Changes of CB1 cannabinoid receptor distribution in temporal lobe epilepsy

PhD Dissertation

Mária Rita Karlócai

János Szentágothai School of Neurosciences
Semmelweis University

Supervisor: Dr. Zsófia Maglóczky, Ph.D.

Official reviewers: Prof. Tibor Wenger, MD, Ph.D., D.Sc.
Dr. József Takács, MD, Ph.D.

Members of the Final Examination Committee:
Prof. József Kiss, MD, Ph.D., D.Sc. -chair
Dr. Andrea Székely, MD, Ph.D.
Dr. Hajnalka Ábrahám, MD, Ph.D.

Budapest, 2012

Hungarian Academy of Sciences, Institute of Experimental Medicine

Table of contents:

1. Abbreviations:

a: alveus

ABC: avidin-biotin-horseradish peroxidase complex

ACSF: artificial cerebrospinal fluid

BSA: bovine serum-albumin

CA: Cornu Ammonis

CB1-R: Type 1 cannabinoid receptor

CCK: cholecystokinin

CR: calretinin

DAB: 3,3'-diaminobenzidine-4HCl

deg: degeneration

EEG: electroencephalogram

ff: fimbria fornix

GABA: γ-amino-butric-acid

GD: gyrus dentatus

h: hilus

HSP72: Heat shock protein 72

KO: knock-out

NeuN: Neuronal Nuclear antigen

NGS: Normal goat serum

PB: phosphate buffer

Pilo: Pilocarpine

s.g.: stratum granulosum

s.lm.: stratum lacunosum-moleculare

s.m.: stratum moleculare

s.o.: stratum oriens

s.p.: stratum pyramidale

s.r.: stratum radiatum

SE: status epilepticus

str.: stratum

TB: TRIS buffer

TBS: Physiological saline buffered with TRIS

TLE: Temporal Lobe Epilepsy

WT: wild type

2. Introduction

2.1. Temporal Lobe Epilepsy

According to the definition of WHO epilepsy is a chronic neurological disorder with various etiologies that affects people of all ages and is characterized by recurrent seizures. Approximately 5 million people have epilepsy worldwide (1-3% of the population (Corsellis & Meldrum, 1976; Houser, 1990). Seizures can vary from the briefest lapses of attention or muscle jerks, to severe and prolonged convulsions (i.e. violent and involuntary contractions, or a series of contractions, of the muscles). Seizures can also vary in frequency, from less than one per year to several per day.

Epilepsy is one of the world's oldest recognized diseases. Fear, misunderstanding, discrimination and social stigma have surrounded epilepsy for centuries. In many countries this condition has a great impact and can impact on the quality of life for people with the disorder and their families. Moreover, it increases a person's risk of premature death by about two to three times compared to the general population.

One seizure does not necessarily indicate epilepsy (up to 10% of people worldwide have one seizure during their lifetimes), thus, epilepsy is defined by two or more spontaneously recurrent seizures (Halász & Rajna, 1990). At the neuronal network level it manifests as states of pathological hyperexcitability and hypersynchronous activity. Imbalanced synaptic input may cause excessive neuronal activity, eventually leading to neuronal death and synaptic reorganization (Engel, 1996; Green, 1991; McNamara, 1999).

Characteristics of seizures vary and depend on where in the brain the disturbance first starts, and how far it spreads later on. Temporary symptoms can occur, such as loss of awareness or consciousness, and disturbances of movement, sensation (including vision, hearing and taste), mood or mental function.

6

Epilepsy syndromes used to be classified based on the classification system accepted by the International League Against Epilepsy (ILAE) in 1989. This classification was based on seizure phenomenology and EEG alterations, it differentiated localized (partial) and generalized forms, and moreover, based on their origin genetic, symptomatic and cryptogenic forms were distinguished as well. However, the development of numerous techniques (electrophysiological techniques, Magnetic resonance imaging (MRI)) and the improvement of our knowledge regarding genetics (mapping of the human genome and uncovering the genetic origin of certain epilepsies) have pointed out the need for a new classification (Berg & Cross, 2010).

According to the most widely accepted concept, the reasons for epilepsies are genes (Salzmann et al, 2008) disposing the network to generate epilepsy under certain circumstances. This notion is strengthened by the fact that epileptic patients often have a history of accidents, febrile seizures, or perinatal disorders (Rocca et al, 1987a; Rocca et al, 1987b). These events do not trigger epilepsy by them selves; however, they may increase the risk of generating seizures in certain people. Thus, most probably the interaction of the entire genome and environmental factors is responsible for this disease.

In adulthood the most common form is Temporal Lobe Epilepsy. The epileptogenic area is mostly found in the hippocampus and quite frequently hippocampal sclerosis occurs.

Though recently a high variety of antiepileptic drugs have been available a significant number of patients are pharmacoresistant (cannot be cured with medication). In case of therapy resistant patients with severe clinical consequences where the epileptic focus can be precisely localized epilepsy surgery is a possible solution (Falconer & Taylor, 1968; Spencer & Spencer, 1994). The aim of the surgery is blocking seizures by lesioning the epileptogenic focus. 85% of partial epilepsies originate from the temporal lobe, thus the surgery most often carried out is anterior temporal lobectomy. After surgery, global cognitive decline can rarely be seen, however certain special functions (like memory) may be modestly impaired. Still, in most cases the quality of life improves following the surgery.

2.2. Anatomy of the mouse hippocampus

The hippocampus is a part of the filogenetically most ancient cortical region, the archicortex. It has a major role in learning and memory and their modifications by emotions. In case of its injury processing of new information may be impaired.

It is a curved elaboration of the edge of cerebral cortex in the floor of the inferior horn of the lateral ventricle; a functional component of the limbic system. The hippocampal formation can be divided into two regions: the cornu Ammonis (CA) and the dentate gyrus (DG), forming two U-shaped semicircles. Based on the morphology, distribution and connectivity of principal cells, the cornu Ammonis can be divided into CA1, CA2 and CA3 (a,b,c) regions (Duvernoy, 1998; Nó, 1934; Seress, 1988) **(Figs 1 and 2)**. These regions (except CA3c) form typical layers: the somata of pyramidal cells are located in str. (stratum) pyramidale. Their basal dendrites can be found in str. oriens, whereas, their apical dendrites localize in str. radiatum and arborize in sr. lacunosum-moleculare (Cajal; Cajal, 1968). The axons of pyramidal cells can be seen in str. oriens and run in the alveus; in the CA3 region axons form recurrent collaterals as well, innervating each other. In the CA3 the region between str. pyramidale and str. radiatum, where mossy fibers terminate is termed str. lucidum (Cajal; Cajal, 1968). In the dentate gyrus granule cell are located in str. granulosum, while their dendrites can be found in str. moleculare. Under the densely packed layer of granule cells the hilus can be seen, where mossy cells are the principal cells.

The human hippocampus differs from rodent hippocampus in certain connectivity patterns; however, the cellular structure is rather similar.

In the hippocampal formation the network of principal cells form a so called trisynaptic loop (Amaral DG, 1990). The perforant path, this glutamatergic pathway originates from the entorhinal cortex, and synapses with apical dendrites of CA1 and CA3 pyramidal cells in str. lacunosum-moleculare, and the dendrites of granule cells in the outer part of str. moleculare (first synapse). Axons of the granule cells (mossy fibers) form

synapses with CA3 dendrites on special complex spines, so called, thorny excrescences in str. lucidum (second synapse). Axons of CA3 pyramidal cells innervate apical dendrites of CA1 pyramidal cells in str. radiatum (third synapse). In addition CA3 pyramidal cells strongly innervate each other forming recurrent collaterals. CA1 pyramidal cells project to the subiculum (Amaral et al, 1991), finally subicular pyramidal cells send axons to the entorhinal cortex (Other fibers lave the hippocampus via fimbria hippocampi).

2.3. Cell types of the hippocampus

The two types of neurons that can be found in the hippocampus are principal and non-principal cells. Principal cells are glutamatergic, pyramidal cells of the cornu Ammonis, whereas, in the dentate gyrus they are granule and mossy cells. Axons of CA1 pyramidal cells project to the subiculum, and these subicular cells innervate the entorhinal cortex forming the main output of the hippocampus. The vast majority of non-principal cells are interneurons with local axonal arborisation (Freund & Buzsaki, 1996).

Though, interneurons form a small portion of hippocampal cells, functionally they are quite important. One single interneuron by its extended axonal tree may innervate numerous pyramidal cells, thus they have a significant role in modifying the firing properties of pyramidal cells.

The functional classification of interneurons is based on their input and output characteristics which can be identified with tracing studies. In addition, interneurons can be categorized based on their neurochemical marker content
(calcium binding proteins, neuropeptides, transmitter receptor-content or neurotroph factors) According to most studies, these cells can be classified into three major groups;
-Perisomatic targeting interneurons
-Dendritic targeting interneurons
-Interneuron specific interneurons

The first two populations target mostly principal cells, perisomatic targeting interneurons (basket and axo-axonic cells) (Halasy et al, 1996; Handelmann et al, 1981; Katsumaru et al, 1988; Kosaka et al, 1987; Kosaka et al, 1985; Li et al, 1992) innervate the perisomatic region, thus, they may control the output of principal cells, whereas dendritic targeting interneurons innervate dendrites, therefore, they can modulate synaptic plasticity and dendritic electrogenesis (Arai et al, 1995; Freund & Buzsaki, 1996; Gulyas et al, 1992; Gulyas et al, 1993; Halasy et al, 1996; Han et al, 1993; Kawaguchi & Hama, 1988; McBain et al, 1994; Miles et al, 1996).

The third population selectively targets interneurons (Freund & Buzsaki, 1996; Gulyas et al, 1996)

2.3.1. Perisomatic targeting interneurons

Interneurons containing the calcium-binding protein parvalbumin (PV) are either perisomatic targeting interneurons (Kosaka et al, 1987) with two distinct subpopulations: basket cells innervating the soma and proximal dendrites and axo-axonic cells innervating the axon-initial segments of principal cells (Katsumaru et al, 1988; Kosaka et al, 1987) . Another basket cell type is known which does not contain parvalbumin, instead, another calcium-binding protein, cholecystokinin (CCK) can be found in it. (Acsady et al, 1996a; Gulyas et al, 1991)

2.3.2. Dendritic targeting interneurons

Dendritic targeting interneurons form a more heterogeneous class compared to perisomatic targeting interneurons. In the dentate gyrus we may distinguish HICAP cells (HIlar Commissural-Associational Pathway-related), where the soma is located in the hilus and the axon in the inner part of str.moleculare, where the input from the commissural and perforant pathways arrive (Freund & Buzsaki, 1996; Han et al, 1993; Sik et al, 1997). Other groups are HIPP (HIlar Perforant Path-associated) and MOPP

(MOlecular layer Perforant Path-associated) cells, where the soma is located in the hilus (HIPP) or in str. moleculare (MOPP) and they innervate the outer part of stratum moleculare where the input from the perforant path can be found (Hampson & Deadwyler,

1992; Sik et al, 1997). HIPP cells can be identified based on their neurochemical marker-content, by containing somatostatin and neuropeptid Y (Katona et al, 1999a; Sik et al, 1997). In addition, certain hilar interneurons innervate CA1 and CA3 regions (Buckmaster & Schwartzkroin, 1995; Sik et al, 1997). In the cornu Ammonis O-LM (oriens-lacunosum-moleculare targeting cells) can be found as well with their soma in str. oriens and axons in stratum lacunosum-molaculare (Cajal, 1968; Nó, 1934). Most probably, these cells have a function similar to HIPP cells by providing feedback-inhibition, since in case of both cell types, the somata and dendrites are located at the output region of principal cells, moreover, they project to the same layer of the entorhinal cortex (Gulyas et al, 1993; McBain et al, 1994; Sik et al, 1995). Moreover, both O-LM cells and HIPP cells contain somatostatin (SOM) and occasionally neuropeptid Y as well (Katona et al, 1999a; Sik et al, 1995) Trilaminar and bistratified cells innervate the more proximal dendritic regions of principal cells. Trilaminar cells innervate strata oriens, pyramidale and radiatum, whereas, bistratified cells send axons only to strata oriens and radiatum (Halasy et al, 1996; Miles et al, 1996; Sik et al, 1995) their somata can be found in the same regions. Dendritic targeting interneurons can be classified according to their neurochemical marker content as well; bistratified cells were shown to be either calbindin-containing (CB)(Sik et al, 1995) or parvalbumin-containing (Klausberger et al, 2004), whereas numerous other interneurons contained Calbindin (Gulyas & Freund, 1996; Sloviter, 1989; Toth & Freund, 1992)or CB1-R (Katona et al, 1999b).

Additionally other interneurons can be distinguished with soma, dendrites and axons located in str. radiatum (Cajal, 1968; Gulyas et al, 1993; Kawaguchi & Hama, 1988; Miles et al, 1996 or in str. lacunosum-moleculare (Nó, 1934 #3164)]. Finally back-projection interunerons located at the border of str. oriens and the alveus of CA1 are dendritic targeting interneurons as well, besides their local axonal arbor, they project back to CA3/hilus (Sik et al, 1995; Sik et al, 1994).

2.3.3. Interneuron-selective (IS) interneurons

These interneurons exclusively innervate other interneurons. Based on their connectivity and morphology, they maybe divided into three groups.

IS-1 cells can be found in all hippocampal regions and contain calretinin (CR) (dendro-dendritic connections are quite frequent between these cells). Their somata are often located in the proximal dendritic region of principal cells. These cells innervate interneurons in the str. radiatum and dentate gyrus (Acsady et al, 1996b; Gulyas et al, 1996).

IS-2 cells were shown to be VIP-positive, with somata and dendrites in str. lacunosum-moleculare, axons in str. radiatum (Acsady et al, 1996a; Acsady et al, 1996b).

IS-3 cells contain VIP as well, however, their axons innervate interneurons in str. oriens and in the hilus (Acsady et al, 1996a; Acsady et al, 1996b).

In the rodent hippocampus an additional interneuron group was identified projecting to the septum, the so-called (Gulyas et al, 2003; Jinno & Kosaka, 2002), HS (hippocampo-septal) cells, with local and projecting axons innervating GABAergic interneurons (Gulyas et al, 2003). These interneurons mostly contain SOM and CB, moreover, spiny, CR-positive interneurons are part of this group as well (Gulyas et al, 2003; Gulyas et al, 1992).
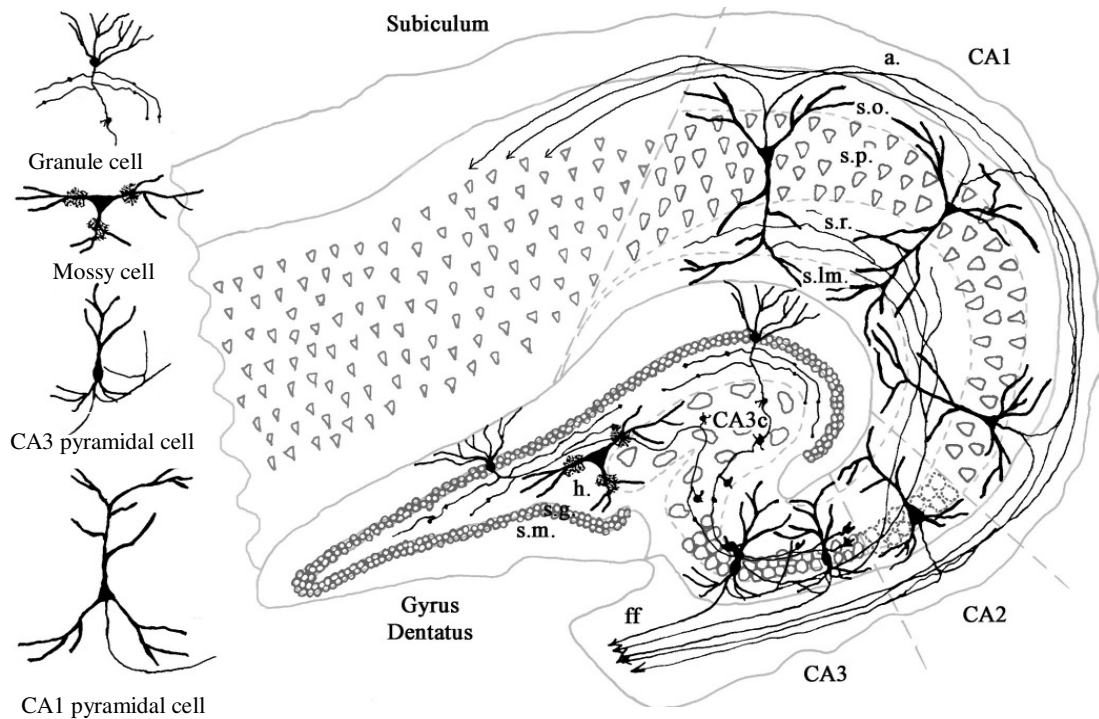
Figure 1: Schematic of human hippocampal formation.

Dentate gyrus and Cornu Ammonis, the two parts of the hippocampal formation, form two U-shaped curves looping into each other. The Cornu Ammonis can be further divided to four subregions: CA1, CA2, CA3 and CA3c (Lorente de Nó, 1934, Seress, 1988). These subregions can be separated by the morphology and connectivity of principal cells (pyramidal cells and mossy cells) found there. Granule cells forming stratum granulosum are the principal cells of the Dentate Gyrus, above this area, stratum moleculare can be found, whereas under it the hilus. The region enclosing the hilus and the CA3c is often mentioned as the endfolium. Abbreviations: CA: Cornu Ammonis, a: alveus, s.p.: stratum pyramidale, s.r.: stratum radiatum, s.lm.: stratum lacunosum-moleculare, ff: fimbria fornix, Figure by Lucia Wittner (PhD thesis 2004)

13
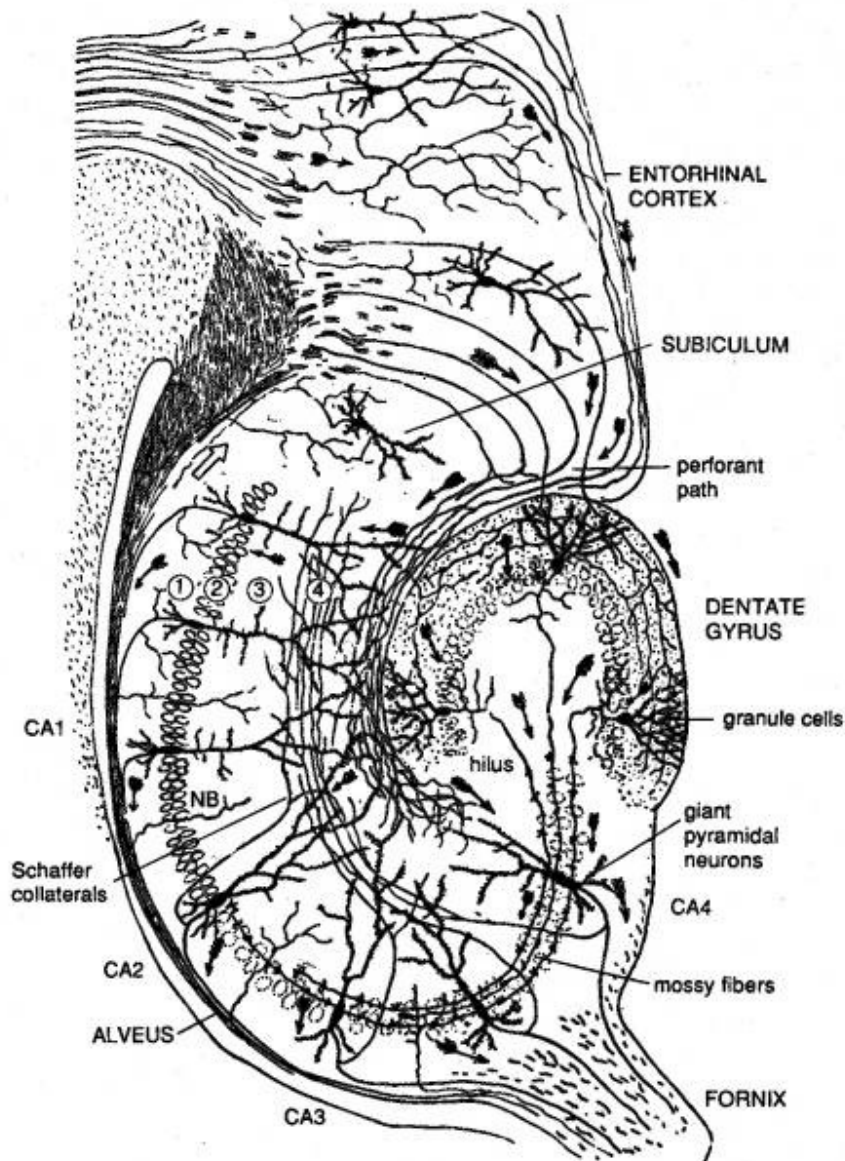
Figure 2: Schematic of rodent hippocampal formation

Similar to the human hippocampus, the rodent hippocampal formation contains two U shaped regions, the Cornu Ammonis and the Dentate Gyrus. The Cornu Ammonis can be divided to CA1, CA2 (not significant in mice), CA3 and CA3c (indicated as CA4 in the figure) subregions. Densely packed granule cells form stratum granulosum in the Dentate Gyrus, with their dendrites in stratum moleculare above, and the hilus underneath them.

Figure by Ramon y Cajal (arrows in CA str. oriens point to the opposite direction of real projection).

2.4. Animal models of epilepsy

Numerous existing animal models demonstrate features typical for human epilepsy. In these models either genetic alterations can be seen, or an acute lesion induces seizures which are followed by a silent period and later by spontaneously occurring recurrent seizures.

-genetic models

A significant proportion of epilepsies have a genetic component. Thus genetic models can provide valuable information regarding the mechanisms underlying neuronal hyperexcitability. The seizure predisposition in these animal models is inherited by the disfunction of certain ion channels, neurotransmitter or neuromodulatory systems.

For example, in the model of genetic absence epilepsy spontaneous seizures occur with age in animals, characterized by motor arrest and head drops that are correlated with generalized spike-wave on the electroencephalogram (EEG). The seizure generating mechanism appears to be located in the lateral thalamic nuclei (Crunelli & Leresche, 2002; Fisher, 1989; Polack & Charpier, 2006).

-kindling models

In the kindling models the development of seizures and epilepsy are acquired by repeated stimulation of the brain (either by electric or chemical stimuli). The stimuli is set at a subthreshold level, however after a certain time, the threshold lowers and acute seizures begin (McNamara, 1986). After the first seizure no further stimulation is required, since a seizure increases the likelihood that more (recurrent) seizures will occur. (Seizures beget seizures) (Brown & Stone, 1973; Lothman et al, 1989; Sutula & Steward, 1986)

-excitatory amino acid analogs

The overexcitation of cells is considered a basic feature of epilepsy. Increase of glutamate release has an important role in causing this overexcitation. Thus by adding additional glutamate or aspartate analogues it is possible to exert toxic effects on the nervous system under certain conditions (Brown & Stone, 1973).

-substances altering the function of ion channels

In epileptic specimens changes in the number and/or function of ion channels can often be seen leading to abnormal extra and intracellular ion concentrations and thus impaired membrane potential. Consequently, by altering the function of ion channels it is possible to mimic abnormal ion concentrations and cause seizure activity (Karnup & Stelzer, 2001; Panuccio et al, 2010). This model is suitable to study the acute phase of epilepsy exclusively, since neither network reorganization nor recurrent seizures occur.

-substances altering the concentration of chations or anions

Similarly to the previous model, the ion balance and thus the membrane potential can be manipulated by changing ion concentrations themselves. Thus, by increasing or decreasing chations and/or anions, the balance of excitation and inhibition can be altered effectively (Gutnick et al, 1982; Heinemann et al, 1986)

In the current studies alterations were examined in pilocarpine induced epilepsy model. Pilocarpine is cholinergic agonist acting on each type of muscarinic acetylcholine receptors (Turski et al, 1986). By activating these receptors it induces status epilepticus (acute seizures) which is followed by a seizures-free latent phase and finally the chronic phase where spontaneously emerging seizures occur (Turski et al, 1984).

2.5. The endocannabinoid system

Physiological and psychological effects of compounds deriving from the plant Cannabis Sativa have been known since the ancient times. The main psychoactive molecule, the terpenoid derivative Δ^9-tetrahydrocannabinol (Northcutt) (Gaoni & Mechoulam, 1971) was described in the 60s, however the site of activation remained hidden. Finally in 1990 the CB1 cannabinoid receptor was cloned from rat brain by Matsuda and co (Felder et al, 1992; Matsuda et al, 1990) and three years later its immune-system counterpart, the CB2 receptor as well (Munro et al, 1993). These findings enlightened the mechanisms of action of THC, and a search began for the brain-derived cannabinoid ligands.

The first ligand described was N-arachidonoyl ethanolamide (anandamide)(Devane et al, 1992), the second 2-arachidonoyl-glycerol (2-AG) (Mechoulam et al, 1995; Sugiura et al, 1995), both extracted from animal tissue (Pertwee, 1997) Even though anandamide was the endocannabinoid described first (Devane et al, 1992), it seems more possible that 2-AG is the one effectively activating the receptor (Sugiura et al, 2006). After identified these two ligands, their synthesizing and degrading enzymes were described as well. Synthesizing (or metabolic) enzyme for anandamide is N-acyl phosphatidylethanolamine phospholipase D (NAPE-PLD) (Okamoto et al, 2004), whereas diacylgycerol lipase- α (DGL-α) (Bisogno et al, 2003) for 2-AG. For degrading anandamide, the enzyme is fatty acid amide hydrolase (FAAH) (Egertova et al, 1998), and monoacylglycerol lipase (mice) (Dinh et al, 2002) for 2-AG.

Activation of the endocannabinoid system is involved in numerous physiological functions like food intake, pain sensation and memory formation. In the brain, the endocannabinoid system is responsible for retrograde synaptic signaling via CB1-R (Type 1 cannabinoid receptor) (Freund et al, 2003; Mackie, 2008; Mackie & Stella, 2006). Endocannabinoids are released from the postsynaptic neurons in an activity-dependent manner, and bind to presynaptic CB1-Rs, thereby suppressing transmitter release from presynaptic terminals (both in excitatory and inhibitory synapses) (Hajos et al, 2000; Hajos et al, 2001; Kathmann et al, 1999; Katona et al, 1999b; Mackie, 2005; Misner & Sullivan, 1999; Ohno-Shosaku et al, 2002; Sullivan, 1999; Varma et al, 2001).

17

In addition to its physiological roles, this system was found to be affected in pathological processes as well. Controversial data were published regarding the effects of cannabinoids in epilepsy. On one hand, in an animal model of TLE (temporal lobe epilepsy), CB1-R agonists displayed anti-epileptic effects (Wallace et al, 2003), in addition, CB1-Rs on glutamatergic axon terminals were shown to mediate anticonvulsant effect, by attenuating glutamate release (Azad et al, 2003; Monory et al, 2006). On the other hand, proconvulsive effects of CB1-R agonists were described as well (Gordon & Devinsky, 2001; Keeler & Reifler, 1967; Lutz, 2004). Moreover, a CB1-R antagonist was shown to prevent the long-term increase in seizure susceptibility when applied in a certain time-window (Chen et al, 2007; Echegoyen et al, 2009).

Human studies showed that recurrent seizures may lead to an adverse reorganization of the endocannabinoid system and to the impairment of its protective effect (Goffin et al, 2011; Ludanyi et al, 2008) which may be accomplished by the downregulation of CB1-Rs located at excitatory synapses occurring in the inner molecular layer of the dentate stratum moleculare (Ludanyi et al, 2008).

Since more numerous CB1-R-positive asymmetric synapses can be found in the hippocampus compared to stained symmetric synapses, previous ultrastructural studies have not demonstrated, what happens to inhibition regulated by the endocannabinoid system at the ultrastructural level. Moreover, the target distribution of CB1-R-positive terminals was not examined either.

Regarding CB1-Rs located at inhibitory synapses, results are restricted to animal models and are contradictory reporting both up and downregulation of the receptor (Falenski et al, 2009; Wyeth et al); (Wallace et al, 2003).

3. Aims

In the present study we wished to uncover anatomical changes affecting the endocannabinoid system in patients with TLE and in pilocarpine treated mice. We focused on two phases of epilepsy in the mouse model (acute and chronic) and to the chronic phase in human TLE, since robust and controversial changes occur at early and later time points post epileptogenesis. (the acute phase obviously cannot be studied in human samples)

The imbalanced ratio of dendritic and perisomatic inhibition has long been regarded as an important feature linked to epilepsy (Magloczky & Freund, 2005; Wittner et al, 2005) , causing cell death and hippocampal reorganization. Increased excitation was shown to originate from mossy fiber sprouting (Houser et al, 1990; Sutula et al, 1989a) and an increased input from the supramammilary nucleus (Abdulla & Campbell, 1993; Magloczky et al, 1994; Magloczky et al, 2000). Although a decreased inhibition was proposed to be associated to the strong excitation, several studies show, that increased inhibition occurs, leading to hyperexcitability through several mechanisms (hypersynchronization, excitatory GABA, etc) (Bernard et al, 2000; Cossart et al, 2001; Karlocai et al, 2011; Wittner et al, 2005; Zhang et al, 2009). The mechanism leading to hypersynchronization can vary; most often the reorganization of excitatory or inhibitory fibers is one of them. Sprouting can often be characterized by changes in target distribution, increase in fiber density or the number of terminals, leading to altered transmitter release. Cannabinoids act as retrograde transmitters, decreasing transmitter release when activating their receptors, thus they are in the position of effectively regulating network activity. Several studies have examined functional and anatomical changes; however no detailed investigation was carried out to quantify the exact changes in number and target distribution of CB1-R-positive fibers.

In the present set of experiments we wished to examine the following issues:

- The correlation between pathological changes and CB1-R distribution in human TLE samples (chronic phase) and in the acute, latent and chronic phases of pilocarpine induced epilepsy.

- Alterations in the target distribution of CB1-R-positive elements in epileptic mice and human patients.

- The correlation between behavioral signs of acute seizures and later emerging cell death and reorganization in the epileptic mice.

- The difference of the seizure susceptibility in CB1-R knock out animals compared to controls.

- We assumed that by understanding the dynamics of changes in CB1-R expression during different phases of epilepsy we could suggest whether CB1-R agonists or antagonists would be suitable candidates for antiepileptic treatment.

4. Materials and methods

4.1. The pilocarpine model of epilepsy

Animals were kept under standard conditions with 12 h dark-light cycle; food and water were supplied ad libitum. Experiments were performed according to the guidelines of the Institutional Ethical Codex & the Hungarian Act of Animal Care & Experimentation (1998, XXVIII, Section 243 ∕ 1998), The Animal Care and Experimentation Committee of the Institute of Experimental Medicine of Hungarian Academy of Sciences and the Animal Health and Food Control Station, Budapest, has approved the experimental design under the number of 2303/003/FŐV/2006. The experiments are in accordance with 86/609/EEC/2 Directives of European Community, which is in full agreement with the regulation of animal experiments in the European Union. All efforts were made to reduce the number of animals used and to minimize pain and suffering. For this animal model 20-30 g male CD1 mice (Harlan, Italy) and CB1-R knock-out CD1 mice were used (Ledent et al, 1999). Animals were assigned to control and experimental groups. Age-matched control mice were injected with physiological saline (12 animals, 0.1 ml/30g) or scopolamine (12 animals 5 mg/kg). Since no difference was found between the two control groups, during the following experiments, control mice were injected with physiological saline.

Experimental mice were injected with intraperitoneal Pilocarpine hydrochloride (340 mg/kg, Sigma) to induce status epilepticus (SE). Scopolamine methyl nitrate (5 mg/kg, Sigma) was injected 30 minutes in advance to prevent peripheral cholinergic effects of pilocarpine. No benzodiazepine treatment was used to stop seizures. By omitting antiepileptic drugs we were able to examine seizure-induced changes 2 hours post SE, without further alteration of the GABAergic function by additional drugs.

Animals were observed for two hours after the pilocarpine injection, and the behavioral signs of seizures were monitored and scored. At every 5 minutes or when behavioral changes occurred a score was determined. Acute seizures started 5-15 minutes after the pilocarpine administration (post pilo). Seizures were classified by using the modified Racine's scale (Racine, 1972) (1-5), animals were separated into "weak" and "strong" groups according to their seizure activity (Magloczky et al). Seizure activity was

defined for every animal by using the maximal value of Racine -scale reached more than once.

In the weak group mice developed only a few mild seizures characterized by few ictal seizure period in the EEG accompanied with startling and shaking, whereas in the strong group the seizures were frequent and EEG showed several ictal seizure periods behaviorally represented by intense motor symptoms including jaw movements, salivation, and forelimb clonus with rearing and tonic-clonic seizures (Magloczky et al; Racine, 1972; Turski et al, 1984).

Acute phase was examined 2 hours after pilocarpine injection. The period examined 1-3 days after the injection was regarded as the latent phase. At day three mass cell loss was observed, therefore this time point was considered as the end of the latent phase. EEG recordings were carried out 1 month after pilocarpine treatment in the chronic phase, at this time point recurrent seizures occurred in most of the strong epileptic animals.

We examined the expression pattern of CB1-Rs in the hippocampus at different survival times: 2 hours after the treatment in the acute phase, 1 and 3 days after the treatment in the latent phase and 1-2 months after the treatment in the chronic phase.

4.2. In vivo electrophysiology

We proved the occurrence of recurrent electrographic seizures with EEG recordings in the chronic phase. Mice were anesthetized with a 1-1.5 % halothane-air mixture (Narcotan, Leciva, Praha, Czech Republic) and secured in a stereotaxic frame (David Kopf, 900 USA, equipped with a SUPERTECH Ltd. made mouse adaptor HU).

Five holes were drilled into the skull above the frontal and parietal lobe bilaterally and above the cerebellum (reference). Stainless steel wire electrodes (MEDWIRE SST1) were placed on the skull and covered with conductive paste (Ten20, USA) to decrease the impedance. The electrodes and the connector were embedded in dental acrylic cement (GS, Japan). This way the electrodes were firmly implanted to the skull but the dura was not pierced. The EEG activity was recorded by a Grass EEG 8B model (Grass Instruments, Quincy, MA, USA), filtered at 1 Hz to 70 Hz and amplified. Data were recorded with a CED 1401 system using SPIKE2 v2.1 software (Cambridge Electronic Design Limited,

Cambridge, UK). Sampling rate was 500 Hz , amplification 20 µV/mm, filter: LP: 70Hz, HP: 1Hz.

Recordings were made for 3 days, in the morning (9 AM) and in the afternoon (4PM) for 1.5 hours. The behavior of the animal was observed during EEG recording. To answer the question whether animals had different diurnal and nocturnal epileptic activity, 24-hour continuous EEG monitoring was also carried out in 4 animals (2 controls, 2 chronically epileptic mice).

4.3. Analysis of the EEG recordings

All EEG recordings were evaluated by three independent and experienced researchers to determine the occurrence of seizures or interictal spikes (Litt et al, 2001). EEG recordings were carried out in 16 mice (6 controls, 4 weak and 6 strong epileptic) in the chronic phase. In 4 animals (2 controls, 2 chronically epileptic ones) 24-hours EEG monitoring was carried out.

Epileptic activity was considered as interictal burst when the amplitude of occasionally appearing EEG spike activity was three times higher than the normal resting control EEG waves. The ictal EEG was determined so that the appearance of large amplitude EEG spikes was continuous and that activity pattern lasted for at least 5 seconds. Occasionally, an increase of frequency and decrease of amplitude of large spikes were seen prior to the ictal event. That phase was considered as interictal activity. Data were analyzed with SPIKE2 v2.1 software (Cambridge Electronic Design Limited, Cambridge, UK).

4.4. Slice preparation

Two hours after pilocarpine injection, control and "strong" epileptic mice (two of each) were deeply anesthetized with isoflurane (Abbott Labs, USA) After decapitation, the brain was quickly removed and placed into ice-cold artificial CSF containing (in mM): sucrose, 252; KCl, 2.5; $NaHCO_3$, 26; $CaCl_2$, 0.5; $MgCl_2$, 5; NaH_2PO_4, 1.25; glucose, 10, and bubbled with 95% O_2 and 5% CO_2 (carbogen gas). We prepared 400- µm-thick coronal slices using a Leica (Nussloch, Germany) VT1000S microtome. Slices containing the hippocampal formation were trimmed from other brain regions. 2 slices of each animal

were immediately transferred to fixative containing 0.05% glutaraldehyde (TAAB, UK), 4% paraformaldehyde (TAAB, UK) and 15% picric acid in 0.1 M phosphate buffer (PB) , whereas other slices were kept in an interface-type holding chamber at room temperature for 2 hours, before fixation. After overnight fixation, CB1-immunostaining was carried out.

4.5. Tissue preparation for morphological examination

Animals were sacrificed at different survival times including 2 hours (n=22), 1 day, 3 days (n=48), 1 month and 2 months (n=105) after pilocarpine administration. Mice were perfused under equithesine anesthesia (chlornembutal 0.3 mL ∕ 100 g), first with physiological saline (1 min) and then with a fixative containing 0.05% glutaraldehyde (TAAB, UK), 4% paraformaldehyde (TAAB, UK) and 15% picric acid in 0.1 M phosphate buffer (PB) for 30 min.

4.6. Human tissue

Hippocampal samples were obtained from patients (n=34) with therapy-resistant temporal lobe epilepsy. The seizure focus was identified by multimodal studies including video-EEG monitoring, MRI, single photon emission computed tomography and/or positron emission tomography. Patients with intractable temporal lobe epilepsy underwent surgery in the National Institute of Neuroscience in Budapest, Hungary within the framework of the Hungarian epilepsy Surgery Program. A written informed consent for the study was obtained from every patient before surgery. Standard anterior temporal lobectomies were performed (Spencer and Spencer, 1985); the anterior third of the temporal lobe was removed together with the temporomedial structures. The study was approved by the ethics committee at the Regional and Institutional Committee of Science and Research Ethics of Scientific Council of Health (TUKEB 5-1/1996, further extended in 2005) and performed in accordance with the Declaration of Helsinki.

Four control post-mortem human hippocampi were used in this study, courtesy of the Lenhossék program. Control brain tissue was obtained from 53-65 years old subjects 2-4 hours post mortem delays. None of the control subjects had any record of neurological

disorders. Brains were removed 2 hours after death, the dissection was performed in the Forensic Pathology Department of the Semmelweis University Medical School.

After surgical removal, the epileptic tissue was immediately dissected to 3-4 mm thick blocks, and immersed into a fixative containing 4% paraformaldehyde, 0.1% glutaraldehyde and 0.2% picric acid in 0.1 M PB (pH=7,2-7,4) (Magloczky et al, 1997). Fixative was changed every 30 minutes to a fresh solution during constant agitation for 6 h, and the blocks were then post-fixed overnight, in the same fixative without glutaraldehyde. In case of control samples the procedure was similar.

4.7. Immunocytochemistry

Brains were removed from the skull and 60 µm thick vibrotome sections were cut from the blocks. Following washing in PB (6x 10 minutes), sections were cryoprotected in 30% sucrose for 1–2 days, followed by freezing three times over liquid nitrogen. Sections were processed for immunostaining with the use of two different antibodies against CB1-Rs (shall be described). Other antibodies used in the study were Neuronal Specific Nuclear Protein (NeuN) and Heat Shock protein 72 (HSP72) as follows. Sections were transferred to Tris-buffered saline (TBS, pH 7.4), then endogenous peroxidase was blocked by 1% H_2O_2 in TBS for 10 min. TBS was used for all the washes (3x10 min between each step) and dilution of the antisera. Non-specific immunostaining was blocked by 5% normal goat serum, 0.1g/ml glycine, 0.1g/ml lysine. A polyclonal guinea pig antibody against CB1-R (1:1000), monoclonal mouse antibody against NeuN (1:4000 Chemicon) and a monoclonal mouse antibody against HSP72 (1:800, Calbiochem) were used for 2 days at 4°C. The specificity of the antibody has been thoroughly tested by the manufacturer and in our laboratory using CB1 knock out mice (Katona et al, 2006). For visualization of immunopositive elements, biotinylated anti-guinea pig or anti-mouse immunoglobulin G (IgG) (1:250, Vector, 2 hours) was applied as secondary antiserum followed by avidin-biotinylated horseradish peroxidase complex (ABC; 1:250, Vector, 1.5 hours). The immunoperoxidase reaction was developed by 3,3'-diaminobenzidine tetrahydrochloride (DAB; Sigma) as a chromogen dissolved in TRIS buffer (TB, pH 7.6). Sections were then

treated with 1% OsO_4 in PB (40 min) and dehydrated in ethanol (1% uranyl acetate was added at the 70% ethanol stage for 40 min) and mounted in Durcupan (ACM, Fluka). The control sections were processed in the same way. For immunogold staining against CB1-R, the sections were blocked in a solution containing 5% normal goat serum, 0.1g/ml glycine and 0.1g/ml lysine (GE Healthcare UK Limited). Incubation in anti-CB1 guinea pig antiserum (1:1000, 2 days) was followed by a second blocking step with 5% normal goat serum, 0.1g/ml glycine, 1g/ml lysine and 0.1% fish gelatin. Secondary antiserum was ultra small gold conjugated goat anti-guinea pig (1:50, overnight incubation, Aurion). Gold labeling was intensified using the R-Gent silver intensification kit (Aurion, Wageningen, The Netherlands). Sections were then osmicated (0.5% OsO_4, 30 min, 4 ^{o}C), dehydrated and embedded in Durcupan. The control hippocampi were processed in the same way.

After light microscopic examination, areas of interest were re-embedded and sectioned for electron microscopy. Ultrathin serial sections were collected on Formvar-coated single slot grids, stained with lead citrate, and examined with a Hitachi 7100 electron microscope.

4.8. CB1-R antibodies

In the first set of experiments (human and mouse target distribution) our antibody against CB1-R (from Prof. Ken Mackie) visualized CB1-Rs only on terminals forming symmetric synapses. Our alternative CB1-R antibody. (from Prof. M. Watanabe, Hokkaido University, Sapporo, Japan) (described by Fukudome (Fukudome et al, 2004)) (**Fig. 3**) stained both symmetric and asymmetric synapses formed by terminals positive for CB1-Rs. This antibody was used in the detailed investigation of CB1-R expression in the pilocarpine model of epilepsy in mice (second part of the study).
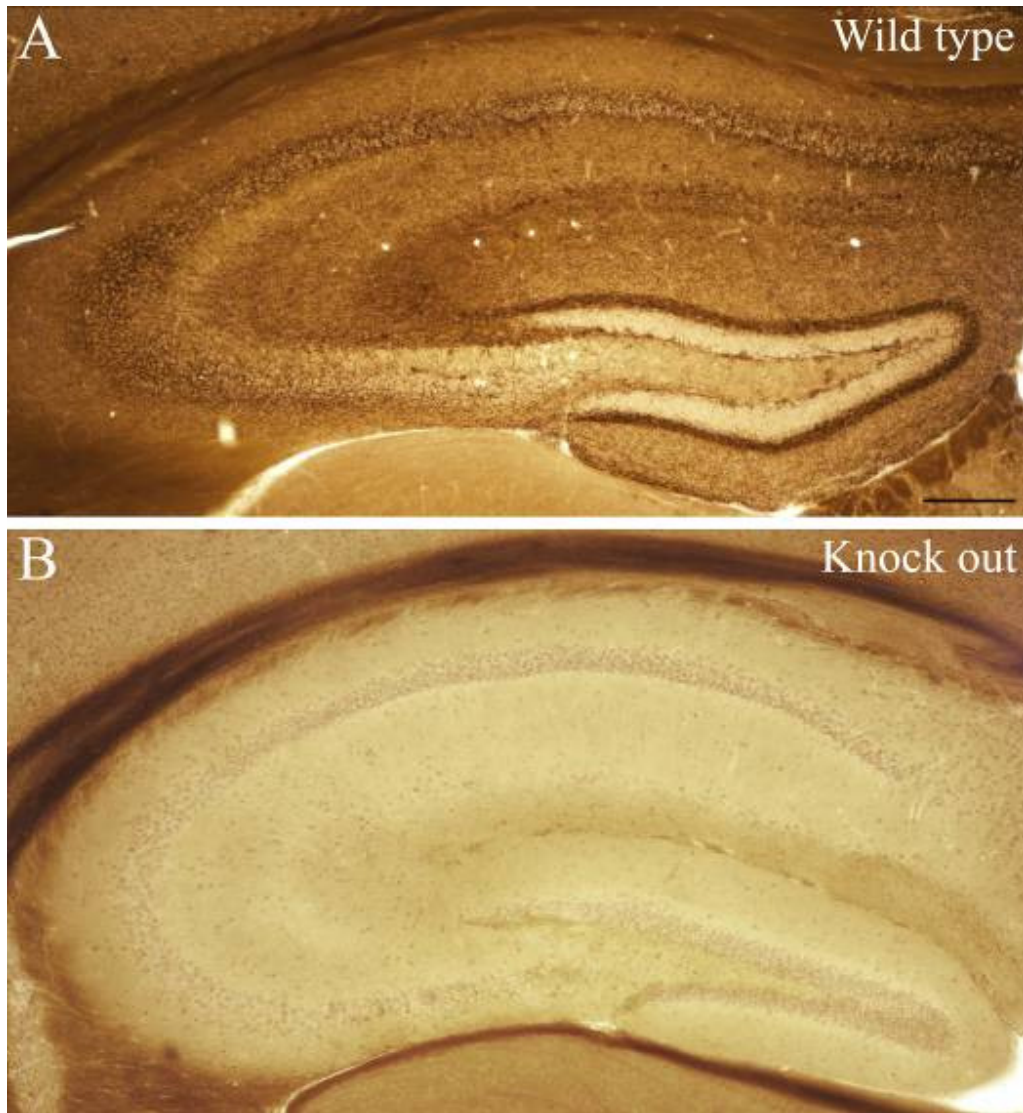
<u>Figure 3: Lack of CB1-R staining in knock out animals</u>

Staining was carried out with the antibody staining CB1R-positive terminals giving symmetric and the ones giving asymmetric synapses as well. In wild type animals (A) CB1-R staining was found in all hippocampal regions as shall be described later. In contrast, in CB1-R knock out animals (B) no specific staining was found, only light background staining occurred in the somatic regions. Lack of staining indicates the specificity of the antibody. Scale: 200 µm

4.9. Gallyas silver impregnation

In the mouse tissue degenerated neuronal elements were visualized with the staining procedure of Gallyas et al. (Gallyas et al, 1980). The steps of this staining are the following: 2x5min in the pretreating solution (2% NaOH and 2.5% NH_4OH), 10 min in the impregnating solution (0–0.8% NaOH, 2.5% NH_4OH, 0.5% $AgNO_3$), 3x5 min in washing solution (0.5% Na_2CO_3 and 0.01% NH_4NO_3 in 30% ethanol), 1 min in developing solution (0.4–0.6% formaldehyde and 0.01% citric acid in 10% ethanol, pH 5.0 –5.5), 3x10 min wash in 0.5% acetic acid. Afterwards sections were mounted on gelatin-coated slides, dehydrated in xylene and covered with XAM neutral medium (BDH, Poole, UK).

4.10. Nissl staining

Cell loss could be visualized with Cresyil violet staining as well. Sections were mounted in chrome-gelatine and air-dried on slides. Afterwards the following steps were carried out: 2 mins in xylene, 3 mins in ethanol abs., 3 mins in 90% ethanol, 3 mins in 70% ethanol, 3 mins in 50% ethanol, 5 mins in cresyle violet (1% in tap water), rinse in 70% ethanol, rinse in 70% ethanol+drops of acetic acid for fixation, rinse in 90% ethanol, 3 mins in ethanol abs., 2x3 mins of xylene, and mounting with DePeX (SERVA Electrophoresis GmbH, Heidelberg, Germay) finally.

4.11. Determination of principal cell loss in epileptic mice

In the chronic phase, the severity of the acute seizures (using the Racine-scale, seizures from 1 to 5) was correlated with the cell-loss found in CA1, CA3 and hilus. Cell loss was determined in case of a large number of animals using a well defined semiquantitative scale by two independent examiners as shown previously (Magloczky & Freund, 1993; Magloczky & Freund, 1995; Wittner et al, 2005). Each region was classified as type 1-3 according to the severity of cell death (type1: cell-loss under 10 %, type2: cell-loss between 10% and 50%, type3: cell-loss above 50%) **(Fig.4)**. Pearson correlation was used to calculate the relationship between cell-loss and seizure strength. Seizure strength was defined for every animal by using the highest number of Racine scale reached during

acute seizures. This number, representative for each animal was correlated with the severity of cell death (types 1-3) in each subregion.
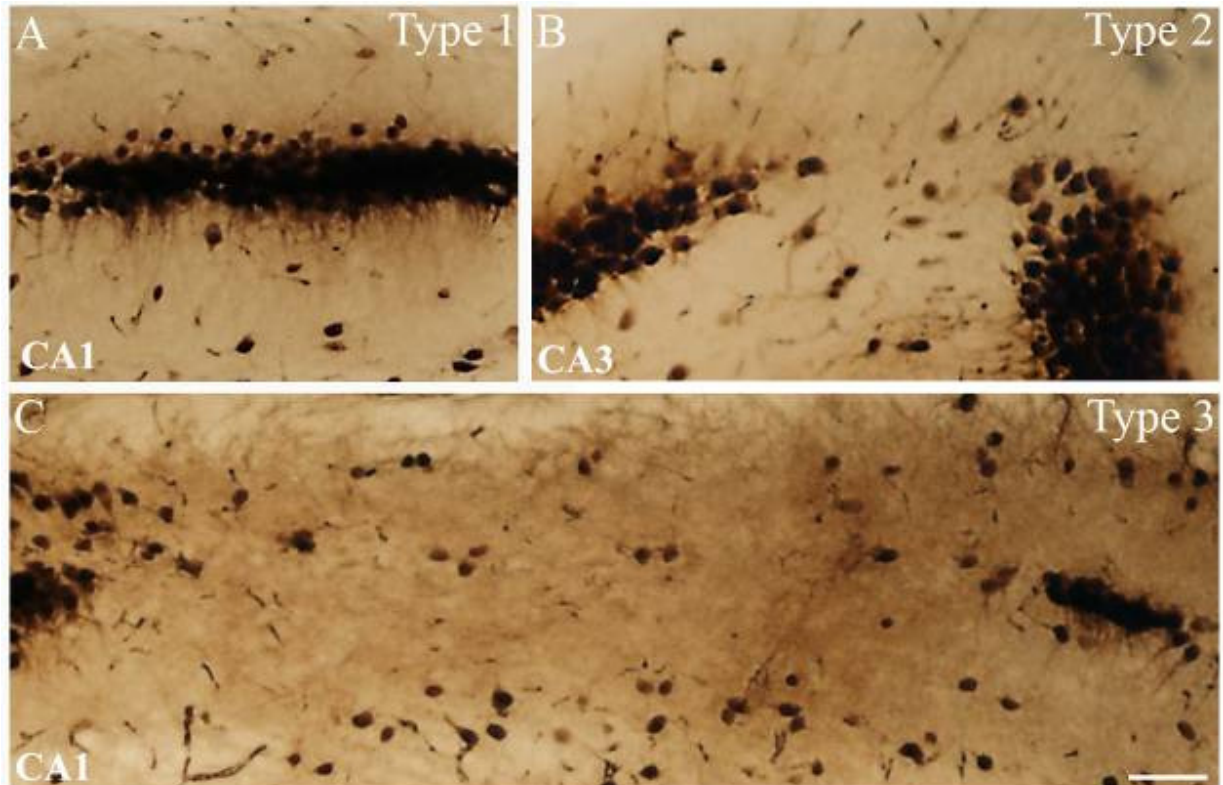
Figure 4: NeuN-staining shows different types of cell loss in the epileptic hippocampus
Based on the severity of principal cell loss, distinct regions were classified as type 1, 2 or 3. In case of type 1 (A) cell loss is quite mild, with only few missing cells (<10% of principal cells are missing in the given region). Type 2 (B) indicated cell loss in patches, affecting more numerous cells (11-50% of principal cells are missing in the given region). Type 3 (C) indicates sclerosis in the given region with more than 51% of principal cells missing. Scale: 50 μm

4.12. Quantitative electron microscopic analysis

4.12.1. Ratio and number of symmetric and asymmetric synapses

Electron microscopic analysis was carried out in the dentate gyrus, since this area is affected by seizure induced changes, however granule cells are well-preserved even in case of robust sclerosis in the CA1 (Houser & Esclapez, 1996; Peng & Houser, 2005) therefore it is possible to examine the surviving elements which may not be the case in CA1.

The quantity of symmetric and asymmetric synapses established by CB1-R-positive axon terminals was examined throughout the str. moleculare of 3 control, 3 chronic epileptic and 3 acute epileptic hippocampi. Serial sections were made from the blocks reembedded from stratum moleculare and examined in the electron microscope. CB1-R stained terminals were analyzed in every 10th section in order, following the rules of systematic random sampling, to avoid sampling of the same axon terminals. Photographs were taken of all terminals in a given area, and the ratio of immunostained symmetric versus asymmetric synapses was determined.

To quantify the exact changes in the number of stained terminals in the chronic and acute phase, we further examined the str. moleculare. The number of CB1-R immunostained terminals forming symmetric and asymmetric synapses was calculated, both in control and in epileptic samples and normalized. The studied areas were measured with NIH ImageJ (U.S. National Institutes of Health, Bethesda, MD) program and were normalized to unit area (40 000 μm^2).

To assess any changes occurring in the density of CB1-Rs per terminals, the number of gold particles located in the membrane of axon terminals was counted and normalized to a unit length of the terminal's perimeter (perimeter length was measured with NIH ImageJ, number of particles was normalized to 1 μm). Significance was tested using Mann-Whitney U-test (Statistica 6.0).

4.13. Target distribution of CB1-R-positive terminals forming symmetric synapses

In the human and mouse tissue target distribution of CB1-R immunopositive elements was studied in the stratum moleculare of the dentate gyrus in control and sclerotic subjects, since in sclerotic samples the highest fiber density can be observed in this area.

Both in controls (N=105, two subjects) and in epileptic patients (N=175, three sclerotic subjects) the postsynaptic target of CB1-immunopositive terminals establishing symmetric synapses were examined (photographed and quantified) at the electron microscopic level.

5. Results

5.1. Reorganization of CB1 receptor expressing GABAergic fibers in temporal lobe epileptic patients

The expression pattern of CB1-receptors associated with inhibitory synapses was studied by immunocytochemistry in epileptic hippocampal tissue derived from intractable TLE patients (N=44). A previous study by Ludanyi et al. has demonstrated a decrease of CB1-Rs associated with asymmetric synapses, thus, we examined changes affecting the number of CB1-R-positive symmetric synapses.

In the hippocampi of human TLE patients the pattern of cell loss was analyzed by light microscope in sections immunostained for different neurochemical markers labeling principal and non-principal cells (Magloczky & Freund, 2005; Toth et al, 2010; Wittner et al, 2005). Based on anatomical alteration observed in the hippocampus patients could be classified into different groups.

5.1.1. Pathological classification of the epileptic samples

All patients examined in the present study had therapy resistant epilepsy of temporal lobe origin. The patients had different degrees of hippocampal atrophy and/or sclerosis. All the examined sections derived from the anterior part of the hippocampal body. Similarly to our previous studies (Clemens et al, 2007; Toth et al, 2010; Wittner et al, 2005; Wittner et al, 2002) and other results (de Lanerolle et al, 2003), patients with epilepsy were classified based on principal cell loss and interneuronal changes examined at the light microscopic level as follows.

(i)   Epileptic Type 1 (mild) (n = 6): similar to control, no considerable cell loss in the CA1 region, pyramidal cells present, layers are visible and intact, their borders are

clearly identified. There is a slight loss in certain interneuron types, mostly in the hilus and the stratum oriens of the CA1 region.

(ii)   Epileptic Type 2 (patchy) (n = 16): pyramidal cell loss in patches in the CA1 pyramidal cell layer but the CA1 region is not atrophic. Interneuron loss is more pronounced.

(iii)   Epileptic Type 3 (sclerotic) (n = 22): the CA1 region is shrunken, atrophic, more than 90% of principal cells are missing. Only the stratum lacunosum-moleculare is present as a distinct layer in the CA1 region, the others could not be separated from each other due to the lack of pyramidal cells and their dendrites and the shrinkage of the tissue. This remaining part should contain the layers identified in the control as stratum oriens, stratum pyramidale and stratum radiatum. Mossy fiber sprouting and considerable changes in the distribution and morphology of interneurons (not shown) can be observed in the samples of this group.

The number, morphology and distribution of cells were similar in patients in the same pathological group, but differed between the groups. The control samples with short (2–4 h) post-mortem delay were similar to each other and differed from the epileptic groups.

Therefore, we concluded that the differences found between control and epileptic tissues in the present study are likely to be caused by epilepsy. (Toth et al, 2010; Toth et al, 2007; Wittner et al, 2005).

In the present study the distribution and localization of CB1-immunoreactive elements was studied in controls, in non-sclerotic (Type 1 and Type 2) and sclerotic cases (Type 3)

5.1.2. Distribution of CB1-R-stained inhibitory synapses in control human hippocampus

In the following set of experiments the antibody used to visualize CB1-Rs stained receptors found in symmetric synapses, but did not stain receptors located at asymmetric synapses.

Immunostaining revealed numerous CB1-positive cell bodies of interneurons scattered in all hippocampal subfields, these cells have been shown to express the neuropeptide CCK (Katona et al, 1999b) and were either perisomatic or dendritic targeting interneurons (Freund & Buzsaki, 1996). Parts of interneuron dendrites were stained, and a dense meshwork of CB1-immunoreactive axons covered the entire hippocampal formation. The strongest axonal labeling was found in stratum moleculare of the dentate gyrus, mostly in the inner part of str. moleculare. Strong staining appeared also in stratum pyramidale of CA1-CA3 containing numerous axon terminals forming basket –like structures surrounding pyramidal cells (Katona et al, 2000). In contrast no labeling occurred in the neuropil in the hilus and str. lucidum, moreover, granule cells were immunonegative.

5.1.3. Distribution of CB1-Rs in epileptic human hippocampus

In the non-sclerotic cases, the distribution of CB1 receptors in the dentate gyrus did not show any major changes compared to the normal post mortem controls. In contrast, a strong increase in CB1 receptor immunostaining was found in the dentate gyrus of epileptic patients with CA1 sclerosis, similar to what we have seen in the mouse model. Immunopositive interneuron somata were preserved both in the dentate gyrus and in the CA1 area. The density of immunostained fibers increased in the dentate molecular layer (**Fig. 5**) and became inhomogeneous in the hilus forming dense arrays of boutons around the surviving mossy cells and interneurons.
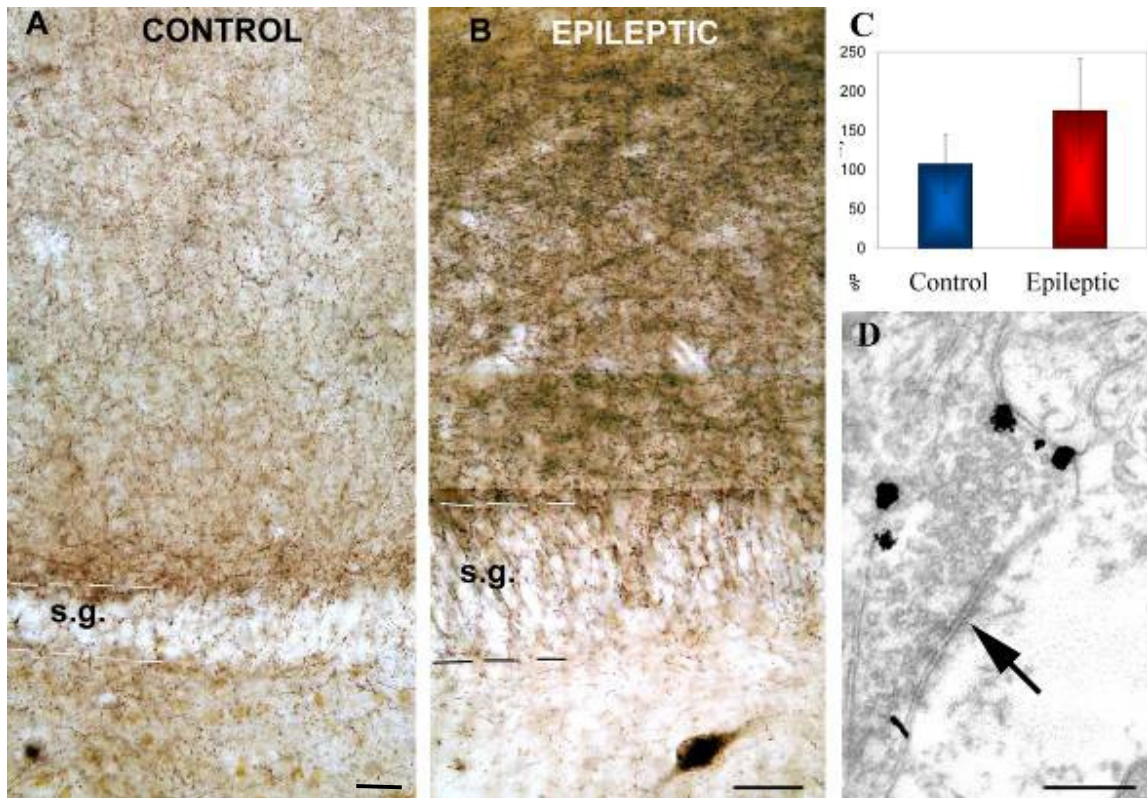
Figure 5. Distribution of CB1-R associated with symmetric synapses at light and electron microscopic level in human dentate gyrus

A) Low power light micrograph showing the distribution of CB1-positive profiles in the control human dentate gyrus. Granule cells are always negative for CB1. B) Tissue from sclerotic epileptic patients remarkably differs from controls. The density and staining intensity of CB1-positive fibers is considerably increased in the stratum moleculare. C) Density of CB1 receptor immunopositive fibers in control (N=3) and sclerotic epileptic patients (N=10) revealed by confocal laeser scanning microscope. The intensity of CB1 receptor staining is elevated in epileptic samples. The difference between control and epileptic samples was highly significant (p<0,05; Student t test). D) A CB1-R-positive terminal from the stratum moleculare of an epileptic patient labeled by immunogold technique establishes symmetric synapse on a dendrite. All of the terminals stained by this CB1 antibody established symmetric synapses. Scales: A,B:50 μm; D:0,5 μm

5.1.4. Qualitative analysis of immunopositive fiber density in human sclerotic tissue

Qualitative analysis revealed an increased density of immunostained axonal meshworks in the sclerotic stratum moleculare compared to the control or non-sclerotic cases. To quantify this increase, sections with fluorescent immunostaining were processed in 3 control and 10 sclerotic cases, and the density of immunolabeling was measured by confocal laser scanning microscopy. The results showed that the density of fibers had significantly increased in epileptic cases (type 3) **(Fig. 5)**.

5.1.5. Ultrastructural analysis of CB1-R distribution in control and sclerotic human tissue

Electron microscopic examination confirmed that the antibody used in this study visualized CB1-Rs only on terminals giving symmetric synapses **(Fig. 5, 6)**. The cellular and subcellular localization of CB1-Rs was similar in the epileptic and control cases. CB1-R-positive terminals form synapses mostly on dendrites and less frequently on spines and somata of granule cells in control and epileptic samples. However, we wished to uncover any potential changes occurring in the target distribution of CB1-R containing terminals in epileptic the tissue.

5.1.6. Target distribution of CB1-immunopositive elements in human TLE

Target distribution of CB1-immunopositive elements was studied in the stratum moleculare of the dentate gyrus in control and sclerotic TLE subjects, where the highest fiber density was observed. Examination of immunogold terminals showed that CB1 receptors were localized in the membrane, outside the synaptic active zone in epileptic patients, as it was shown previously in the control human hippocampus (Katona et al, 2000) **(Graph 1)**. Both in controls (N=105, two subjects) and in epileptic patients (N=175, three subjects) the CB1-immunopositive terminals established symmetric synapses mostly on dendrites (75 v.72,5 %, spines 13,2 v. 15,5 %, and cell bodies 11,8 v. 13 %, in control and epileptic subjects, respectively).

Therefore, we can conclude that the target distribution was not changed, although the density of fibers has been elevated greatly.
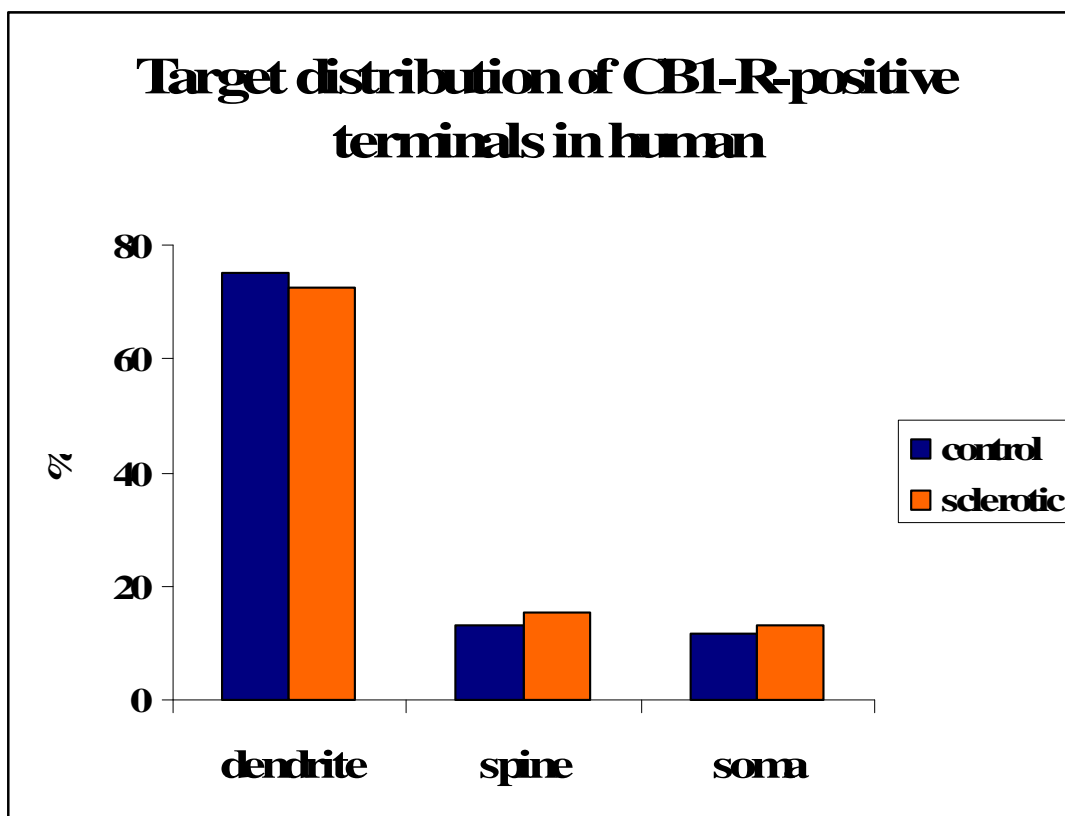
Graph 1: Target distribution of CB1-R-positive terminals establishing symmetric synapses in human TLE samnples

The ratio of CB1-R-positive fibers synapsing on distinct neuronal elements does not change in the epileptic tissue compared to controls.

A previous study by Ludanyi et al (Ludanyi et al, 2008) has demonstrated a downregulation of CB1-Rs linked to asymmetric synapses, whereas, our results show an upregulation in CB1-Rs related to symmetric synapses. These results are quite surprising and indicate that epileptic reorganization affects CB1-R-positive excitatory and inhibitory networks in a different way. To understand the time course of the dynamics of CB1-R expression, we established an animal model of TLE (pilocarpine model, we shall describe it

later) showing similar pathological changes to human TLE. First we characterized changes affecting CB1-Rs linked to symmetric synapses and studied alterations in the target distribution of immunopositive terminals in the mouse model with the same antibody as we used for human tissue (Antibody staining CB1-R-containing terminals establishing symmetric synapses).

5.2. Changes of CB1-receptor immunostained inhibitory fibers in a model of temporal lobe epilepsy

Similar to human TLE tissue, upregulation of CB1-Rs linked to symmetric synapses could be seen in the mouse model as well (using the same antibody as in case of human tissue). The expression pattern of CB1-Rs in the hippocampi of both strong and weak CD1 mice was studied at a survival time of 4-8 weeks (chronic phase).

In control samples numerous immunostained cell bodies were seen (previously shown to be CCK-positive (Katona, 1999 #3054) and could be either dendritic or perisomatic targeting interneurons (Freund & Buzsaki, 1996)). The most intense staining of CB1-positive fibers was found in the molecular layer of the dentate gyrus (DG), in stratum pyramidale of the cornu Ammonis (CA), and in the subiculum. In contrast, faint labeling was observed in the strata radiatum and granulosum **(Fig. 3)**. CB1-immunostaining showed no change in the hippocampi of weak animals compared to controls. In the sclerotic samples CB1-R-positive cell bodies were preserved, however, the general CB1-immunostaining was much stronger throughout the hippocampus. The most striking difference was found in the strata moleculare and granulosum of the DG **(Fig. 6)**, in the strata pyramidale and radiatum of the CA1.)
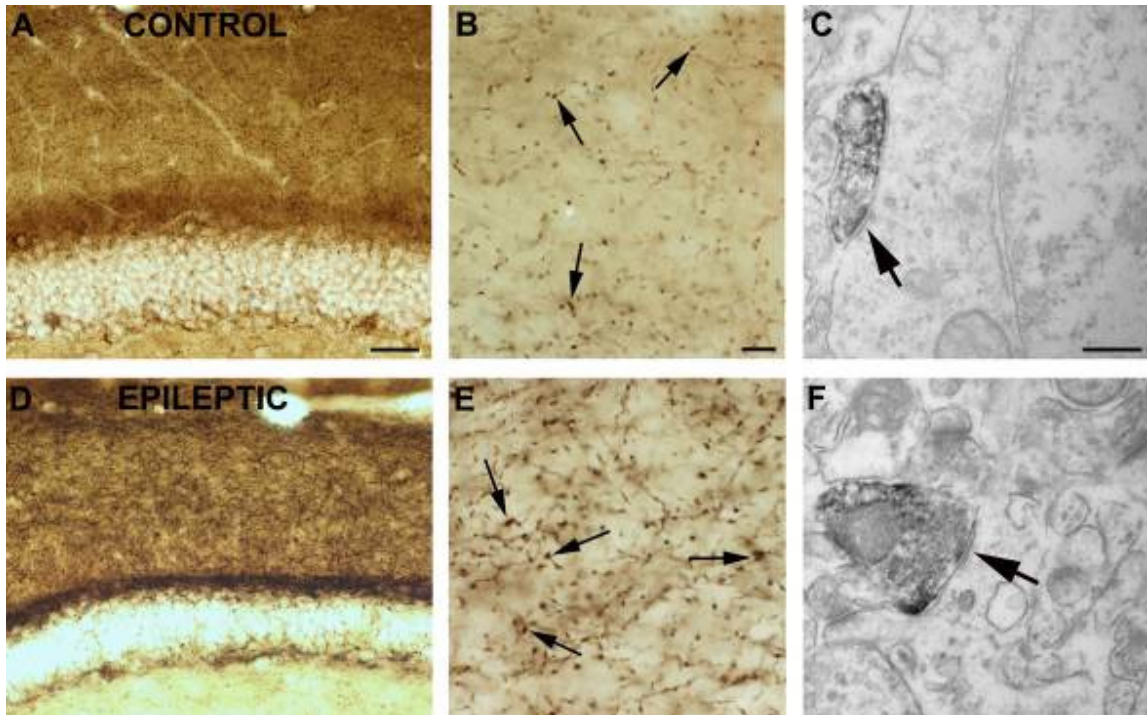
Figure 6: Demonstration of CB1-Rs at light and electron microscopic level in mice

CB1 immunostaining in the dentate gyrus of a control (A, B, C) and a "strong" epileptic (D, E, F) mouse. In control samples (A,B), dense staining of CB1-positive fibers can be found in the molecular layer of the DG. In the stratum moleculare of sclerotic animals (D, E) the intensity of CB1 immunostaining is elevated. The most frequent postsynaptic targets of CB1 receptor-positive terminals establishing symmetric synapses (arrows) are cell bodies (C) and dendrites (F) Scales: A,D: 200 μm; B,E: 50 μm; C,F:1 μm.

5.2.1. Target distribution of CB1-immunopositive elements in sclerotic mouse tissue

Quantification of CB1-immunopositive element's target distribution was carried out in the mouse model as well to examine whether the unchanged target distribution is human specific or not. Stratum moleculare of the dentate gyrus was studied in control and sclerotic animals, since the highest fiber density was observed in this area. Similar to controls and human tissue, CB1 receptors were localized in the membrane, outside the synaptic active zone (Nyiri et al, 2005). Both in controls (N=53) and sclerotic cases (N=48) the target

distribution of CB1-R immunopositive fibers was examined. Stained terminals established symmetric synapses mostly on dendrites (77.4 v.77.1%, spines 22.6 v.20.8% and cell bodies 0 v. 2.1 %) **(Graph 2)**. Thus, target distribution was not changed, similar to the human tissue.
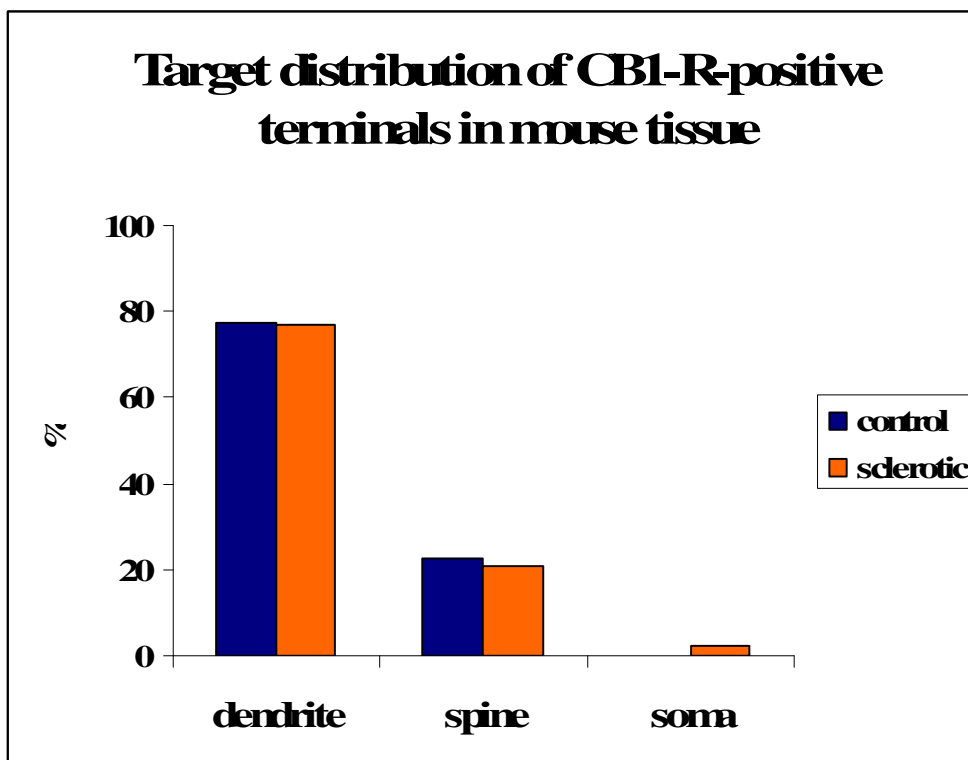
Graph 2: Target distribution of CB1-R-positive terminals establishing symmetric synapses in mouse TLE samples

The ratio of CB1-R-positive fibers synapsing on distinct neuronal elements does not change in the epileptic tissue compared to controls.

As the next step we carried out a more detailed investigation to reveal changes in the receptor protein expression in different phases of pilocarpine induced epilepsy (acute, latent and chronic). For this set of experiments we used an antibody staining CB1-R-positive symmetric and asymmetric synapses as well (see materials and methods).

5.3. Description of the pilocarpine model of epilepsy

5.3.1. The pattern of cell loss in pilocarpine induced epilepsy

To clarify the alterations of the hippocampal circuits on the pilocarpine model of epilepsy using CD1 mice, we carried out detailed investigation. Based on the behavioral signs during the acute seizures, animals were classified as "weak" or "strong" epileptic using the modified Racine scale (Magloczky et al, 2010; Racine, 1972; Turski et al, 1984). Animals showing seizure severity from Racine 1 to Racine 4 (shaking, chewing, nodding, forelimb clonus, rearing but no tonic-clonic seizures) were assigned to the weak group. However, in the strong group all animals showed tonic-clonic seizures (Racine 5) with other less severe seizure manifestations **(Fig. 7).** We examined the cell loss pattern in the hippocampi at different survival times using NeuN-immunostaining **(Fig. 8)**, GluR2/3-immunostaining **(Fig. 9)** Nissl staining **(Fig. 10)**. Since cell loss observed was similar in case of all three staining further on in the study, NeuN staining was used to determine cell-loss.

In the acute phase (2 hours after the treatment) cell loss was not observed neither in the weak nor in the strong animals, nor did signs of hippocampal reorganization occur (data not shown).

In the latent phase, (1-3 days post-pilocarpine) loss of sensitive interneurons (calretinin positive) and few principal cells could already be seen in the CA1 and CA3 regions (3 days) (not shown). Three days post pilocarpine, cell loss was usually patchy in the CA1-3; occasionally pyramidal cells disappeared in long segments of areas.

In the chronic phase, patchy cell loss was found infrequently in "weak" animals, but none of their hippocampi showed sclerosis **(Fig. 8B, 9B, 10B)**. In contrast, hippocampi of the "strong" mice showed sclerosis in most cases (70%) meaning that CA1 and CA3 regions were shrunken, atrophic and more than half of the cells were missing from the CA1 region. Loss of vulnerable interneurons was also observed in all regions **(Fig. 7) (Fig. 8C, 9c, 10C).** In our model calretinin-containing cells were used as a marker to monitor early cell death, since these cells were the most sensitive to epileptic insult (not shown) (Magloczky & Freund, 2005; Toth et al, 2010) .

40

Based on the severity of cell death, the degree of damage affecting different subregions (CA1, CA3, dentate gyrus) was classified as type 1 (mild cell loss), type 2 (patchy cell loss) and type 3 (sclerotic), defined according to the following semiquantitative scale: type 1, up to 10% of the cells are damaged; type 2, 11-50% of the cells are missing; type 3: more than 50% of the cells are missing. CA1 and CA3 were considered sclerotic when cell loss exceeded 50 %, especially when strata oriens, pyramidale and radiatum could not be separated any more (Magloczky & Freund, 1993; Magloczky & Freund, 1995) **(Fig 4)**.

Statistical analysis revealed a significant correlation (Pearson correlation) between the degree of cell-loss and seizure strength in Racine scale values ($p < 0.05$) (105 animals) **(Fig. 7)**. Thus, behavioral signs of the acute seizures could be used to predict the degree of cell loss in the chronic phase.
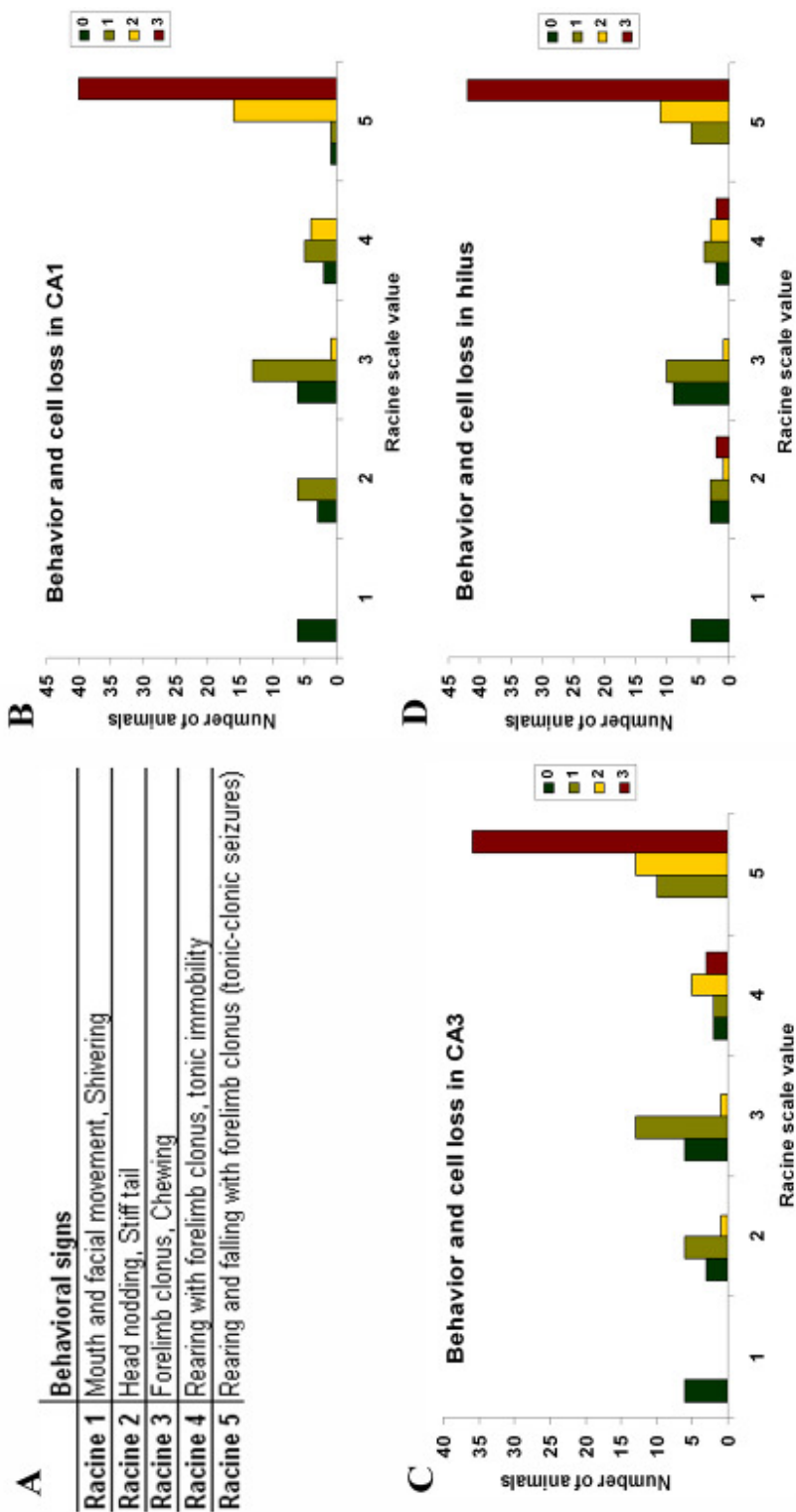
Figure 7: Correlation between behavioral signs and cell loss.

Table A describes seizure behavioral scoring for each Racine scale value. Graphs B, C and D show the correlation between seizure intensity (Racine scale value) and cell loss (color code indicates cell loss from 0 to 3, where 0 refers to no cell loss, 1: cell-loss under 10 %, 2: cell-loss between 10% and 50%, 3: cell-loss above 50%) in CA1, CA3 and the hilus respectively. Correlation between Racine scale value and cell loss in the regions proved to be significant using Pearson correlation ($p < 0.05$)
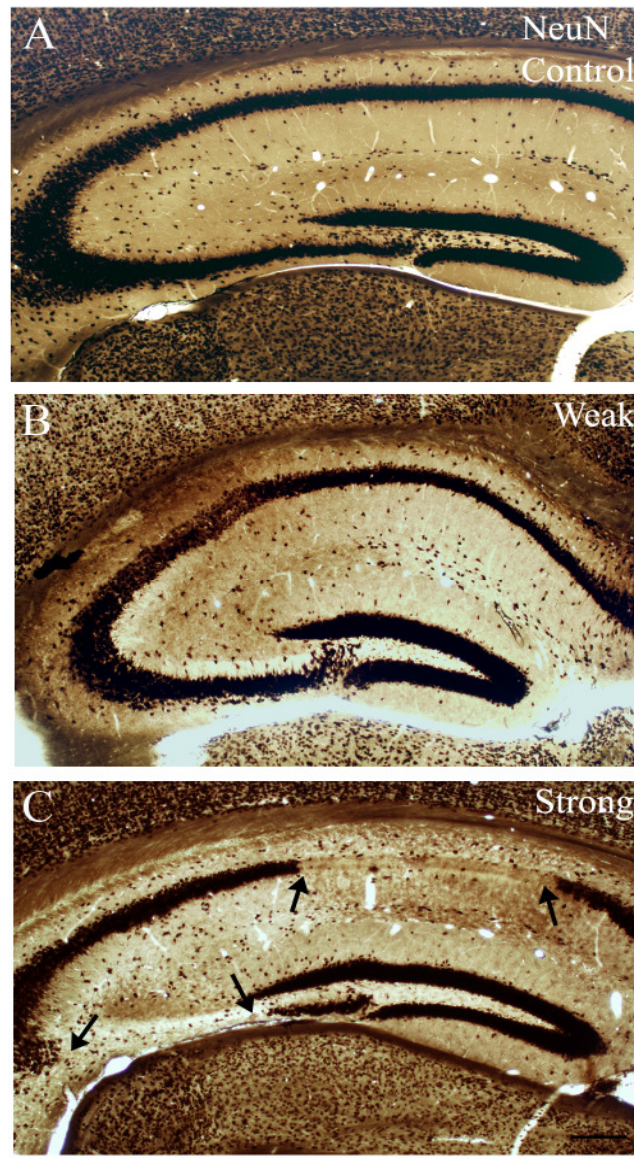
Figure 8: Pathological changes in pilocarpine induced epilepsy with NeuN immunostaining

Light micrographs of control (A) and epileptic (B, C) animals immunostained for NeuN. Animals survived for 1 month after pilocarpine treatment. Compared to control mice (A), in non-sclerotic „weak" animals (B) only mild, restricted changes are seen in the hippocampus occasionally. In the sclerotic hippocampi of "strong" animals (C) a characteristic pattern of neuronal damage appears. The principal cell loss is over 50% (sclerosis) mostly in CA1 and CA3 (arrows) and in the hilus. Scale: 200µm
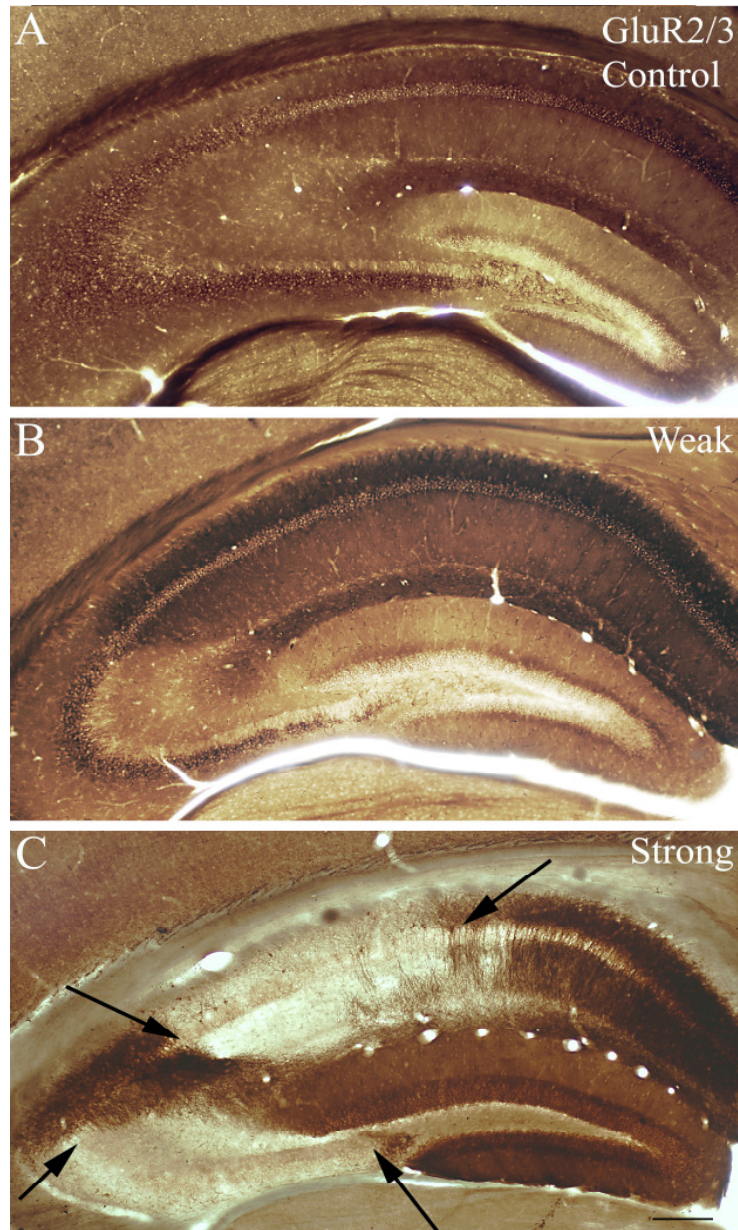
Figure 9: Pathological changes in pilocarpine induced epilepsy with GluR2/3 immunostaining

Light micrographs of control (A) and epileptic (B, C) animals immunostained for GluR2/3. Animals were sacrificed in the chronic phase of epilepsy (1 month post pilo). Compared to control mice (A), in non-sclerotic „weak" animals (B) no mass cell loss occurs. In the sclerotic hippocampi of "strong" animals (C) however, robust cell loss (principal cell loss above 50%) appears affecting the CA1, CA3 regions (arrows) and the hilus. Scale: 200µm
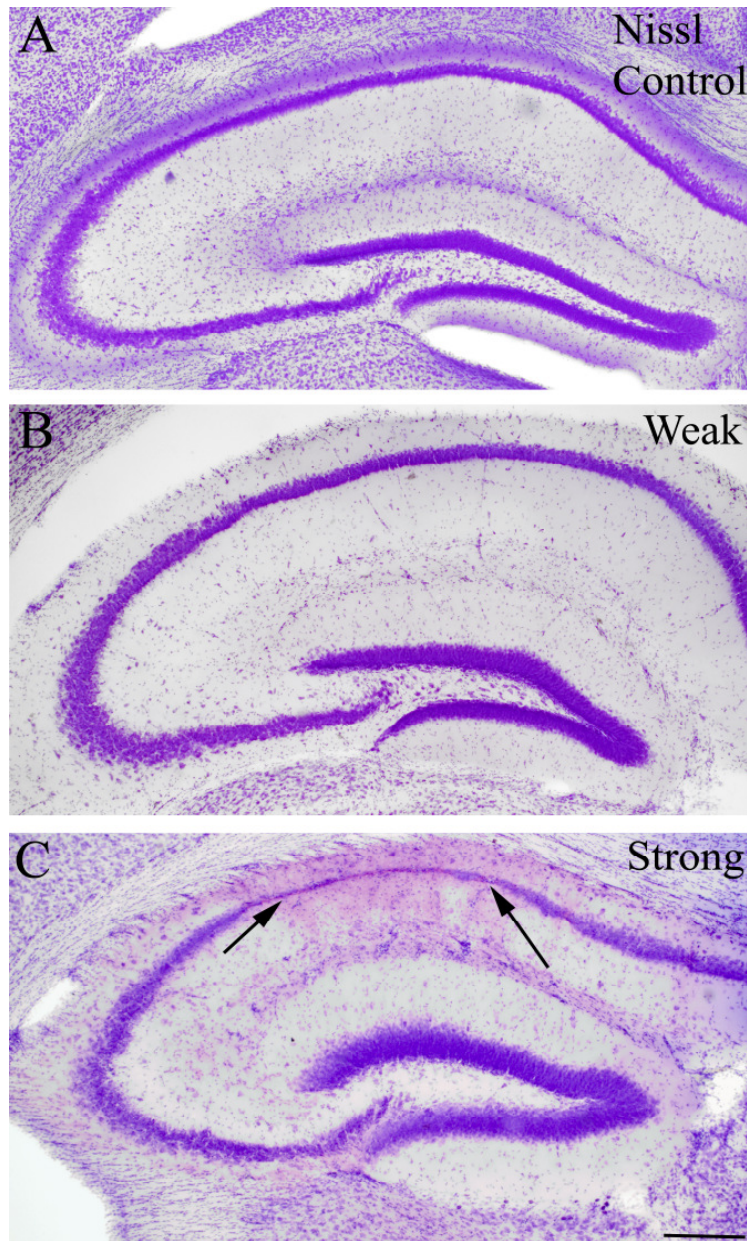
Figure 10: Anatomical changes in pilocarpine induced epilepsy with Nissl staining

Light micrographs of control (A) and epileptic (B, C) animals with Nissl staining. Animals were sacrificed 1 month after pilocarpine treatment. In control (A) and non-sclerotic „weak" animals (B) no considerable difference can be seen. In contrast, the hippocampi of "strong" animals (C) shows typical signs of sclerosis, robust neuronal damage appears affecting the CA1 (white arrows), however, less severe cell loss occurs in the hilus. Scale: 200µm

5.3.2. In vivo electrophysiological recordings

To prove the appearance of epileptic activity and recurrent seizures, EEG recordings were carried out in 16 mice (6 controls, 4 weakly and 6 strongly epileptic) in the chronic phase. On the basis of these recordings, the EEG activity of pilocarpine treated mice differed from controls **(Graph 3, Figs. 11,12,13)** considerably. Strong synchronization and numerous interictal spikes were seen separately or in clusters. In members of the weak group **(Fig. 12)** recurrent seizures were rarely seen (in 1 mouse out of 4), while interictal spikes (incidence 2.2 ± 2.26Hz, amplitude $581\pm160\,\mu$V) occurred in all cases. In members of the strong group recurrent seizures appeared (ictal spikes with a frequency of 5.9 ± 2.3Hz, amplitude $546\pm112\,\mu$V) in nearly every animal (5 out of 6) **(Fig 13)**. Thus, the occurrence of recurrent seizures in the chronic phase showed strong association with the severity of acute seizures **(Graph 3)**.

One month after pilocarpine injection in 4 animals (2 controls, 2 strong) 24 hours long EEG monitoring was carried out to investigate nocturnal epileptic activity. We observed seizure activity in the EEG represented by spikes in all animals. No animals showed exclusively nocturnal seizures, but they performed recurrent seizures during the whole day. Seizure incidence was the highest in the afternoon compared to other periods of the day.
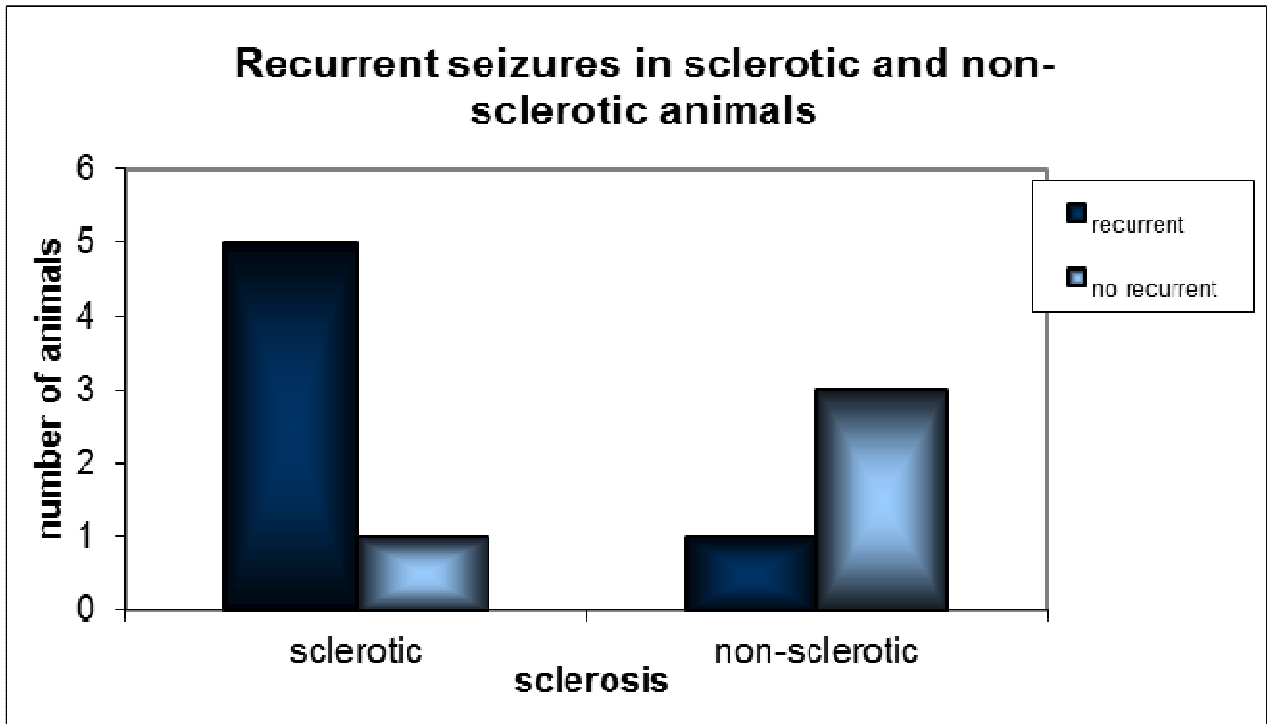
Graph 3: Correlation of cell loss and the existence of recurrent seizures

In pilocarpine treated animals recurrent seizures occurred in most strong animals. After perfusion and immunostaining these animals turned out to be sclerotic. In contrast, in pilocarpine treated animals not showing recurrent seizures sclerosis was rarely found, suggesting a link between sclerosis and the occurrence of recurrent seizures.
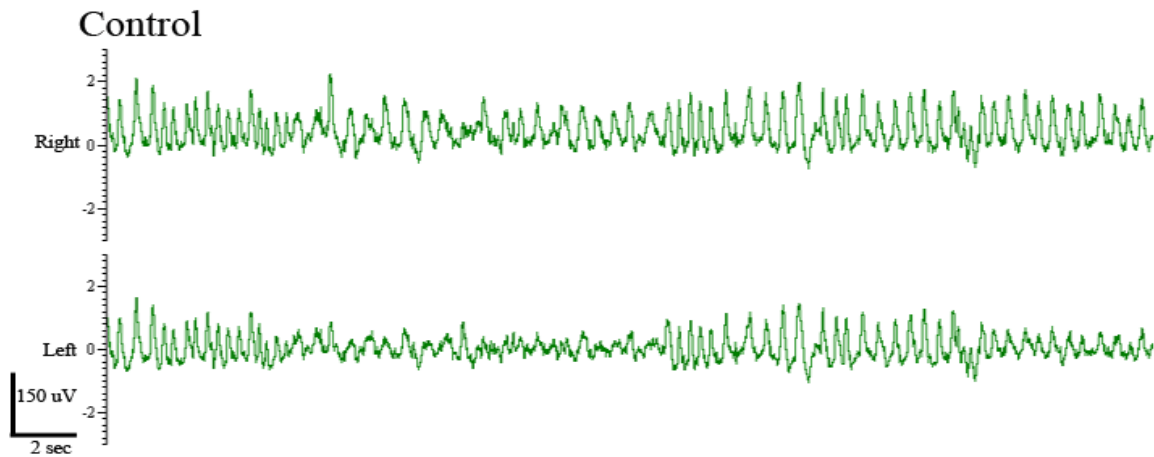
Figure 11: Properties of EEG recording from control mice

In the EEG recordings of control animals no ictal or interictal activity occurs, animals were sleeping quite often during the recording. Higher and lower amplitude activity was seen consecutively.
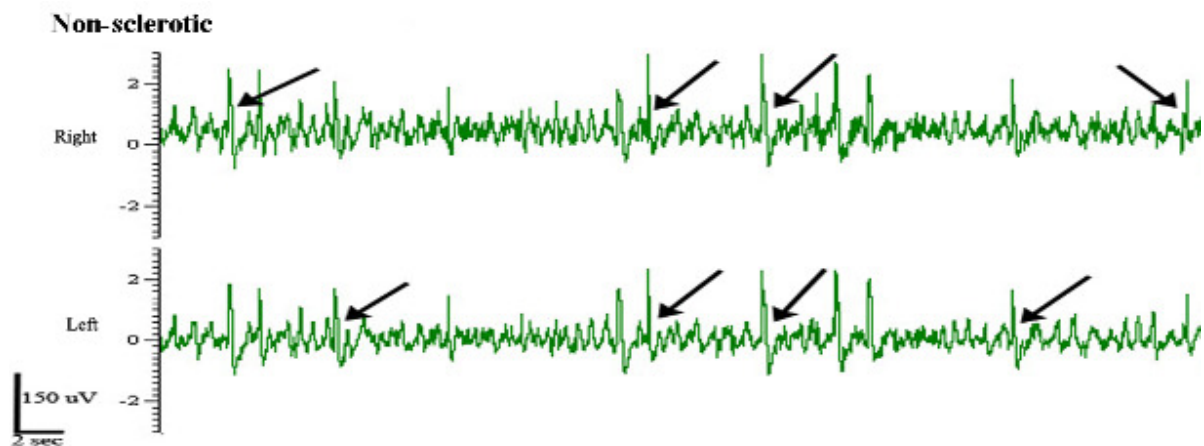
Figure 12: Physiological changes in non-sclerotic animals in pilocarpine induced epilepsy

The EEG recording of "weak" animals 1 month after pilocarpine treatment differs from control EEGs. In case of these animals interictal spikes (arrows) occur frequently, however ictal events were hardly ever seen.
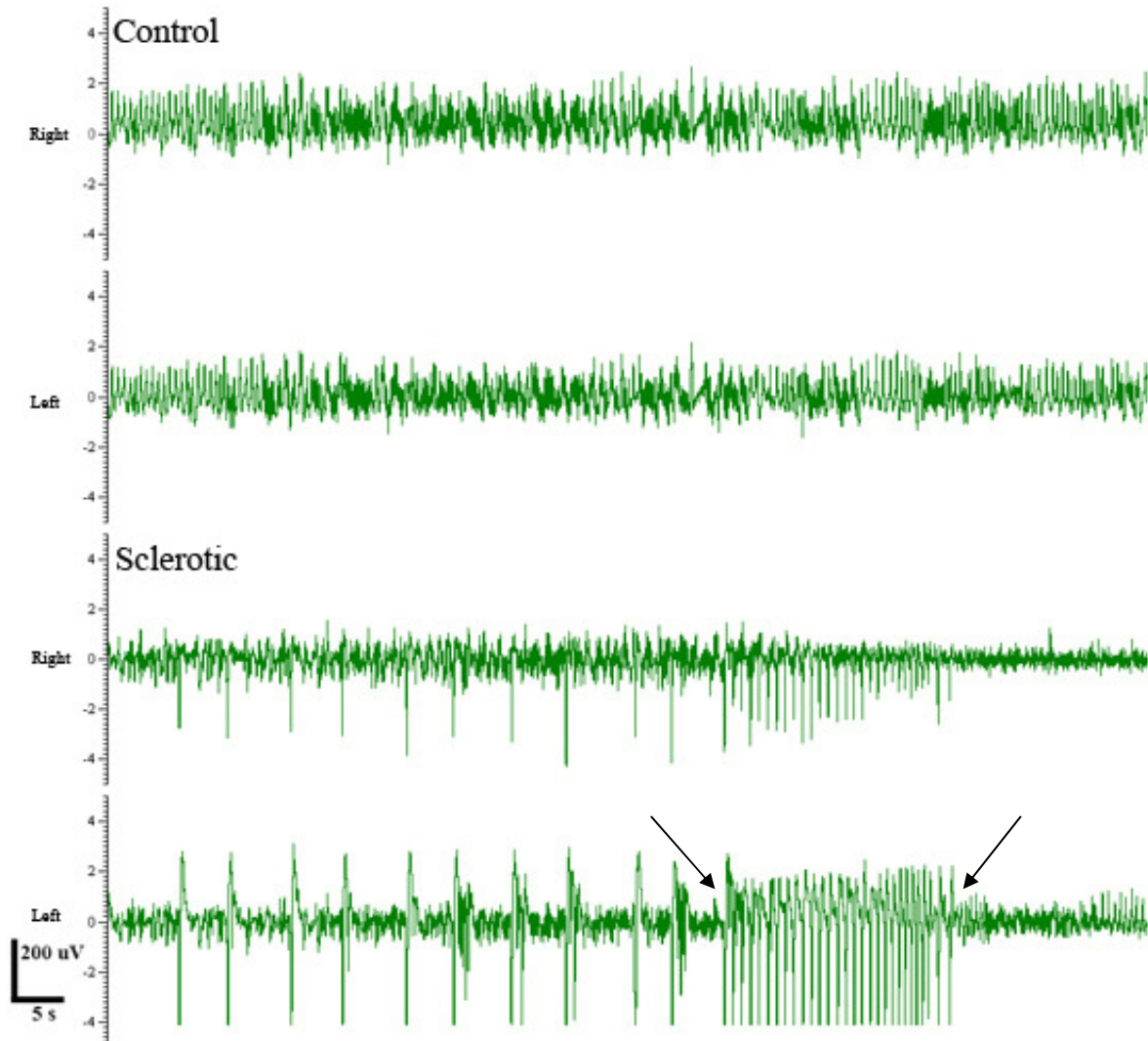
Figure 13: Physiological changes in pilocarpine induced epilepsy

Animals survived for 1 month after pilocarpine treatment. Compared to the EEG recordings of control animals in strong mice an increased activity appears. In these animals recurrent seizures are observed in most cases, both interictal and ictal (arrows) activity appears. An increase in frequency and decline in amplitude can be seen immediately preceding and after the seizures.

49

5.3.3. Anatomical changes in the acute phase of epilepsy (2 hours)

We examined potential changes with several markers that may indicate the presence of very early cell loss (CR), degeneration (Gallyas) or excitotoxic damage (HSP72). However, none of the mentioned markers pointed out cell loss in any cases, thus we concluded, that degeneration and mass cell loss is not a direct consequence of acute seizures themselves.

5.3.4. Morphological changes in the latent phase of epilepsy (1, 3 days post pilo)

To examine whether morphological differences between animals with strong or weak seizures occur at an early time point, immunostaining against Heat Shock Protein 72 (HSP72) was carried out to visualize cells suffering from excitotoxic damage, since this protein confirms the emergence of abnormal proteins due to various damaging effects (Gass et al, 1995; Lowenstein et al, 1990; Magloczky & Freund, 1995).
In control hippocampi **(Fig. 14A)** immunostained cells were never seen, light background staining appeared occasionally in the layers of principal cells.

However, in the acute phase of epilepsy (2 hours after injection) no significant alteration was observed with HSP72 immunostaining, the hippocampi of both weak and strong animals were control-like (data not shown).

In the latent phase positive cells were not seen in weak epileptic animals **(Fig. 14B)**, however, in members of the strong group robust changes occurred 1 day after the induction of the seizures **(Fig. 14C)**. Principal cells with Golgi-like HSP72-staining appeared occasionally in mossy cells of the hilus **(Fig. 15A)** in some granule cells in the dentate gyrus **(Fig. 15B, D)** and in the str. pyramidale of the CA3 **(Fig. 15C)**. Occasionally few immunopositive cells were seen in the CA1 str. pyramidale as well (not shown).
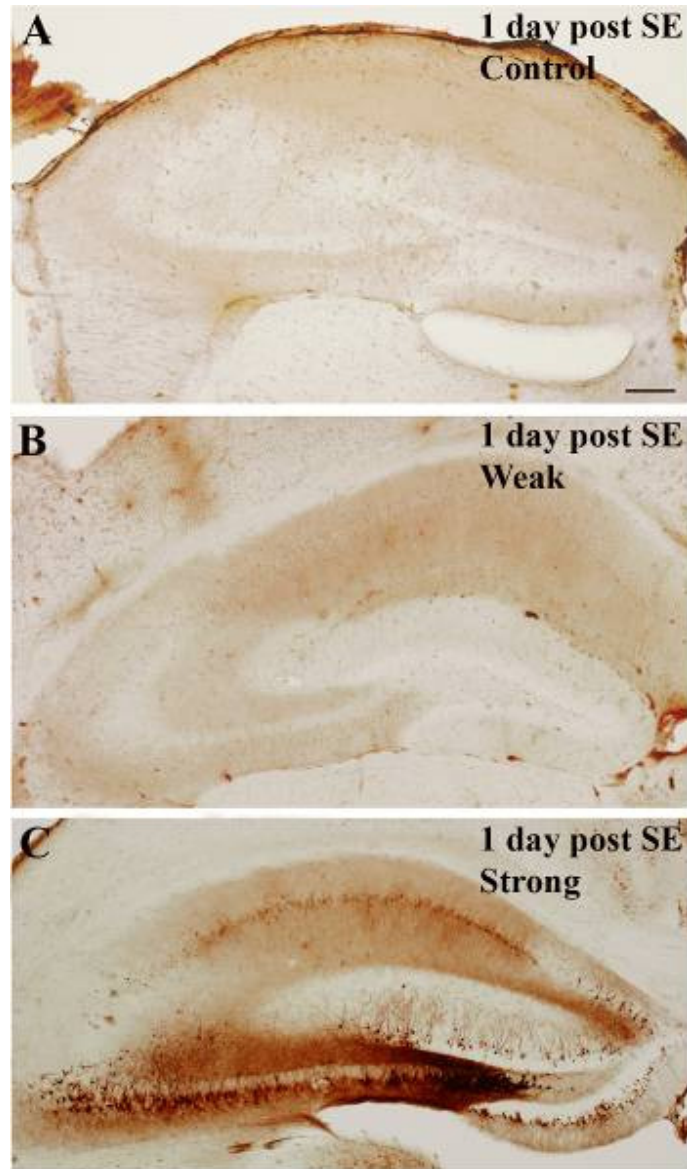
Figure 14: Demonstration of excitotoxic insult 1 day after pilocarpine treatment

In animals of the "weak" group (B) HSP72-immunostaining is control-like (A), only a slight increase in background-staining can be seen, but no stained cells with processes appear. Although there are no morphological signs of neuronal degeneration at this early stage in the hippocampi of "strong" epileptic animals (C), the vulnerable cells as well as the resistant granule cells start to express HSP72, and are stained in a Golgi-like manner. Faint homogeneous staining of CA1 pyramidal cells can also be seen. Scale: 200μm
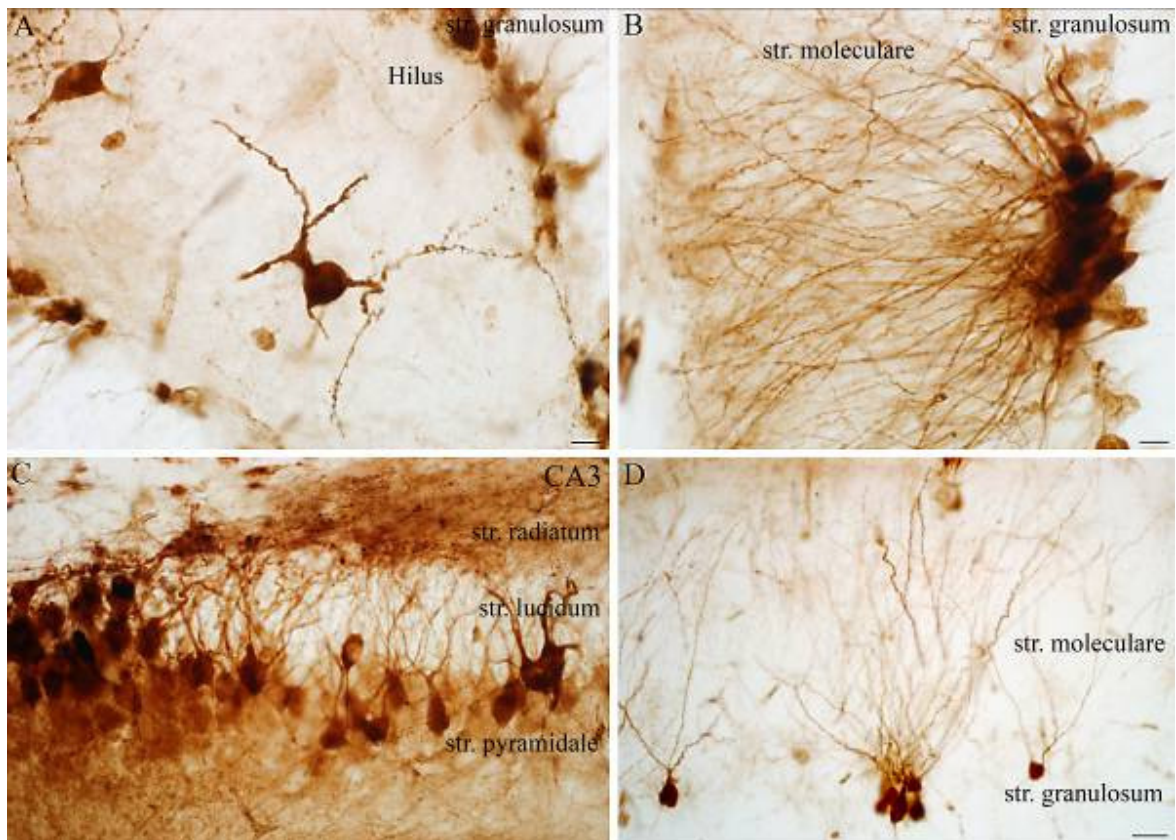
Figure 15: HSP72 expression of distinct cell types 1 day after pilocarpine treatment

In strong animals 1 day after status epilepticus, Mossy cells of the hilus (A) express HSP72 in the soma and processes. Similar Golgi-like staining can be seen in numerous granule cells (B, D). Even though, mass principal cell loss is not observed, several CA3 pyramidal cells express the protein. Scale: 50µm

53

Three days after pilocarpine treatment weak samples displayed the same appearance seen in controls **(Fig. 16A, B)**, with a modest increase in background staining. In contrast, in the hippocampi of strongly epileptic animals a marked increase in HSP72 expression was found in CA1 pyramidal cells **(Fig. 16C, 17C)**, and in the mossy cells of the hilus **(Fig. 17 A, C)**. Three days post pilocarpine fewer granule cells were stained compared to samples 1 day after pilocarpine **(Fig. 17B)**, yet granule cells did not degenerate, indicating that cells expressing HSP72 may survive the insult.
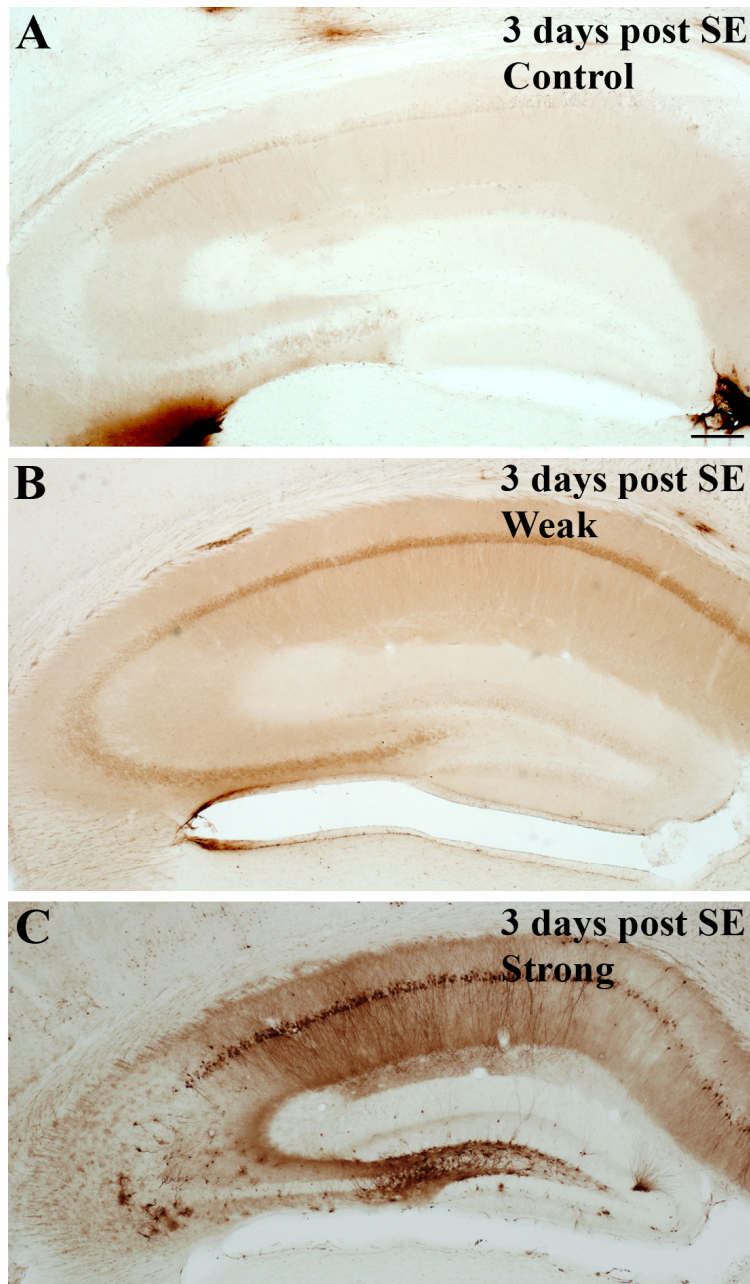
Figure 16: Degeneration of hippocampal cells 3 days post pilocarpine

In the control (A) tissue no HSP72-positive elements can be seen, only a light background staining appears. Similarly, in the hippocampi of weak animals (B) only a slight increase in background-staining occurs. In contrast, in tissue from the strong animals, HSP72 is heavily expressed in a large population of pyramidal cells (C) and in some mossy cells, indicating that they were exposed to excitotoxic insult. Scale: 200 µm
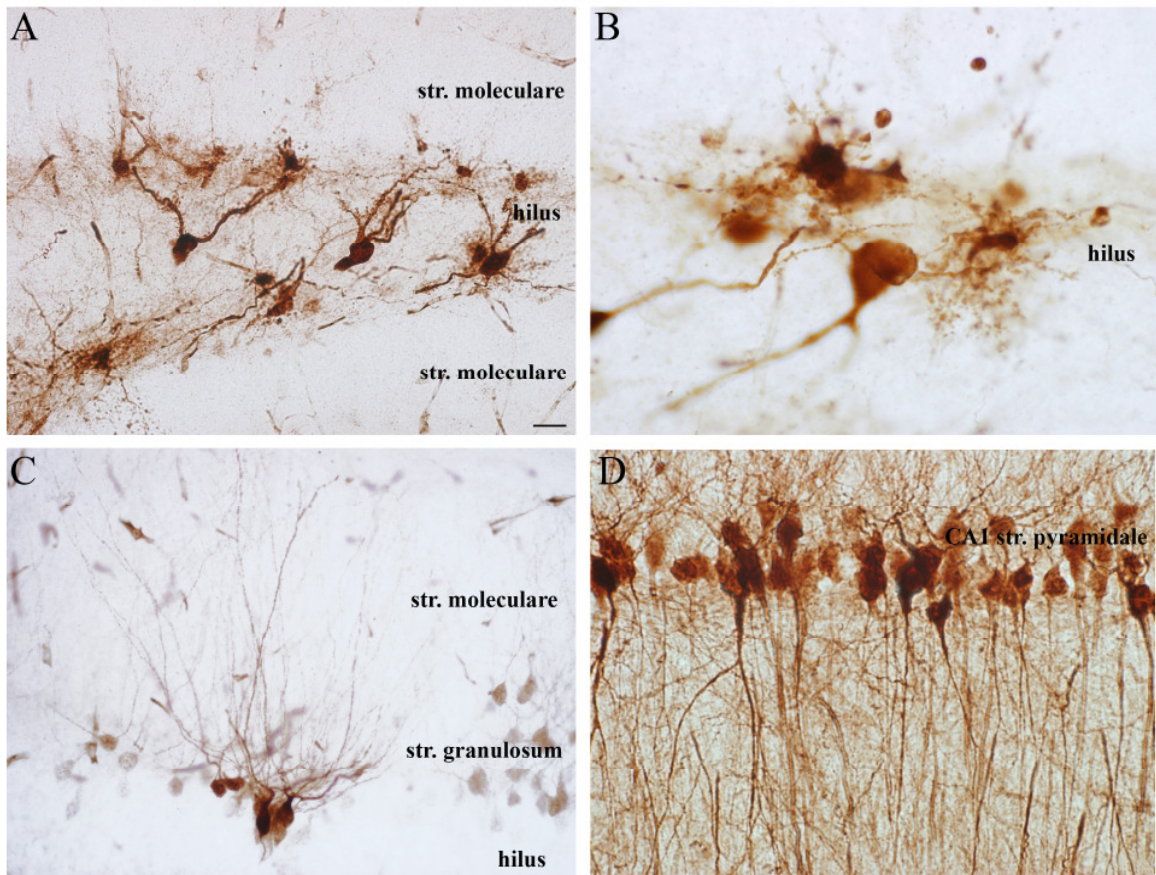
Figure 17: Degeneration of principal cells and interneurons days 3 post pilocarpine

3 days after pilocarpine injection Golgi-like stained mossy cells (A, B) appeared in the hilus with numerous stained processes (dendrites, spines, and thorny excrescences). Some granule cells (C) appeared to be positive as well, but less in number than in samples 1 day after the treatment. In addition, granule cells did not degenerate, which indicates, that HSP72-expression does not signal irreversible damage. In the CA1 region numerous principal cells (D) expressed HSP72 in a Golgi-like manner. Scale: 50 µm

These results prove that cellular differences can be seen between animals with different acute behavior; validating our classification into "weak" and "strong" groups. Irreversibly damaged cells were visualized with Gallyas silver impregnation **(Fig. 18, 19)** during this reaction silver binds to abnormal proteins; therefore, irreversibly damaged cells accumulate silver granules, in contrast to other living cells with red/orange staining.

One day after pilocarpine injection no visual changes could be seen in weak animals compared to controls **(Fig. 18A, B)**. In the strong animals most regions of the hippocampus appeared to be control-like, however, a dark silver deposit was present in hilar neurons undergoing argyrophilic degeneration **(Fig. 18C, D)** and occasionally in stratum oriens of the CA1 **(Fig, 18E)** or CA3 **(Fig. 18F)** pyramidal cells.
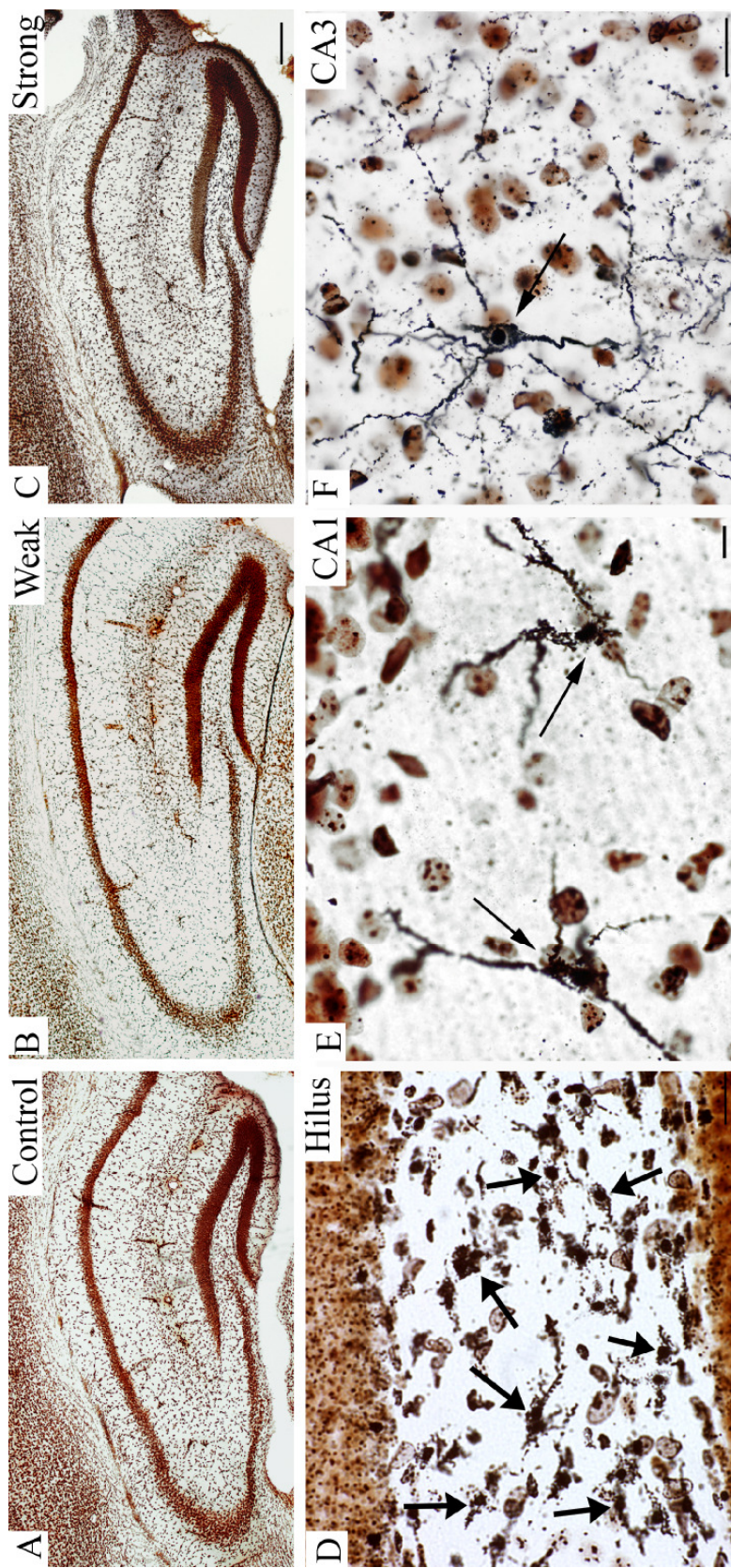
Figure 18: Demonstration of excitotoxic cell death 1 day after pilocarpine treatment

In animals of the "weak" group (B) Gallyas-staining remained control-like (orange cells are healthy) (A), with very few cells degenerating. Though 1 day post injection is a quite early stage of epilepsy, in the hippocampi of "strong" epileptic animals (C, D, E, F) degenerating cells appeared. Dark silver deposit was present in neurons irreversibly damaged. Cells with degenerated processes and accumulating silver densely appear mostly in the hilus (D), however, other vulnerable cells could be seen in str. oriens and str. radiatum or CA1 (E) and CA3 (F). Scale: A, B, C: 200μm; D, E, F: 50 μm

Three days after pilocarpine administration, Gallyas-staining was control-like in weak animals **(Fig. 19A, B)**; however, in strong animals cell-loss was quite severe compared to that in animals 1 day after pilocarpine injection **(Fig. 19C)**. Silver accumulation appeared in additional subregions; besides stratum oriens, numerous degenerated, shrinked cells or dendrites were present in strata pyramidale and radiatum of the CA1 **(Fig. 19D)** and CA3 **(Fig. 19E)** moreover, several degenerating somata and dendrites appeared in the hilus **(Fig 19F)**.
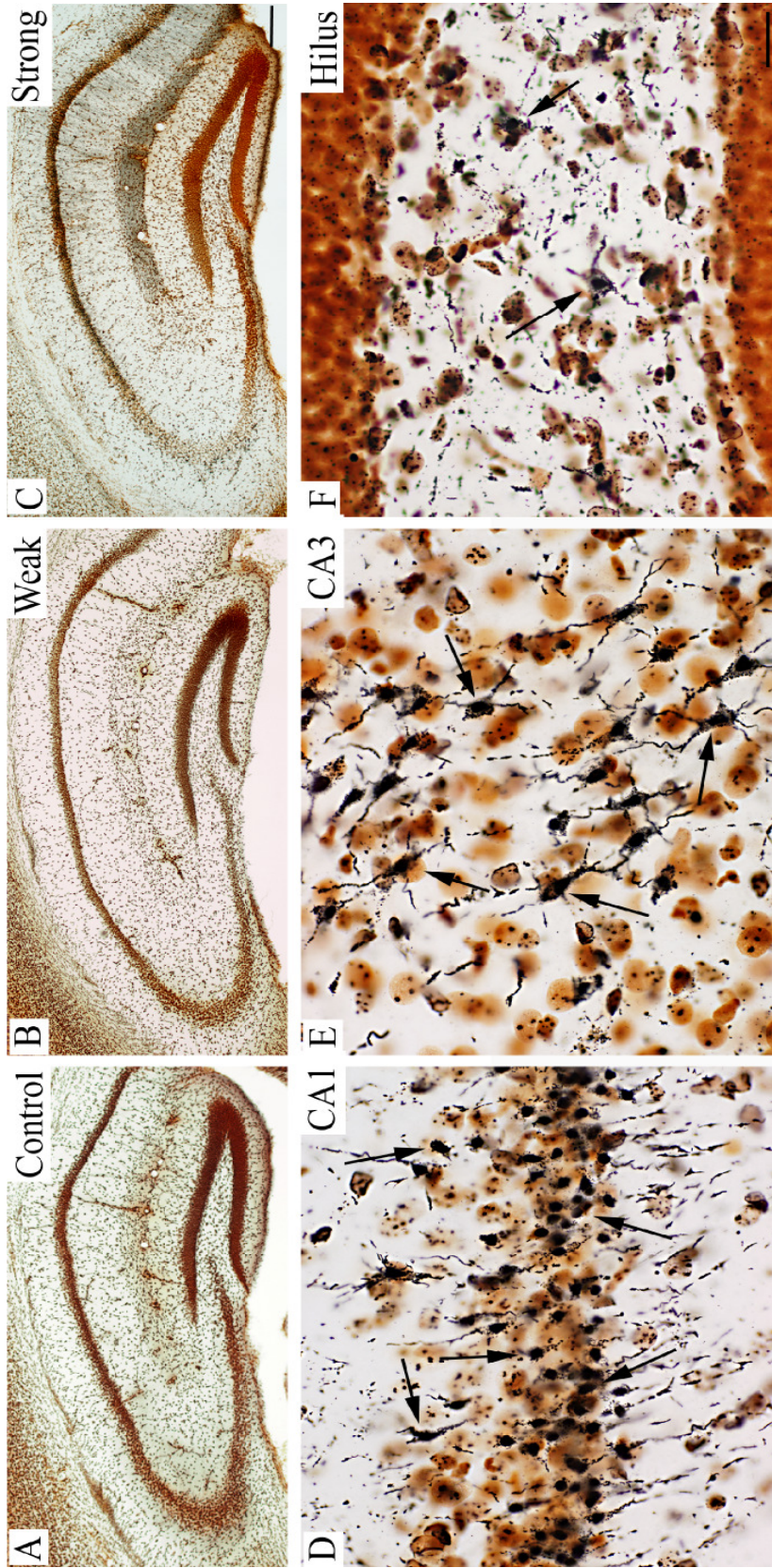
Figure 19: Demonstration of excitotoxic cell death 3 days post pilocarpine

Gallyas silver impregnation reveals that 3 days after pilocarpine administration, the hippocampi of weak (B) animals remain control-like (A). However, in strong animals principal cell loss begins at a large scale (orange cells are alive, black are degenerating). (C, D, E, F). Argyrophilic cell degeneration can be seen in the vulnerable regions of the hippocampus, like the CA1 and CA3 pyramidal cell layer (D, E) and the hilar region (F) (arrows). Scale: A, B, C: 200 µm, D, E, F: 50 µm

5.4. Analysis of CB1-R distribution in different phases of pilocarpine-induced epilepsy

5.4.1. Distribution of CB1 receptors in control tissue

In control samples intense CB1-R immunostaining was found throughout the hippocampus **(Fig. 20A)**. Immunopositive cell bodies of interneurons were seen in all hippocampal subfields, mostly in strata radiatum and lacunosum-moleculare of CA1 and CA3, as well as at the border of the hilus and in the inner molecular layer of the dentate gyrus. These cells are known to be CCK-positive as well (Katona et al, 1999b) and are dendritic or perisomatic targeting interneurons (Freund & Buzsaki, 1996). Intense staining of CB1-R-positive fibers was found in stratum pyramidale of the cornu Ammonis **(Fig. 20 B, C)** and in the molecular layer of the dentate gyrus (DG) **(Fig. 20C)**. The most intense staining appeared in the inner third of str. moleculare where the terminals of mossy cells can be found (these terminals express great amount of CB1-R protein). In contrast, less dense labeling was observed in the strata lucidum **(Fig. 20C)** and granulosum **(Fig. 20D)** (Haller et al, 2007; Katona et al, 2006; Matyas et al, 2004)
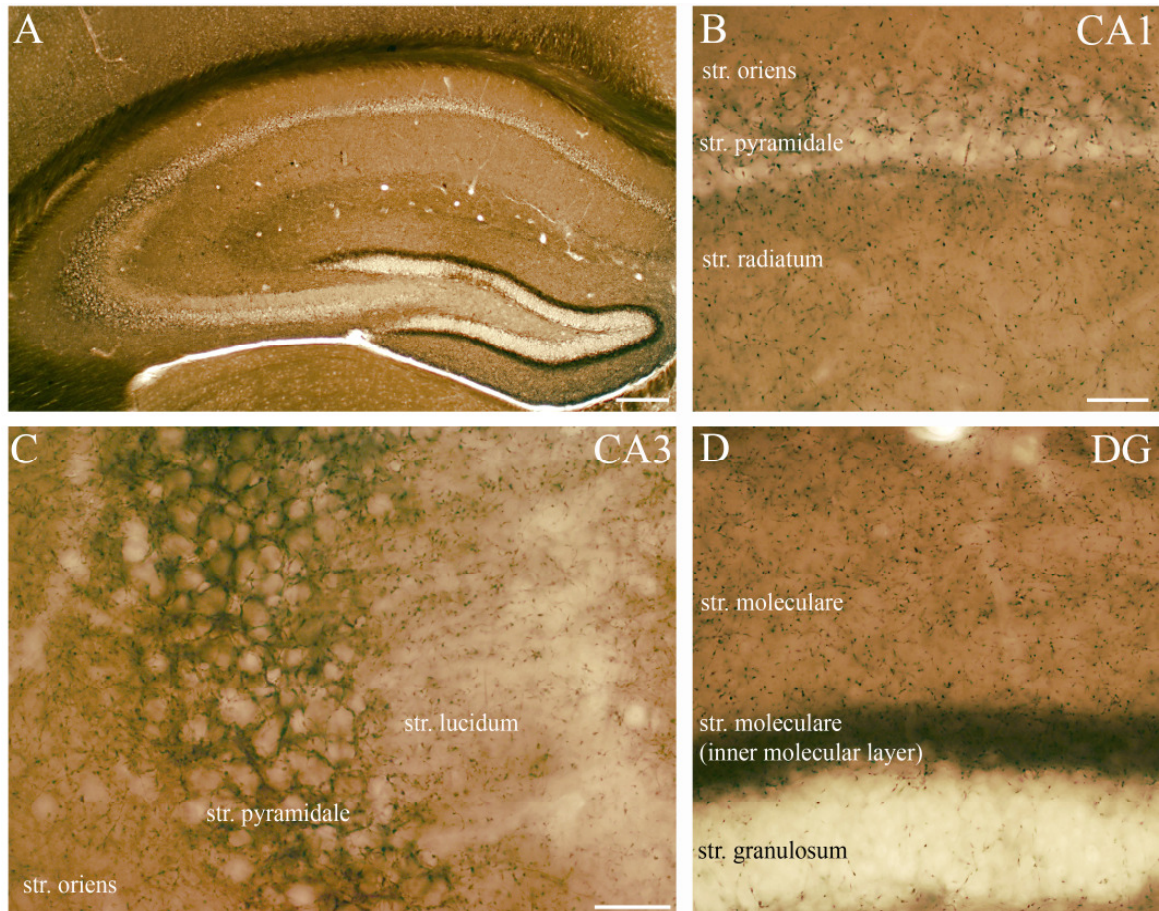
<u>Figure 20: Distribution of CB1-Rs in control hippocampus</u>

In control tissue CB1 receptors were found throughout the hippocampus (A). Pyramidal layers of CA1 (B), CA3a (C) and the inner molecular layer of str. moleculare (D) were strongly labeled due to intensely stained terminals. Less intense staining was found in dendritic regions like strata oriens, radiatum and lacunosum-moleculare, and pyramidal layer of CA3 b and c. In contrast, very light staining occurred in str. lucidum (C) and str. granulosum D). Scale: A: 200µm, B, C, D: 50 µm.

At the electron microscopic level numerous immunopositive axon terminals were found forming symmetric or asymmetric synapses. Immunogold particles indicating the presence of CB1-Rs was located predominantly perisynaptically and presynaptically (typically in terminals) as described earlier (Katona et al, 1999a; Nyiri et al, 2005).

5.4.2. Distribution of CB1 receptors in the acute phase of epilepsy (2 hours)

In the acute phase, epileptic hippocampi from members of the weak group showed control-like phenotype: no major changes were seen in the distribution and density of immunolabelled elements. Compared to controls **(Fig. 21A, C)**, in tissue from the strong group a robust decrease in immunopositivity was observed throughout the hippocampus, namely, the dense axonal meshwork seen in the strata moleculare, radiatum and oriens of controls was substantially reduced **(Fig. 21B, D).** Moreover, CB1-R immunopositive boutons forming baskets in the principal cell layers could hardly be seen at light microscopic level **(Fig. 21B)**. In this phase a global downregulation of the protein appeared.
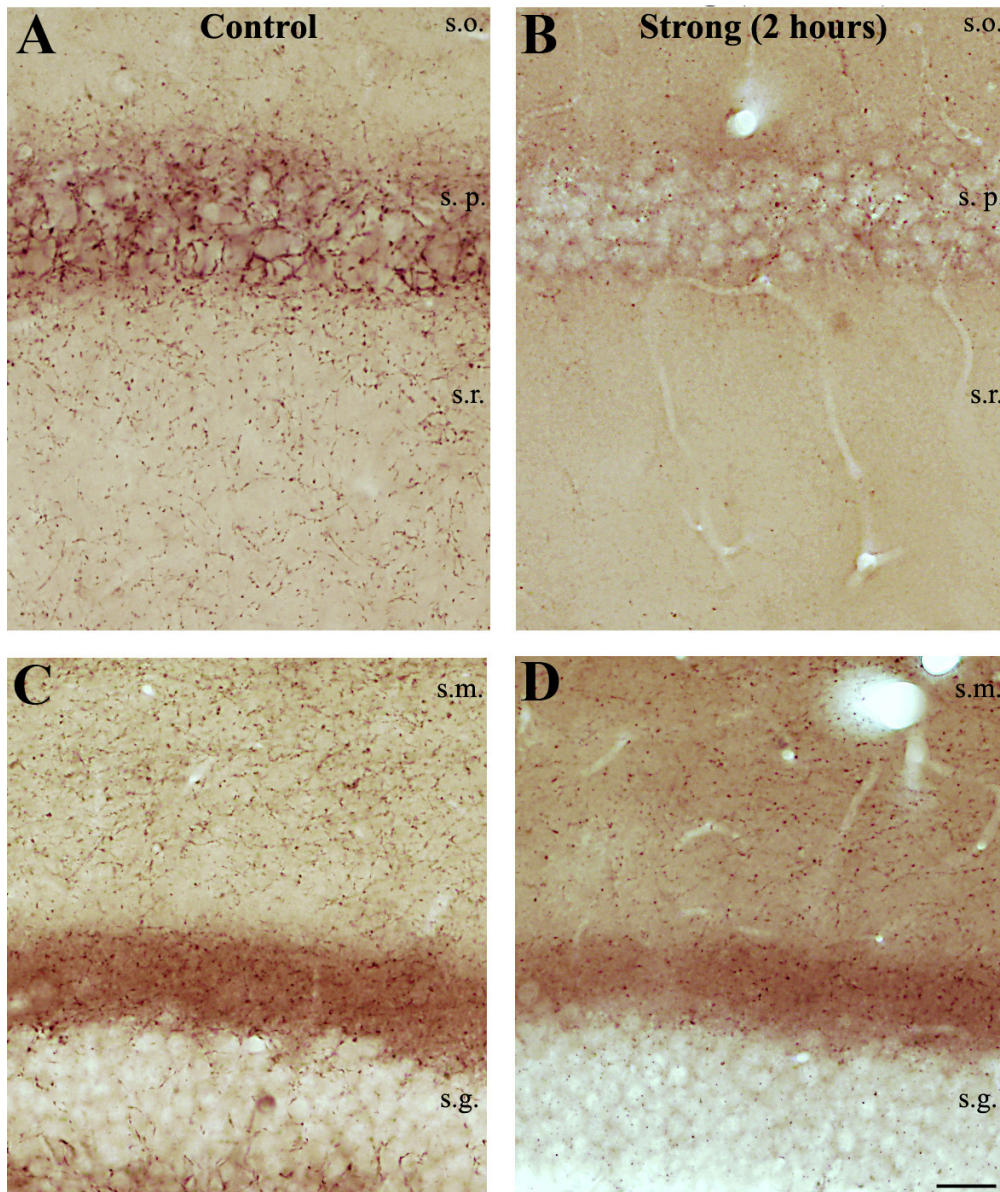
Figure 21: Changes of CB1-R-staining in the acute phase

In control samples intense staining of CB1-R-positive fibers can be seen in CA1 stratum pyramidale and radiatum (A) and in the molecular layer of the dentate gyrus (C).

In the acute phase of epilepsy (2 hours after pilocarpine injection) the hippocampi of strongly epileptic animals show decrease of CB1-R staining (B, D) compared to controls (A, C). The change is more remarkable in CA1 than in the DG, where the faint diffuse staining of the inner str. moleculare is hardly affected. Scale: 50 μm

5.4.3. Reversible changes in CB1-R expression in acute slices (2 hours post pilo)

To investigate the electrophysiological correlates of our anatomical findings observed in acute phase, we planned to record the effects of CB1–R activation on hippocampal function. *In vitro* slices were prepared from the hippocampi of control and strongly epileptic animals. As a first step, immunostaining for CB1-Rs was carried out on the slices at two time points: immediately fixed after the slice cut and after 2 hours of incubation in an interface-type holding chamber. Surprisingly, we observed that after 2 hours of incubation, slices from strongly epileptic animals showed control-like distribution of CB1-Rs **(Fig. 22A, C,** and **D)**. However, when slices from the same animals were immediately fixed after cutting, a similar decrease in CB1-R distribution was found as seen in perfusion fixed animals (compared to controls) **(Fig. 22B)**.
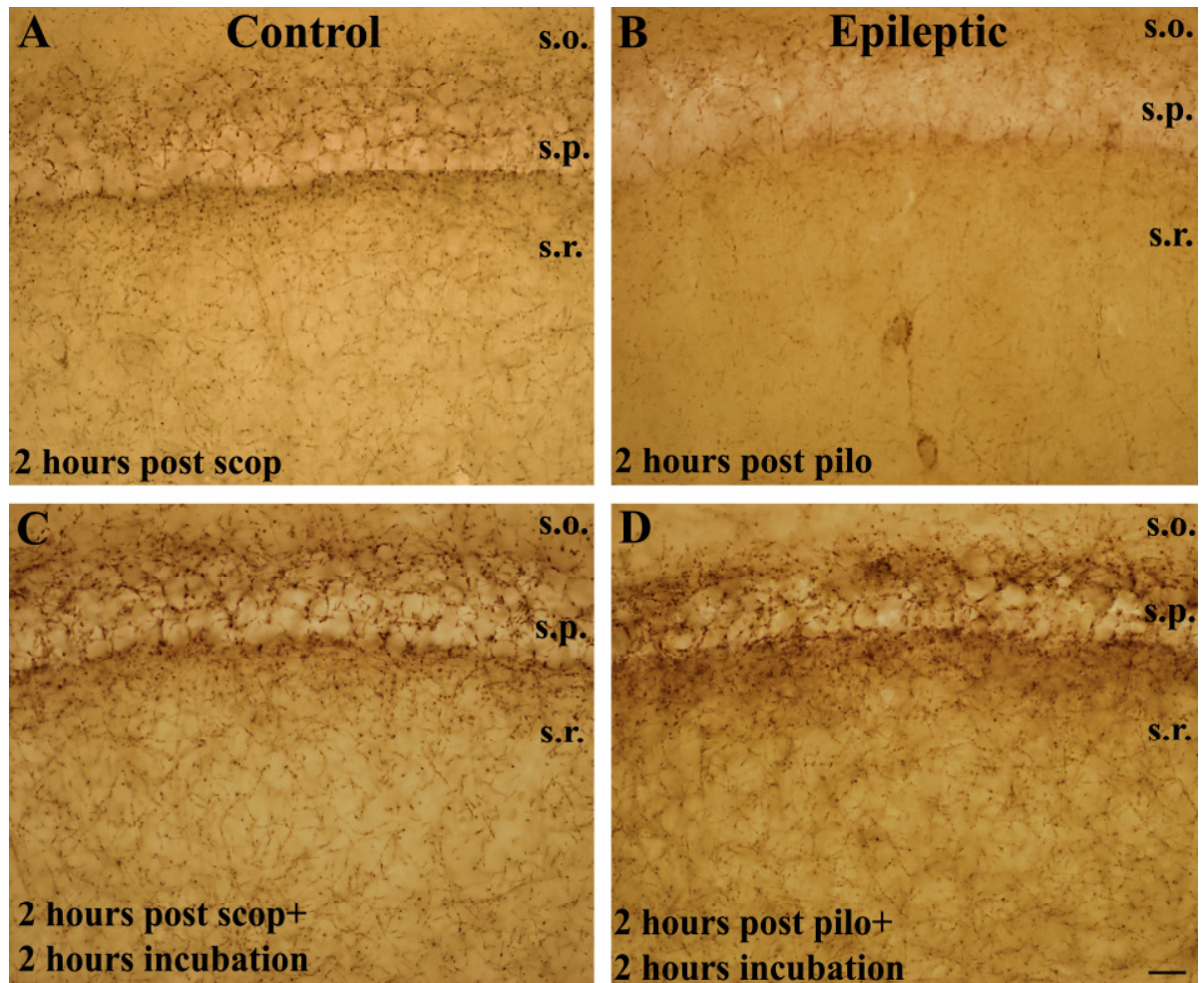
Figure 22: Reversible changes in CB1-R-staining in slice preparation (acute phase)

In CA1 region of surviving brain slices 2 hours post pilocarpine a massive decrease is seen in CB1-R staining in strongly epileptic animals (B) compared to scopolamine treated controls (A) as it was seen in perfusion-fixed epileptic animals. In contrast, the slices from the same animals which were incubated in ACSF for an additional 2 hours the CB1-R staining in the epileptic tissue (D) did not differ from control slices (C). Scale: 50 µm

These data suggest that under our circumstances the consequences of the acute phase on hippocampal CB1-R function cannot be studied using in vitro slice preparations, since the changes in CB1-R distributions after acute seizures recovers within the incubation time that has to precede recording.

Since functional consequences of CB1-R decrease could not be established with *in vitro* methods, we studied the seizures of animals *a priori*, lacking CB1-Rs (CB1-R knock-out animals).

5.4.4. Increased mortality after seizures in CB1 KO animals

We addressed the question how seizure susceptibility changes in CB1-R knock out mice, therefore 22 controls were examined, 22 CB1-R knock out animals and 21 wild type littermates were injected with pilocarpine in a different set of experiments. CB1-R KO animals received very intense seizures (typical for strong epileptic animals) they were more susceptible to epilepsy as only 3 animals had mild seizures out of 22 and all 19 animals showing strong seizures died in 15 minutes **(Graph 4)**.
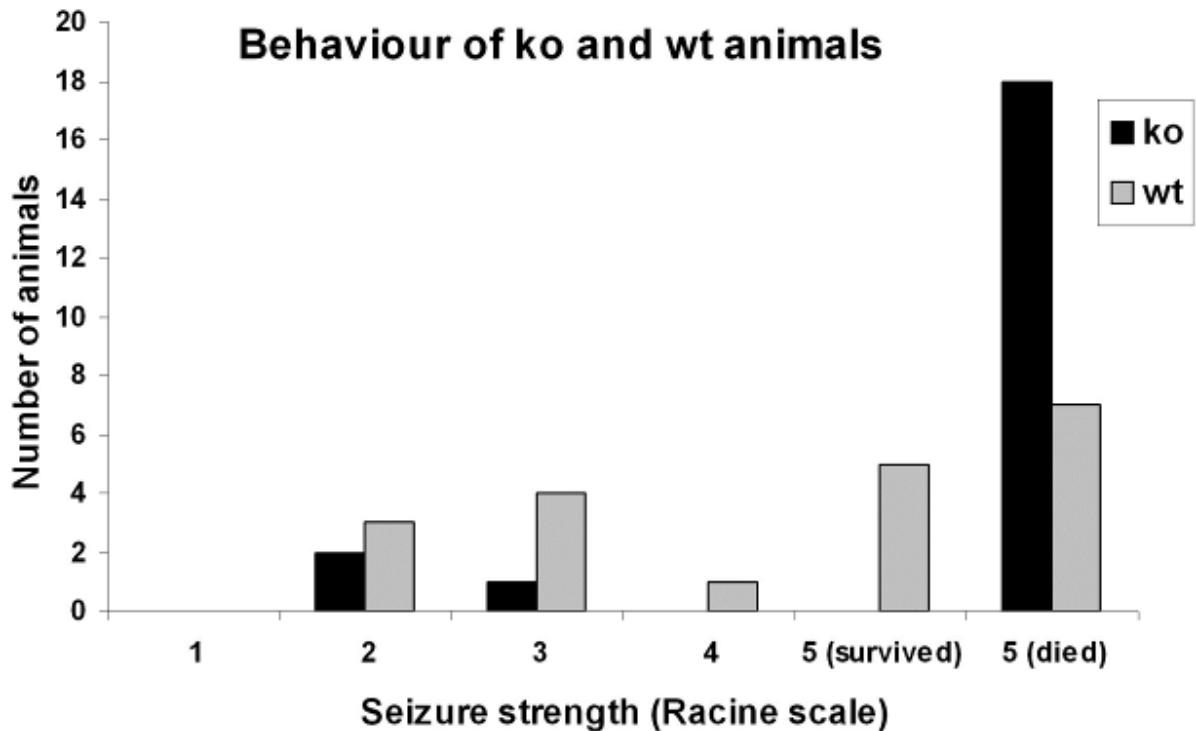
Graph 4: Seizure severity and survival rates displayed by of KO and wild type animals

Graph showing the number of animals as a function of seizure strength demonstrates that knock out animals had more severe seizures compared to wild types and never survived tonic-clonic (Racine 5) seizures.

Mice receiving only mild or no seizures (members of the weak group), survived and were sacrificed in the chronic phase. These animals showed no signs of pathological alterations, NeuN and Gallyas labeling was similar to the staining in weak wild type littermates (not shown).

These results demonstrate a protective role of CB1-R activation in epilepsy (during strong seizures) as it has been shown previously (Bhaskaran & Smith, 2010; Guggenhuber et al, 2011; Monory et al, 2006).

5.4.5. Ultrastructural changes of CB1-R expression in the acute phase of epilepsy

At the electron microscopic level degenerating profiles were observed occasionally throughout the hippocampus. They were mostly oedemic dendritic profiles, axon terminals and spines; however, they were not selectively CB1-R-positive.

To quantify the changes of CB1-R expression, systematic random sampling was carried out in the str. moleculare of the dentate gyrus. We could not take advantage of dissector method, since one cannot obtain accurate counts in a reasonable time when structures of interest form a very small fraction (da Costa et al, 2009) as it is the case in this study. Moreover, we wished to minimize alterations caused by the sprouting of positive or non-positive fibers in the examined area, therefore, we have examined a large area ($>40.000 \, \mu m^2$) in a single plane.

A total of 298 terminals were digitized (169 of control tissue, 129 of strong epileptic tissue) and analyzed. First we compared the ratio of immunolabelled axon terminals establishing symmetric versus asymmetric synapses in the same sample of 298 terminals **(Graph 5, Fig. 23)**.

The percentages of CB1–R immunopositive axon endings forming symmetric and asymmetric synapses found in acute epileptic samples were calculated and compared to the percentage observed in controls **(Graph 5, Fig. 23)**. The analysis revealed no significant change in these ratios (control: 79.6 ± 7.6 % in case of asymmetric and 20.4 ± 7.6 % in case of symmetric synapses; strong epileptic: 80 ± 4 % in case of asymmetric and 20 ± 4 % in case of symmetric synapses, $p>0.05$; Mann-Whitney test) **(Graph 5)**. To uncover changes in the overall number of stained terminals, we counted every stained terminal in the entire width of the reembedded part of str. moleculare, and normalized the results to unit area (40 000 μm^2). Compared to control tissue, a significant decrease was found in the number of labeled asymmetric and symmetric synapses (control asymmetric: 18.9 ± 2.3; symmetric: 6 ± 0.2; strong epileptic asymmetric: 11.8 ± 3.7, symmetric: 3.2 ± 0.7; $p<0.05$; Mann-Whitney test) **(Graph 6)**.

In the next step we counted the number of gold particles in the membrane of CB1-R-stained terminals and normalized it to the perimeter of the terminal membrane (particle /1 μm) to uncover any changes occurring on a smaller scale. No difference was found in the

normalized quantity of gold particles either in case of symmetric (control: 0.69±0.29, strong epileptic: 0.59±0.34) or in case of asymmetric synapses (control: 0.64±0.27, strong epileptic: 0.63± 0.33) **(Graph 7)**. However, when measuring the perimeter of immunopositive terminals an increase occurred in case of symmetric synapses indicating swelling of these terminals ($p < 0.05$; Mann-Whitney test) (control: 2±0.67 µm, strong epileptic: 2.63±0.87 µm).

Nevertheless, no such difference was observed among stained terminals forming asymmetric synapses (control: 1.9±0.76 µm, strong epileptic: 2.12±0.9 µm).

Taken together, the results imply that mechanism(s) other than axon terminal degeneration could account for the loss of CB1-R staining in the acute phase of epilepsy; though it may cause serious alterations in transmitter release.

To understand further changes in CB1-R expression we examined other phases as well.
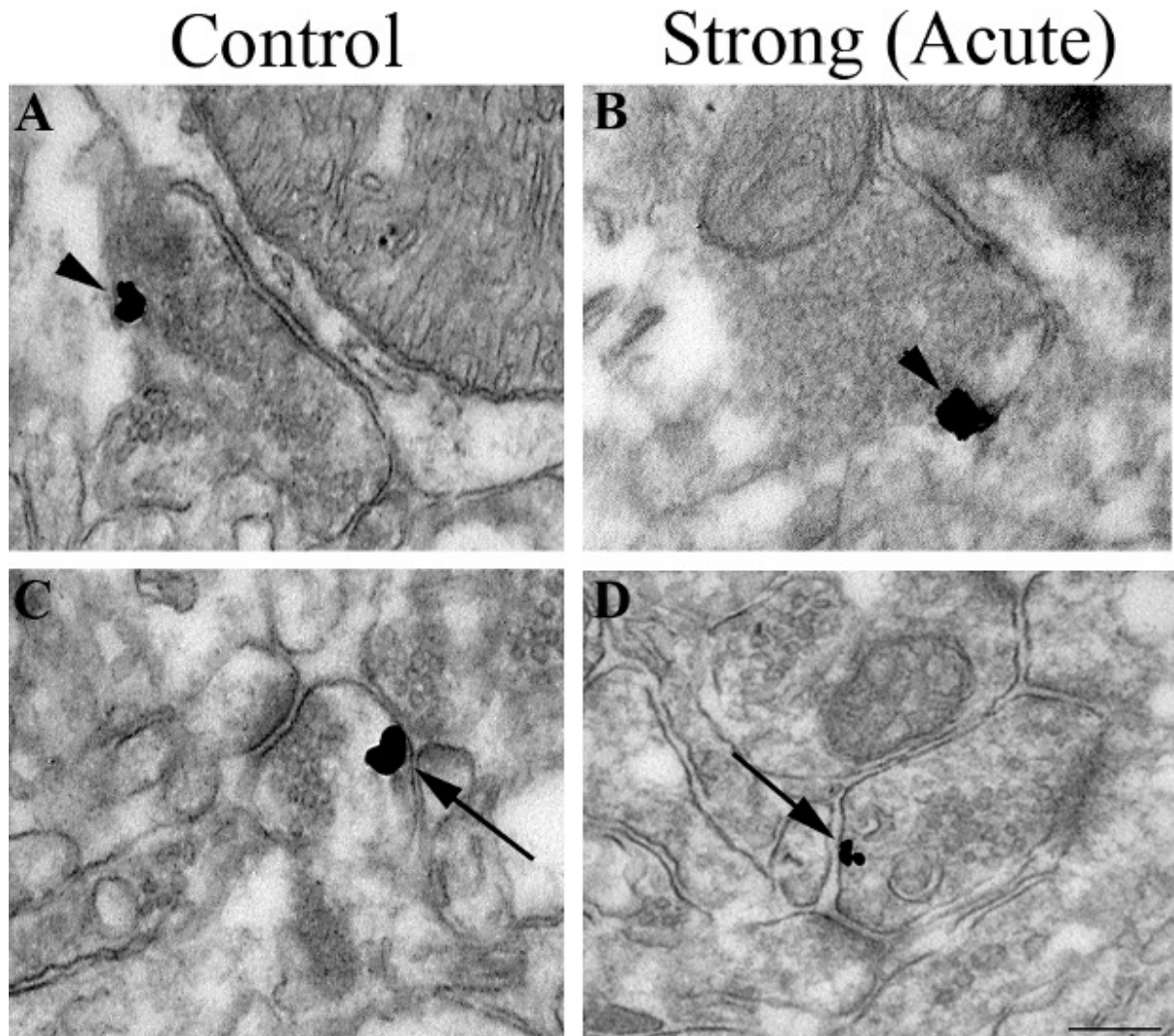
Figure 23: Ultrastructure of CB1-R-positive terminals in the acute phase of epilepsy

High power electron micrographs of CB1-R immunolabelled axon terminals from the str. moleculare of the DG of controls (A,C) and acute epileptic animals (2 hours) (B, D) post pilo. Our antibody labels both CB1-R-positive terminals giving symmetric (A, B) and asymmetric (C, D) synapses. Gold particles are located extrasynaptically. Scale: 200 nm.

Ratio of asymmetric and symmetric CB1-R-positive synapses
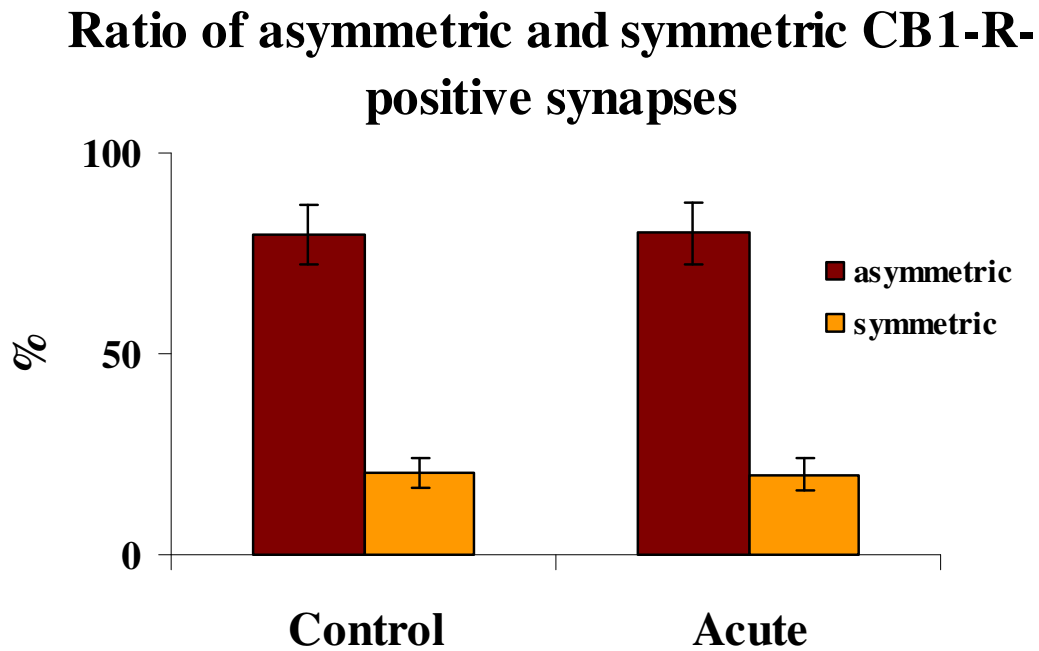
Graph 5: **Unchanged ratio of CB1-R-stained symmetric versus asymmetric synapses in the acute phase**

Graph shows no changes in the ratio of CB1-R immunopositive terminals establishing symmetric versus asymmetric synapses in control and epileptic tissue in str. moleculare of the DG. No difference was found in the ratio of immunopositive asymmetric versus symmetric synapses in the DG of strong animals in the acute phase.

Absolute number of CB1-R-positive asymmetric and symmetric synapses
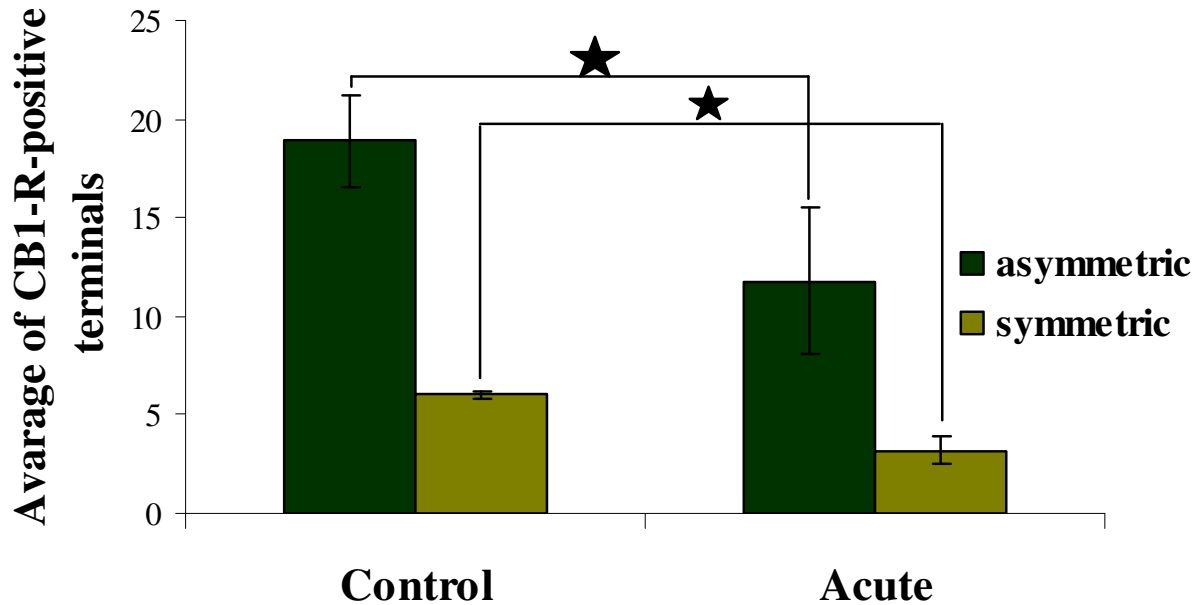
Graph 6: Quantitative changes of CB1-R immunostained terminals in the acute phase of epilepsy

Graph shows changes in the absolute number of symmetric versus asymmetric synapses in control and epileptic tissue. Significant decrease was found in the number of CB1-R immunostained asymmetric and symmetric synapses in the DG of strong animals in the acute phase, compared to controls.

Statistics were calculated with Mann-Whitney test (p<0.05).

Normalized number of gold particles in CB1-R-positive asymmetric and symmetric synapses
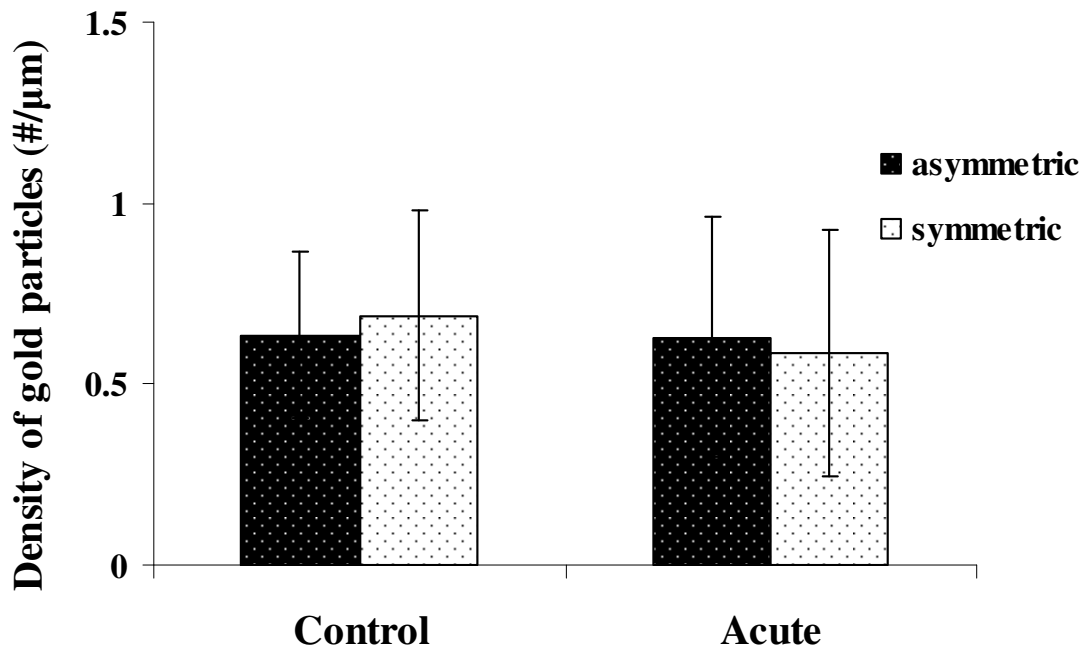
Graph 7: Quantitative changes of gold particles indicating the presence of CB1-Rs in the acute phase of epilepsy

Changes occur in the normalized number of gold particles indicating the presence of CB1-Rs in control and strong epileptic tissue. No difference appears in the mean density of gold particles in asymmetric or symmetric synapses in acute epileptic tissue compared to control tissue. Statistics were calculated with Mann-Whitney test ($p < 0.05$).

5.4.6. Distribution of CB1 receptors in the latent phase of epilepsy (1 and 3 days post pilo)

One day after pilocarpine injection CB1-R levels were control-like both in weak and strong animals. Three days after pilocarpine injection upregulation of CB1-R immunoreactivity occurred in some animals of the strong group. There was a gradual recovery in CB1-R intensity 1 and 3 days post pilo. 3 days after SE principal cells began to degenerate and HSP72 staining was more extended referring to excitotoxic damage caused

by the initial seizures **(Fig. 16,17)**. However, in the latent phase the decrease in the intensity of the receptor staining was not observed any longer. CB1-R staining proved to be control-like or moderately increased.

5.4.7. Distribution of CB1 receptors in the chronic phase of epilepsy (1 and 2 months) in mice

To study the long-term changes in CB1-R levels, their distribution was examined one month after pilocarpine injection, in the chronic phase. In general, similar alterations in CB1-R staining were found in these animals as we observed earlier with antibody recognizing only CB1-R at inhibitory terminals (Magloczky et al., 2010). In epileptic animals of the weak group the distribution of CB1-Rs was mostly control-like. In the sclerotic samples the general CB1-R immunostaining was enhanced throughout the hippocampus compared to controls **(Fig. 24A,C)**. The density of immunostained fibers in CA1 increased heavily in surviving elements of strata pyramidale and radiatum **(Fig. 24B)**. Similarly, in DG a dense CB1-R-positive axonal plexus was found in strata moleculare and granulosum **(Fig. 24D)**. Immunopositive interneuron somata were present both in the dentate gyrus and in the CA1 and CA3 areas.
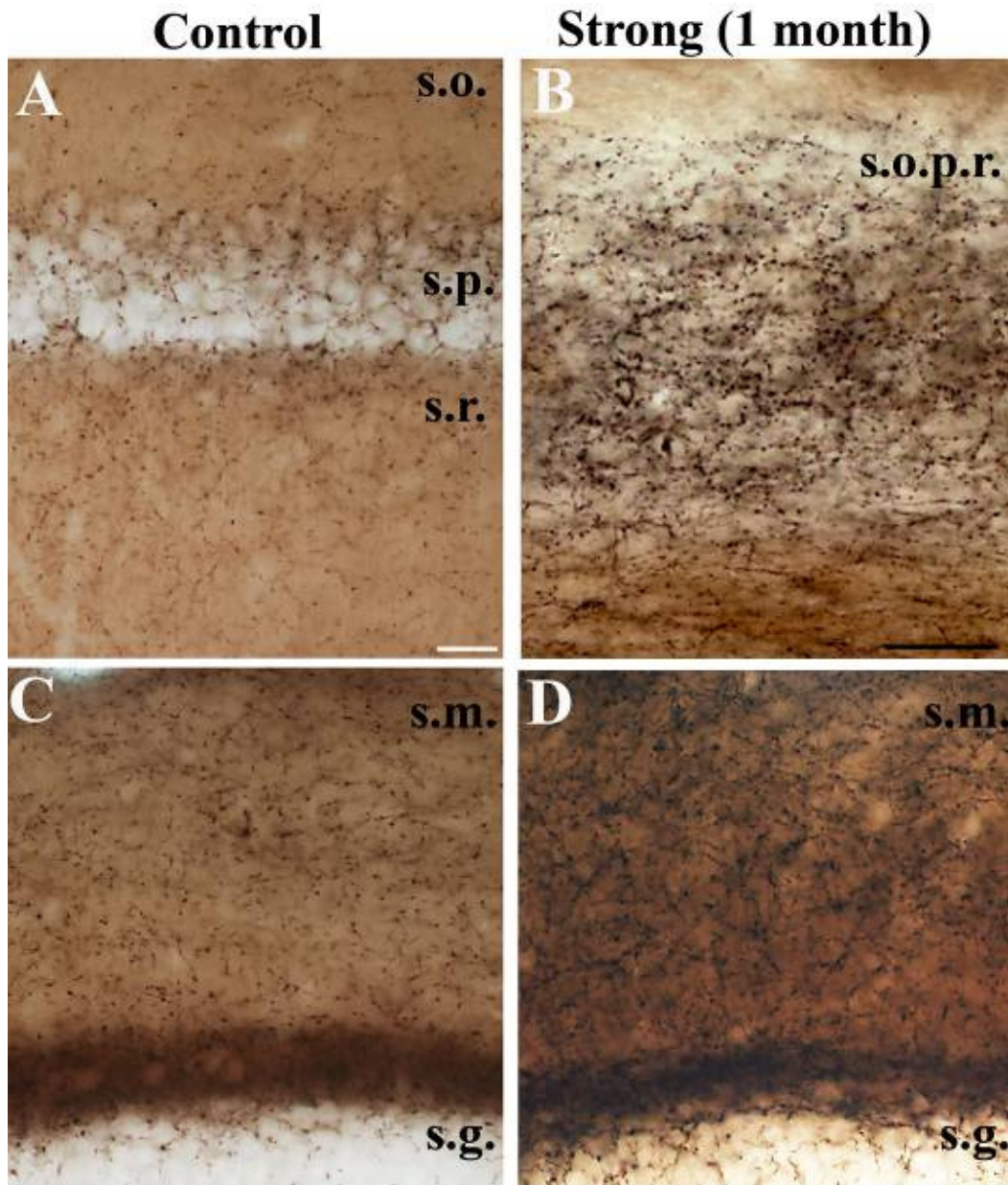
Figure 24: Changes in CB1-R-staining in the chronic phase

CB1-R immunostaining in the hippocampi of control (A, C) and chronically epileptic, sclerotic mice (1 month post pilocarpine)(B, D). In the sclerotic samples the general CB1-R immunostaining is much stronger throughout the hippocampus. In the CA1 (A) a dense immunostained axonal plexus can be seen in the sclerotic CA1 region (layers cannot be distinguished) (B). In the dentate gyrus stained fibers establish more dense meshworks than in control tissue (D). Scales: A, C, D: 50 μm B: 20 μm

5.4.8. Ultrastructural analysis of CB1-R distribution in the chronic phase (in mice)

At the electron microscopic level, numerous glial elements and occasionally degenerating profiles were seen, changes that are typical for epileptic tissues (Corsellis & Meldrum, 1976), however glial elements did not seem to be positive for CB1-R staining (CB1-R-staining in glial elements was around detection threshold). The general ultrastructural features of CB1-R-positive elements were unchanged; nevertheless, the number of stained terminals increased significantly (p<0.05) **(Fig. 25)**. Changes in the ratio of CB1-R-stained terminals establishing symmetric versus asymmetric synapses were analyzed (3 control and 3 strong epileptic mice, number of quantified terminals: 169 controls, 178 strong epileptic). In epileptic animals the ratio was significantly changed; the mean percentage in control tissue was 79.6 ± 7.64% in case of asymmetric **(Fig. 25D)** and 20.4 ± 7.6% in case of symmetric synapses **(Fig.25B)**, in strong epileptic tissue 51.4 ± 3.9% of the examined terminals proved to be asymmetric whereas 48.6 ± 3.9% was symmetric **(Graph 8)** (p<0.05; Mann-Whitney test). These results may suggest either a loss of stained asymmetric synapses or an increase of symmetric synapses, or both.

To address this question, we used systematic random sampling as described above and digitized every stained terminal throughout the entire width of the reembedded part of str. moleculare, and normalized the results to unit area (40.000 µm^2). Compared to control tissue a significant increase was found in the number of CB1-R-positive asymmetric and symmetric synapses (control asymmetric: 18.9 ± 2.3 symmetric: 6 ± 0.2; epileptic: asymmetric: 34.9 ± 10.9, symmetric: 32.3 ± 18.5, p<0.05; Mann-Whitney test), **(Graph 9)**. During the analysis of immunogold-labeled axon terminals, we noticed an increase in the number of immunogold particles located at symmetric synapses in the hippocampi of chronically epileptic animals of the strong group **(Fig. 25B)** (Karlocai et al, 2011).

To quantify these changes, immunogold particles were counted in 3 control and 3 strong epileptic animals in 302 (125 controls and 177 strong epileptic) terminals. The number of gold particles in the membrane of CB1-R stained axon terminals forming symmetric or asymmetric synapses was counted and normalized to unit perimeter of the axon terminal membrane (particle/1 µm). No difference was found between asymmetric synapses in control and epileptic tissue in the average quantity of gold particles (control:

0.64 ± 0.27, strong epileptic: 0.633 ± 0.46, p>0.05, Mann-Whitney test). In contrast, the number of immunogold particles significantly increased in axon terminals forming symmetric synapses (control: 0.69 ± 0.29, strong epileptic: 0.99 ± 0.49, p<0.05, Mann-Whitney test) **(Graph 10)**. Furthermore, the perimeter of immunopositive terminals establishing symmetric synapses significantly increased in strong epileptic animals in the chronic phase (control: 1.99±0.67 µm, strong epileptic: 2.7±0.9 µm). No such change was observed in terminals establishing asymmetric synapses (control: 1.89±0.8 µm, strong epileptic: 2.22±0.93 µm).
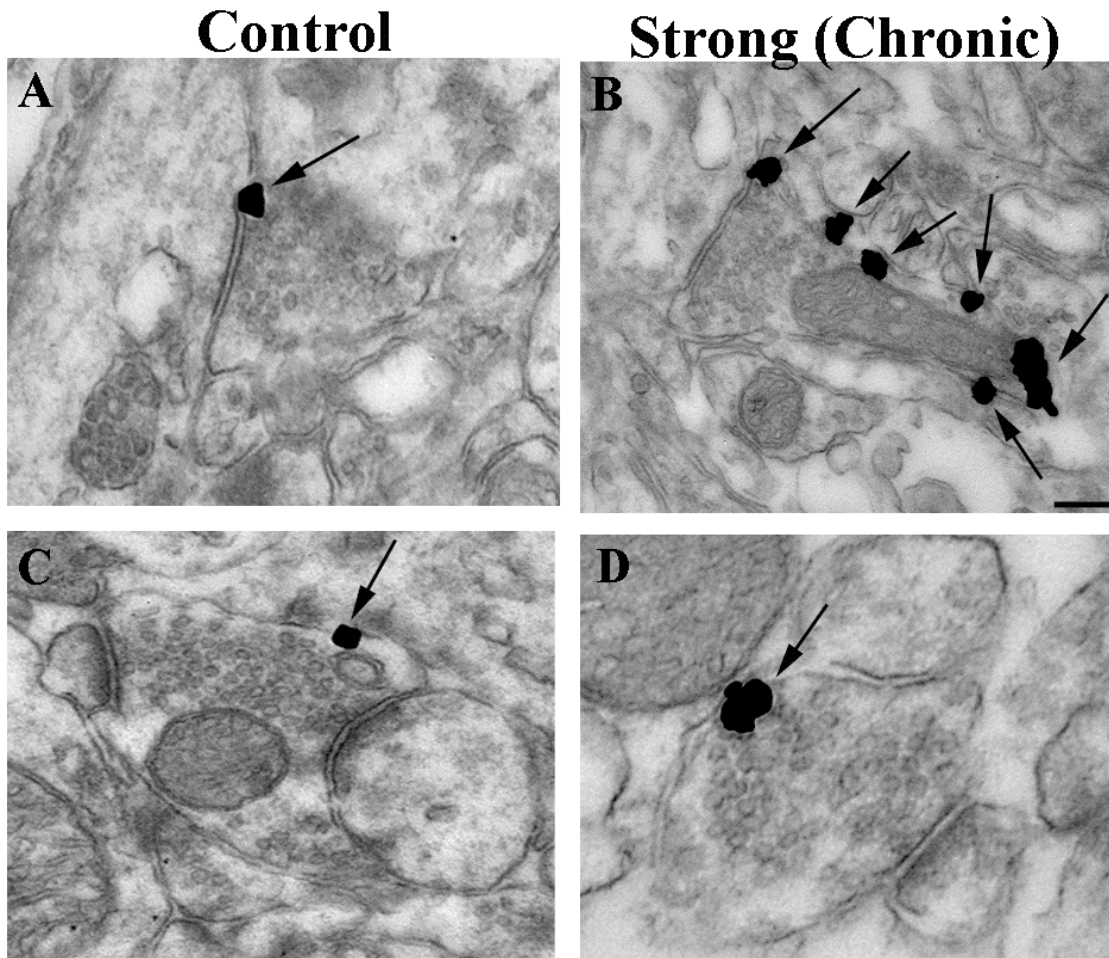
Figure 25: Ultrastructure of CB1-R-positive terminals

High power electron micrographs of CB1-R immunolabelled axon terminals from the str. moleculare of the DG of controls (A,C) and chronic epileptic animals (1 month) (B, D) post pilo. Our antibody labels both CB1-R-positive terminals giving symmetric (A, B) and asymmetric (C, D) synapses. Gold particles are located extrasynaptically. In the chronic, strong tissue the number of gold particles on terminals forming symmetric synapses has increased (B). Scale: 200 nm.

Ratio of asymmetric and symmetric CB1-R-positive synapses
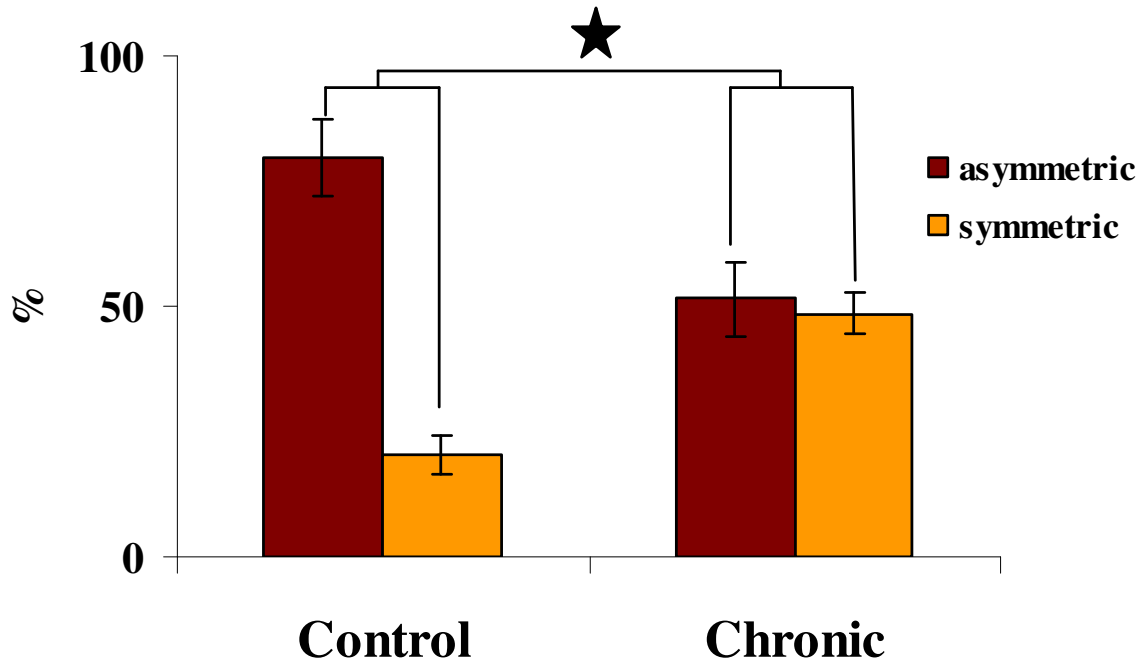
Graph 8: Changes in the ratio of CB1-R immunostained terminals in the chronic phase of epilepsy

Graph shows changes in the ratio of CB1-R immunopositive terminals establishing symmetric versus asymmetric synapses in control and chronic epileptic tissue in str. moleculare of the DG. Compared to controls, a significant increase can be seen in the ratio of CB1-R-stained symmetric versus asymmetric synapses in strong epileptic animals.

Absolute number of CB1-R-positive asymmetric and symmetric synapses
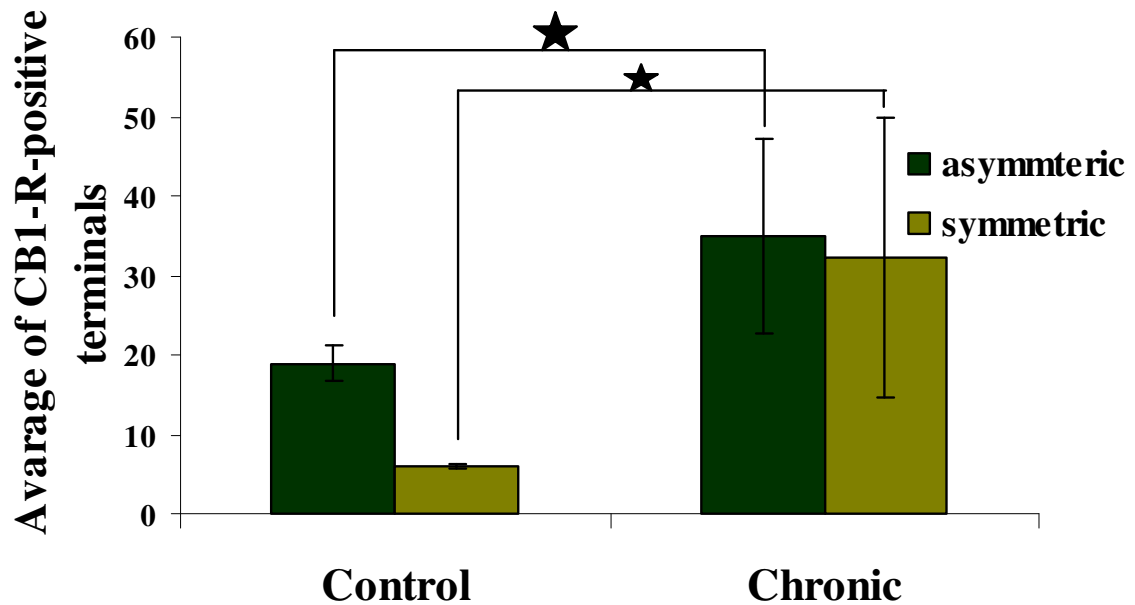
Graph 9: Quantitative changes of CB1-R immunostained terminals in the chronic phase of epilepsy

Graph shows changes in the absolute number of symmetric versus asymmetric synapses in control and chronic epileptic tissue. In strong animals in the chronic phase, a significant increase was found in the number of immunostained terminals forming asymmetric and symmetric synapses. Statistics were calculated with Mann-Whitney test (p<0.05).

Normalized number of gold particles in CB1-R-positive asymmetric and symmetric synapses
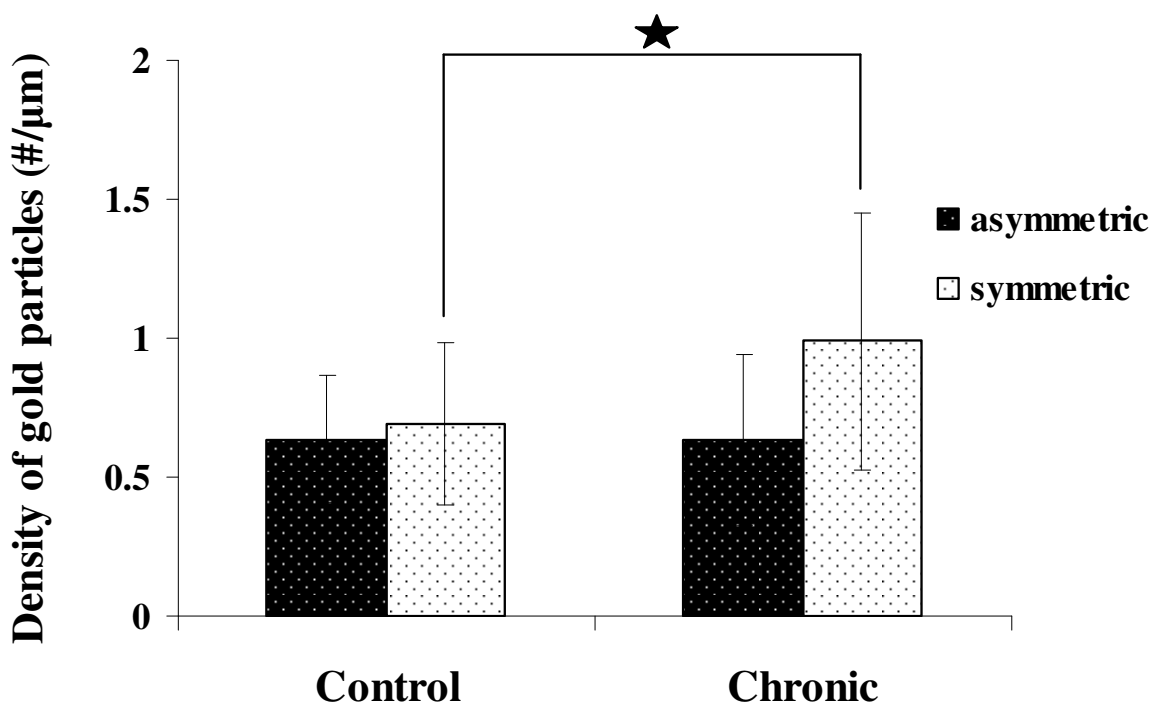
Graph 10: Quantitative changes in the number of gold particles in terminals (chronic phase of epilepsy)

Graph shows changes in the normalized number of gold particles indicating the presence of CB1-R protein in control and epileptic tissue. No difference appears in the mean density of gold particles in epileptic tissue in case of asymmetric synapses. However, the number of gold particles located in symmetric terminals increase significantly in the epileptic tissue. Statistics were calculated with Mann-Whitney test ($p<0.05$).

In summary, we found that the ratio of stained symmetric versus asymmetric synapses was unchanged in the acute phase, whereas, it has significantly changed in the chronic phase. The number of immunolabelled axon terminals forming asymmetric and symmetric synapses was decreased in the acute and increased in the chronic phase. In addition, the number of gold particles indicating the presence of CB1-Rs was increased on terminals forming symmetric synapses but only in the chronic phase (no such difference occurred in case of asymmetric synapses). These results may indicate a transient decrease of the receptor function in the acute phase leading to abnormally high transmitter release. In contrast, the elevation of CB1-R density in the chronic phase, may secure the balance of transmitter release, acting as an extremely powerful circuit-breaker on GABAergic and glutamatergic transmission (Cinar et al, 2008).

6. Discussion

Endocannabinoids as retrograde signal molecules are released by large intracellular Ca^{2+} transients, complex-spike burst-firing, and/or phospholipase C activation via metabotropic receptors in neurons (Freund et al, 2003; Kano et al, 2009). They bind to presynaptic CB1-Rs located on glutamatergic and GABAergic axon terminals, and thereby decrease transmitter release from excitatory and inhibitory boutons arriving primarily onto the same neurons (Hajos et al, 2000; Sullivan, 1999).

In our model various aspects of epileptic cell loss and reorganization are similar to that seen in human TLE (Clemens et al, 2007; Leite & Cavalheiro, 1995; Magloczky et al, 1997; Toth et al; Wittner et al, 2005; Wittner et al, 2001). On the basis of our results the strength of seizures in the acute phase can be used to predict future changes (e.g. cell loss) in the chronic phase. The vulnerability of cells differed between "weak" and "strong" groups, as indicated by HSP72-expression in the latent phase. The expression of CB1-Rs related to the GABAergic and glutamatergic axon terminals was strongly decreased without specific degeneration in the acute phase, but in the chronic phase a significant upregulation occurred in the number of immunostained terminals. In addition, a significant increase was seen in the number of CB1-Rs in a single terminal, but only in terminals forming symmetric synapses. In human tissue an upregulation was seen in CB1-R-positive terminals forming symmetric synapses similar to the mouse model. Despite quantitative changes in the number of stained terminals, the target distribution was not altered neither in human nor mice TLE.

The question arises whether the different changes in the endocannabinoid-mediated reduction of GABA and glutamate release (Bragin et al, 2002; Freund & Hajos, 2003) contribute to seizure generation and maintenance, or should it rather be considered as a neuroprotective reaction (Guggenhuber et al, 2011; Monory et al, 2006).

6.1. Changes in the acute phase of epilepsy

Earlier investigations of short term changes in the endocannabinoid system revealed a robust downregulation in the acute phase (Falenski et al, 2009; Wyeth et al). In these studies the loss of staining was explained by initial cell death or the degeneration of terminals. In contrast, in our samples mild degeneration was observed involving different profiles which were rarely CB1-R-positive; moreover, swelling was observed in case of immunostained terminals forming symmetric synapses. In addition, in our study the acute phase was examined 2 hours after pilocarpine injection. Previous studies examined the "acute" phase at e.g. 9 hours to 1 week post SE (Wyeth et al, 2010). We were able to examine the acute changes as early as 2 hours post SE since we did not use benzodiazepines to terminate seizures. This way we could demonstrate that acute changes of CB1-R distribution are independent of cell loss and likely the consequence of initial seizure activity.

Furthermore, the decrease of CB1-Rs in acute slices proved to be a reversible change, since they were redistributed in the membranes in a short time after "ending the seizures"/sacrificing the animals. Therefore, *in vitro* electrophysiology may not suitable to examine functional changes in the acute phase. These examinations suggest the occurrence of internalization and recycling (Hsieh et al, 1999), or degradation shortly followed by de novo synthesis.

Endocannabinoids are known to be synthesized in an activity-dependent manner (Freund et al, 2003; Lutz, 2002; Piomelli et al, 2007). In case of epileptic hyperexcitation an increase may occur in endocannabinoid levels as proposed previously and shown in kainic acid model of TLE (Cadas et al, 1996; Howlett, 2002; Katona & Freund, 2008; Lourenco et al, 2011; Lutz, 2004; Marsicano et al, 2003), thus CB1 receptors become strongly activated. Although CB1 receptor agonists are potent anticonvulsants both in animal models and human patients with TLE (Cunha et al, 1980; Monory et al, 2006; Wallace et al, 2003), their constant presence may cause internalization of the receptor (Coutts et al, 2001; Tappe-Theodor et al, 2007) or changes in conformation (forming homo- or heterodimers) (Gomes et al, 2001; Rios et al, 2001) leading to proconvulsive effects (Gordon & Devinsky, 2001; Keeler & Reifler, 1967) **(Fig. 26)**. Therefore, the controversial

effects of cannabinoid agonists may be explained by the timing of their application (Echegoyen et al, 2009).

6.2. Changes in the chronic phase of epilepsy

In the chronic phase of epilepsy a massive increase of CB1-staining located both at symmetric and asymmetric synapses was found throughout the hippocampus **(Fig. 26)**. Our results differ from that of Falenski et al (Falenski et al, 2007) and Wyeth et al.(Wyeth et al), since in these studies the loss of staining was sustained throughout the chronic phase as well, at least in certain hippocampal subregions. This discrepancy could be explained by differences between the models. In our study we examined sclerotic animals with a cell loss pattern similar to that seen in human TLE patients. In animal models described earlier (Falenski et al, 2007; Wyeth et al) different results were found depending on the model conditions (e.g. termination of seizures by benzodiazepines or severity of cell loss pattern which was less then 10% in certain studies).

6.2.1. Sprouting of excitatory fibers

Increased number of glutamatergic terminals with CB1-Rs was found in the hippocampi of sclerotic (strong epileptic) animals, most probably due to the sprouting of CB1-R expressing fibers. This highlights the importance of endocannabinoid mechanisms in reducing glutamate release during epilepsy (Aguado et al, 2006; Azad et al, 2003). Recent findings show that the overexpression of CB1-Rs on glutamatergic synapses can protect against excitotoxic damage (Guggenhuber et al). Moreover, increased effects of CB1-R agonists and elevated levels of receptor protein were shown in the dentate gyrus of pilocarpine treated mice (Bhaskaran & Smith, 2010) **(Fig. 26)**.

Controversially, the innermost part of stratum moleculare was examined previously by Ludanyi et al. showing that a downregulation of CB1-Rs related to glutamatergic terminals occurs in the inner molecular layer of the dentate gyrus in human TLE patients (Houser, 1990; Ludanyi et al, 2008; Nadler et al, 1980; Sutula et al, 1989b). In the study of Ludanyi et al. the ratio of CB1-R stained asymmetric synapses was calculated by comparing the number of stained terminals to the number of unstained terminals in a given

area. However, intensive sprouting of excitatory axon terminals in the stratum moleculare occurs in the epileptic tissue as it has been described recently (Goffin et al, 2011) . The increased amount of CB1-R unstained terminals may explain the decreased ratio of CB1-R-positive boutons found by Ludanyi et. al.. Another reason for this discrepancy can be the different method for quantification. In our study exclusively CB1-R-postive terminals were quantified in the entire width of str. moleculare.

In addition, a recent study showed that an increased CB1-R availability could be observed in human TLE, which correlated negatively with the latency following the last seizure (Goffin et al, 2011; Ludanyi et al, 2008; Magloczky et al, 2010), therefore CB1-R expression seems to be regulated very dynamically, which may easily explain differences between the results.

6.2.2. Sprouting of inhibitory fibers, changes in perisomatic inhibition

In the chronic phase of epilepsy CB1-R-positive (and also CCK-positive) cell bodies were preserved in the dentate gyrus and in the CA1 area, despite the mass principal cell loss. Enhancement of the immunostained terminal density deriving from the surviving CB1-R-positive interneurons was associated with the degree of cell loss (Magloczky et al).

In case of CB1-Rs located in terminals establishing symmetric synapses a strong increase in CB1-R-immunostaining was found both in the hippocampi of epileptic patients and in mice with CA1 sclerosis (Magloczky et al, 2010). Moreover, we found an increase of CB1-R level on single GABAergic terminals in parallel with an increase of terminal perimeter (Karlocai et al, 2011; Magloczky et al, 2010; Nusser et al, 1998; Wittner et al, 2002). Results of Chen et al. (Chen et al, 2003) show a chronic increase of CB1-Rs on axons of cholecystokinin-containing inhibitory cells following febrile seizure-like events. Our previous study, showing the sprouting of CB1-R-expressing interneuronal fibers and the elevation of CB1-R levels both in a chronic model (pilocarpine) and in human patients highlights the involvement of the reorganized endocannabinoid system in the chronic phase of temporal lobe epilepsy (Katona et al, 1999b). In addition, the increase in the size of inhibitory terminals may have a role in altering the effect of inhibition as proposed previously (Chen et al, 2007).

Sprouting of CB1-R expressing neurons related to GABAergic fibers (mostly CCK-containing cells) (Cohen et al, 2002; Cossart et al, 2005; Fujiwara-Tsukamoto et al, 2003; Stein & Nicoll, 2003; Szabadics et al, 2006; van den Pol et al, 1996; Woodin et al, 2003) may have controversial effects depending on the depolarizing or hyperpolarizing effect of GABA **(Fig. 26)**. If GABA is hyperpolarizing, proconvulsant effects of CB1-Rs could occur, by reducing GABAergic inhibition (Chen et al, 2003; Cossart et al, 2001; Magloczky & Freund, 2005; Wittner et al, 2005; Wittner et al, 2001). However, in case of altered ion homeostasis, $GABA_A$ receptors may have depolarizing effects (Magloczky & Freund, 2005; Wittner et al, 2005), thus reduced GABA release would be anticonvulsive in a restricted area.

GABA release causing hyperpolarization may be anticonvulsant as well, since enhanced perisomatic inhibition in chronic epilepsy was proposed to have a role in synchronizing seizure activity (Echegoyen et al, 2009). In addition, in epileptic tissue the axons of perisomatic targeting interneurons often sprout, suggesting an enhancement in this type of inhibition (Coutts et al, 2001).

Consequently, the effect of altered CB1-R distribution may depend on the current network state and ion homeostasis. Reduced transmitter release may decrease seizure intensity in case of glutamate release, and also in case of GABA release, when GABA has a hypersynchronizing or depolarizing effect. These scenarios, if they occur during epileptic seizures, may lead to an antiepileptic network effect of the increased density of CB1-Rs.
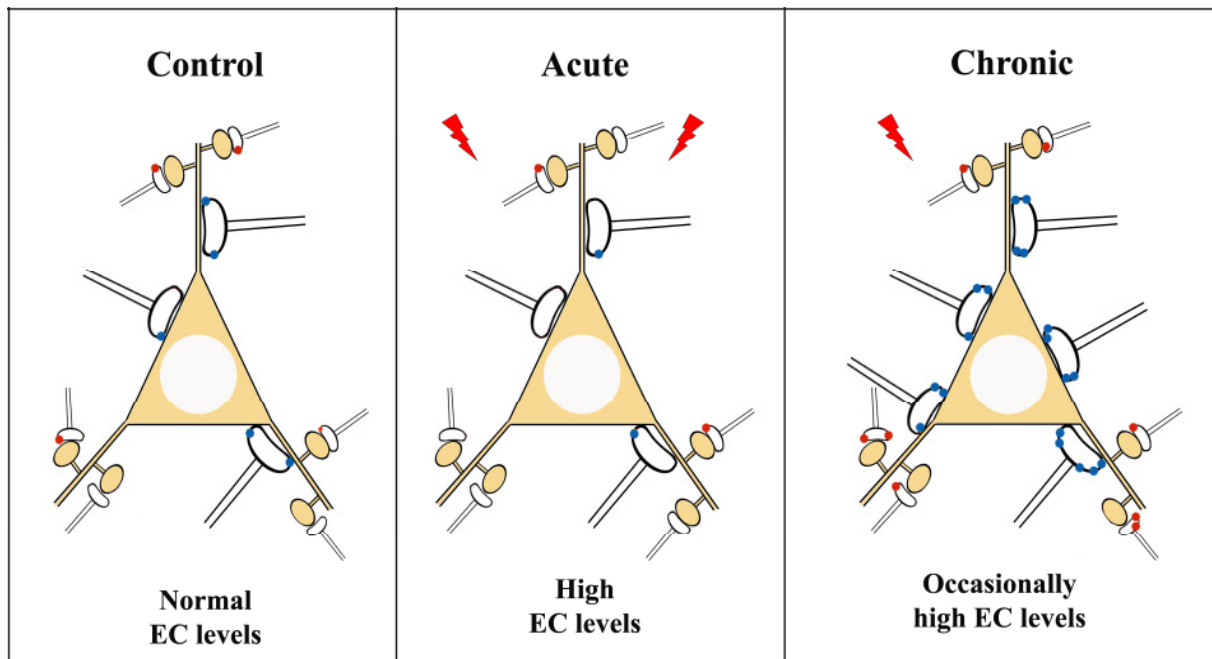
Figure 26: Changes in CB1-R-expression in different phases of TLE

During the acute phase due to intense early seizures endocannabinoid levels increase, leading to receptor internalization Thus, transmitter release becomes increased which aggravates seizures. In contrast, during the chronic phase, compensatory mechanisms activate, more numerous CB1-cantaining terminals can be found, this way reducing the activity of the network.

6.3. Preserved target distribution in human TLE and in the animal model of epilepsy

Both in epileptic and human tissue we found an unchanged target distribution of CB1-R immunopositive elements. This result indicates that the reorganization of the endocannabinoid system affects only the density of receptors. Thus, the target selectivity of CB1-R-expressing terminals follows a strict guideline; indicating, that an unchanged endocannabinoid-mediated decrease of transmitter release on distinct domains seems to be crucial in order to effectively decrease the abnormal transmitter release. The fact that the studied features of the endocannabinoid system were similarly changed or unchanged in human TLE and in the mouse model indicates that these alterations are strongly linked to

epileptic activity and reorganization. Thus, they may be considered changes widely occurring among species due to neuronal hyperexcitation.

6.4. Therapeutic implications

Previous studies by Echegoyen et al (Hsieh et al, 1999) showed that the application of SR141716, a CB1 receptor antagonist, in the early acute phase can prevent long term hyperactivity of the neuronal network. This raises the possibility of an antiepileptogenic therapy which may prevent the evolution of chronic seizures. The internalization of CB1-Rs caused by the application of WIN55212 can be rescued by the application of the antagonist SR141716 (Jones et al; Pertwee, 2008) acutely. This mechanism most likely underlies results found in the study of Echegoyen. However timing is critical in case of adding antagonists since it should be applied immediately and promptly after seizure onset.

Another possible therapy is the use of CB1-R agonists. The agonist causing the smallest internalization is THC (delta9-tetrahydrocannabinol) (Coutts et al, 2001; Hsieh et al, 1999) which is not used in therapy due to its addictive and hallucinogenic effects. Nevertheless, non-psychotropic analogs of tetrahirdocannabinol, like cannabidiol have antiepileptic properties as well (Guggenhuber et al, 2011), moreover they cause only little internalization (Falenski et al, 2007; Marsicano et al, 2003; Wyeth et al) and therefore, they might be suitable candidates (Echegoyen et al, 2009; Goffin et al, 2008; Naderi et al, 2008).

However, one should take into account that various changes can be seen in different models of epilepsy (Goffin et al, 2011; Guggenhuber et al, 2011; Karlocai et al, 2011) and in epileptic patients the original therapeutic drugs may counteract with endocannabinoid ligands. Thus, additional studies are required targeting other members of the endocannabinoid system as potent targets of antiepileptic therapies.

7. Conclusions

We showed that early seizures can determine the severity of future epileptic events. With the neurochemical marker HSP72 different mechanisms were shown to be activated in strong and weak animals leading to profound differences also in the chronic phase.

In case of CB1-R-staining, robust changes were only found in animals with strong acute seizures. In animals with mild seizures and hardly any cell loss, CB1-R distribution was not altered considerably. However, it is important to consider that in human TLE patents sclerosis is the most common cell loss pattern; therefore, alterations in animals with similar cell loss are likely to be relevant in human TLE.

The death of CB1 KO animals with strong acute seizures suggest that CB1 receptors may have a key role in the control of the first seizures, and thereby may prevent the seizures from reaching the "no-return" state. Thus, the decrease of CB1-Rs in animals with strong acute seizures may lead to elevation of glutamate release during acute seizures, as well as to the subsequent development of recurrent seizures, reorganization and cell loss. The increased density of CB1-Rs in the chronic phase may serve as a protective mechanism in most cases as confirmed in earlier studies.

The unchanged target distribution of CB1-R-positive elements indicate that the increased endocannabinoid tone is necessary on all cellular domains, thus; the greater input affects the somatic and dendritic regions as well.

8. Summary

The endocannabinoid system plays a central role in retrograde synaptic communication and may control the spread of activity in an epileptic network. In human and mouse TLE samples the intensity of CB1-R-staining in inhibitory synapses was increased in sclerotic samples. Analysis of target distribution did not show any changes neither in case of epileptic human nor in case of epileptic mice.

Using the pilocarpine model of temporal lobe epilepsy we examined the expression pattern of the Type 1 cannabinoid receptor (CB1-R) in the hippocampi of CD1 mice at survival times of 2 hours, 1 day, 3 days and 2 months (acute, latent and chronic phases). Based on the behavioral signs of the acute seizures, animals were classified as "weakly" or "strongly" epileptic using the modified Racine scale. Mice of the weak group had mild seizures, whereas seizures in the strong group were frequent with intense motor symptoms and the majority of these animals developed sclerosis in the chronic phase.

In control samples the most intense staining of CB1-R-positive fibers was found in the molecular layer of the dentate gyrus and in str. pyramidale of the cornu Ammonis. In weak animals no significant changes were seen at any survival time compared to controls. In strong animals, however, in the acute phase, a massive reduction in CB1-R-stained terminals occurred in the hippocampus. At electron microscopic level the absolute number of immunostained terminals decreased in DG. However 2 hours after ending the seizures the CB1-R-staining recovered in *in vitro* slices.

In the chronic phase, CB1-immunostaining in sclerotic samples was stronger throughout the hippocampus. Quantitative electron microscopic analysis showed an increase in the number of CB1-R-positive terminals in the dentate gyrus. Moreover, the number of immunogold particles significantly increased in GABAergic terminals.

Our results suggest a proconvulsive downregulation of CB1 receptors in the acute phase most probably due to receptor internalization, followed by compensatory upregulation and sprouting in the chronic phase of epilepsy. In conclusion, the changes in CB1 receptor expression pattern revealed in this study are associated with the severity of hippocampal injury initiated by acute seizures that ultimately leads to sclerosis in the vulnerable regions in the chronic phase.

9. Összefoglalás

Az endocannabinoid rendszer központi szerepet játszik a retrográd szinaptikus kommunikációban és képes befolyásolni az aktivitás terjedését egy epileptikus hálózatban. Jelen munkában temporális lebeny eredetű epilepsziás emberi és egér mintákban erősödést tapasztaltunk a gátló szinapszisokat érintő CB1-R festésben. A immunpozitív terminálisok célelemeinek vizsgálata nem mutatott változást epilepszia hatására sem az emberi, sem az egér hippokampuszban.

Állat modellünkben (pilokarpin) elemeztük az 1-es típusú kannabonoid receptor expressziójának változását CD1-es hím egerek hippokampuszában 2 órával, 1-és 3 nappal, valamint 2 hónappal a pilokarpin kezelés után (akut, latens, krónikus fázis).

Az akut rohamok során megfigyelt viselkedés alapján az állatokat "erősen" és "gyengén" epilepsziás csoportokra osztottuk a módosított Racine-skála segítségével. A gyenge csoport tagjai kevés és enyhébb rohamokat kaptak, míg az erős csoport tagjai gyakran mutattak tónusos-klónusos rohamokat. Ezen állatok a krónikus fázisban többnyire szklerotikusnak bizonyultak. Kontroll állatokban a legerősebb CB1-R festést a str. moleculareban és a str. pyramidaleban találtuk. Gyengén epilepsziás állatokban nem volt jelentős különbség a kontrollokhoz képest semelyik fázisban sem. Ezzel szemben az erős állatokban, az akut fázisban, jelentős csökkenés volt tapasztalható az egész hippokampuszban. Elektronmikroszkópos vizsgálatok kimutatták, hogy a CB1-R-pozitív terminálisok száma szignifikánsan lecsökken, ám 2 órával a rohamok vége után a festés fokozatosan visszatért kontroll-szerűvé *in vitro* szeltekben.

A krónikus fázisban a CB1-R festés az egész hippokampuszban megerősödött. Kvantitatív elektronmikroszkópos vizsgálatunk kimutatta, hogy a CB1-R-pozitív terminálisok száma megnő a str. moleculare-ban. Ezen túl, a fehérjét jelölő arany szemcsék száma is megnőtt gátló terminálisok esetén.

Eredményeinkből arra következtethetünk, hogy a CB1-R-ok csökkenése egy prokonvulzív folyamat, melynek legvalószínűbb oka a receptor internalizáció. A krónikus fázisban megjelenő növekedés és sarjadzás pedig egy kompenzációs folyamat eredménye lehet. Összességében a CB1-R expresszió változása a hippokampusz károsodásának mértékével arányos.

10. References

Abdulla EM, Campbell IC (1993) L-BMAA and kainate-induced modulation of neurofilament concentrations as a measure of neurite outgrowth - implications for an invitro test of neurotoxicity. *ToxicolInVitro* **7:** 341-344

Acsady L, Arabadzisz D, Freund TF (1996a) Correlated morphological and neurochemical features identify different subsets of vasoactive intestinal polypeptide-immunoreactive interneurons in rat hippocampus. *Neuroscience* **73:** 299-315.

Acsady L, Gorcs TJ, Freund TF (1996b) Different populations of vasoactive intestinal polypeptide-immunoreactive interneurons are specialized to control pyramidal cells or interneurons in the hippocampus. *Neuroscience* **73:** 317-334.

Aguado T, Palazuelos J, Monory K, Stella N, Cravatt B, Lutz B, Marsicano G, Kokaia Z, Guzman M, Galve-Roperh I (2006) The endocannabinoid system promotes astroglial differentiation by acting on neural progenitor cells. *J Neurosci* **26:** 1551-1561

Amaral DG, Dolorfo C, Alvarez-Royo P (1991) Organization of CA1 projections to the subiculum: a PHA-L analysis in the rat. *Hippocampus* **1:** 415-435.

Amaral DG IR (1990) Hippocampal formation. In *The Human Nervous System,*, G. P (ed), pp 711-755. San Diego, CA: Academic Press

Arai A, Silberg J, Lynch G (1995) Differences in the refractory properties of two distinct inhibitory circuitries in field CA1 of the hippocampus. *Brain research* **704:** 298-306

Azad SC, Eder M, Marsicano G, Lutz B, Zieglgansberger W, Rammes G (2003) Activation of the cannabinoid receptor type 1 decreases glutamatergic and GABAergic synaptic transmission in the lateral amygdala of the mouse. *Learn Mem* **10:** 116-128

Berg AT, Cross JH (2010) Towards a modern classification of the epilepsies? *Lancet neurology* **9:** 459-461

Bernard C, Cossart R, Hirsch JC, Esclapez M, Ben-Ari Y (2000) What is GABAergic inhibition? How is it modified in epilepsy? *Epilepsia* **41 Suppl 6:** S90-95

Bhaskaran MD, Smith BN (2010) Cannabinoid-mediated inhibition of recurrent excitatory circuitry in the dentate gyrus in a mouse model of temporal lobe epilepsy. *PloS one* **5:** e10683

Bisogno T, Howell F, Williams G, Minassi A, Cascio MG, Ligresti A, Matias I, Schiano-Moriello A, Paul P, Williams EJ, Gangadharan U, Hobbs C, Di Marzo V, Doherty P (2003)

Cloning of the first sn1-DAG lipases points to the spatial and temporal regulation of endocannabinoid signaling in the brain. *J Cell Biol* **163:** 463-468

Bragin A, Mody I, Wilson CL, Engel J, Jr. (2002) Local generation of fast ripples in epileptic brain. *J Neurosci* **22:** 2012-2021

Brown DJ, Stone WE (1973) Glutamate and aspartate in cortical subarachnoid fluid in relation to convulsive activity. *Brain Res* **54:** 143-148

Buckmaster PS, Schwartzkroin PA (1995) Physiological and morphological heterogeneity of dentate gyrus-hilus interneurons in the gerbil hippocampus in vivo. *Eur J Neurosci* **7:** 1393-1402

Cadas H, Gaillet S, Beltramo M, Venance L, Piomelli D (1996) Biosynthesis of an endogenous cannabinoid precursor in neurons and its control by calcium and cAMP. *J Neurosci* **16:** 3934-3942

Cajal Ry *Histologie du systeme nerveux de l'homme et des vertébrés*: Maloine.

Cajal Ry (1968) *The structure of Annon's horn*: Springfield.

Chen K, Neu A, Howard AL, Foldy C, Echegoyen J, Hilgenberg L, Smith M, Mackie K, Soltesz I (2007) Prevention of plasticity of endocannabinoid signaling inhibits persistent limbic hyperexcitability caused by developmental seizures. *J Neurosci* **27:** 46-58

Chen K, Ratzliff A, Hilgenberg L, Gulyas A, Freund TF, Smith M, Dinh TP, Piomelli D, Mackie K, Soltesz I (2003) Long-term plasticity of endocannabinoid signaling induced by developmental febrile seizures. *Neuron* **39:** 599-611

Cinar R, Freund TF, Katona I, Mackie K, Szucs M (2008) Reciprocal inhibition of G-protein signaling is induced by CB(1) cannabinoid and GABA(B) receptor interactions in rat hippocampal membranes. *Neurochem Int* **52:** 1402-1409

Clemens B, Bessenyei M, Piros P, Toth M, Seress L, Kondakor I (2007) Characteristic distribution of interictal brain electrical activity in idiopathic generalized epilepsy. *Epilepsia* **48:** 941-949

Cohen I, Navarro V, Clemenceau S, Baulac M, Miles R (2002) On the origin of interictal activity in human temporal lobe epilepsy in vitro. *Science* **298:** 1418-1421.

Corsellis JAN, Meldrum BS (1976) Epilepsy. In *Greenfield's Neuropathology*, Blackwood W, Corsellis JAN (eds), 0 edn, pp 771-795. London: Arnold

Cossart R, Bernard C, Ben-Ari Y (2005) Multiple facets of GABAergic neurons and synapses: multiple fates of GABA signalling in epilepsies. *Trends Neurosci* **28:** 108-115

Cossart R, Dinocourt C, Hirsch JC, Merchan-Perez A, De Felipe J, Ben-Ari Y, Esclapez M, Bernard C (2001) Dendritic but not somatic GABAergic inhibition is decreased in experimental epilepsy. *Nat Neurosci* **4:** 52-62.

Coutts AA, Anavi-Goffer S, Ross RA, MacEwan DJ, Mackie K, Pertwee RG, Irving AJ (2001) Agonist-induced internalization and trafficking of cannabinoid CB1 receptors in hippocampal neurons. *J Neurosci* **21:** 2425-2433

Crunelli V, Leresche N (2002) Childhood absence epilepsy: genes, channels, neurons and networks. *Nature reviews* **3:** 371-382

Cunha JM, Carlini EA, Pereira AE, Ramos OL, Pimentel C, Gagliardi R, Sanvito WL, Lander N, Mechoulam R (1980) Chronic administration of cannabidiol to healthy volunteers and epileptic patients. *Pharmacology* **21:** 175-185

da Costa NM, Hepp K, Martin KA (2009) A systematic random sampling scheme optimized to detect the proportion of rare synapses in the neuropil. *J Neurosci Methods* **180:** 77-81

de Lanerolle NC, Kim JH, Williamson A, Spencer SS, Zaveri HP, Eid T, Spencer DD (2003) A retrospective analysis of hippocampal pathology in human temporal lobe epilepsy: evidence for distinctive patient subcategories. *Epilepsia* **44:** 677-687

Devane WA, Hanus L, Breuer A, Pertwee RG, Stevenson LA, Griffin G, Gibson D, Mandelbaum A, Etinger A, Mechoulam R (1992) Isolation and structure of a brain constituent that binds to the cannabinoid receptor. *Science* **258:** 1946-1949

Dinh TP, Carpenter D, Leslie FM, Freund TF, Katona I, Sensi SL, Kathuria S, Piomelli D (2002) Brain monoglyceride lipase participating in endocannabinoid inactivation. *Proc Natl Acad Sci U S A* **99:** 10819-10824

Duvernoy HM (1998) *The human hippocampus*, 2 edn. Berlin: Springer-Verlag.

Echegoyen J, Armstrong C, Morgan RJ, Soltesz I (2009) Single application of a CB1 receptor antagonist rapidly following head injury prevents long-term hyperexcitability in a rat model. *Epilepsy Res* **85:** 123-127

Egertova M, Giang DK, Cravatt BF, Elphick MR (1998) A new perspective on cannabinoid signalling: complementary localization of fatty acid amide hydrolase and the CB1 receptor in rat brain. *Proc Biol Sci* **265:** 2081-2085

Engel J, Jr. (1996) Excitation and inhibition in epilepsy. *Can J Neurol Sci* **23:** 167-174.

Falconer MA, Taylor DC (1968) Surgical treatment of drug-resistant epilepsy due to mesial temporal sclerosis. Etiology and significance. *Archives of neurology* **19:** 353-361.

Falenski KW, Blair RE, Sim-Selley LJ, Martin BR, DeLorenzo RJ (2007) Status epilepticus causes a long-lasting redistribution of hippocampal cannabinoid type 1 receptor expression and function in the rat pilocarpine model of acquired epilepsy. *Neuroscience* **146:** 1232-1244

Falenski KW, Carter DS, Harrison AJ, Martin BR, Blair RE, DeLorenzo RJ (2009) Temporal characterization of changes in hippocampal cannabinoid CB(1) receptor expression following pilocarpine-induced status epilepticus. *Brain Res* **1262:** 64-72

Felder CC, Veluz JS, Williams HL, Briley EM, Matsuda LA (1992) Cannabinoid agonists stimulate both receptor- and non-receptor-mediated signal transduction pathways in cells transfected with and expressing cannabinoid receptor clones. *Molecular pharmacology* **42:** 838-845

Fisher RS (1989) Animal mdels of the epilepsies. *Brain ResRev* **14:** 245-278

Freund TF, Buzsaki G (1996) Interneurons of the hippocampus. *Hippocampus* **6:** 347-470

Freund TF, Hajos N (2003) Excitement reduces inhibition via endocannabinoids. *Neuron* **38:** 362-365

Freund TF, Katona I, Piomelli D (2003) Role of endogenous cannabinoids in synaptic signaling. *Physiological reviews* **83:** 1017-1066

Fujiwara-Tsukamoto Y, Isomura Y, Nambu A, Takada M (2003) Excitatory GABA input directly drives seizure-like rhythmic synchronization in mature hippocampal CA1 pyramidal cells. *Neuroscience* **119:** 265-275

Fukudome Y, Ohno-Shosaku T, Matsui M, Omori Y, Fukaya M, Tsubokawa H, Taketo MM, Watanabe M, Manabe T, Kano M (2004) Two distinct classes of muscarinic action on hippocampal inhibitory synapses: M2-mediated direct suppression and M1/M3-mediated indirect suppression through endocannabinoid signalling. *Eur J Neurosci* **19:** 2682-2692

Gallyas F, Wolff JR, Bottcher H, Zaborszky L (1980) A reliable and sensitive method to localize terminal degeneration and lysosomes in the central nervous system. *Stain Technol* **55:** 299-306

Gaoni Y, Mechoulam R (1971) The isolation and structure of delta-1-tetrahydrocannabinol and other neutral cannabinoids from hashish. *Journal of the American Chemical Society* **93:** 217-224

Gass P, Prior P, Kiessling M (1995) Correlation between seizure intensity and stress protein expression after limbic epilepsy in the rat brain. *Neuroscience* **65:** 27-36

Goffin K, Bormans G, Casteels C, Bosier B, Lambert DM, Grachev ID, Van Paesschen W, Van Laere K (2008) An in vivo [18F]MK-9470 microPET study of type 1 cannabinoid receptor binding in Wistar rats after chronic administration of valproate and levetiracetam. *Neuropharmacology* **54:** 1103-1106

Goffin K, Van Paesschen W, Van Laere K (2011) In vivo activation of endocannabinoid system in temporal lobe epilepsy with hippocampal sclerosis. *Brain* **134:** 1033-1040

Gomes I, Jordan BA, Gupta A, Rios C, Trapaidze N, Devi LA (2001) G protein coupled receptor dimerization: implications in modulating receptor function. *J Mol Med* **79:** 226-242

Gordon E, Devinsky O (2001) Alcohol and marijuana: effects on epilepsy and use by patients with epilepsy. *Epilepsia* **42:** 1266-1272

Green RC (1991) Neuropathology and behavior in epilepsy. In *Epilepsy and Behavior*, 0 edn, pp 345-359. Wiley-Liss, Inc.

Guggenhuber S, Monory K, Lutz B, Klugmann M (2011) AAV vector-mediated overexpression of CB1 cannabinoid receptor in pyramidal neurons of the hippocampus protects against seizure-induced excitoxicity. *PloS one* **5:** e15707

Gulyas AI, Freund TF (1996) Pyramidal cell dendrites are the primary targets of calbindin D28k-immunoreactive interneurons in the hippocampus. *Hippocampus* **6:** 525-534

Gulyas AI, Hajos N, Freund TF (1996) Interneurons containing calretinin are specialized to control other interneurons in the rat hippocampus. *J Neurosci* **16:** 3397-3411

Gulyas AI, Hajos N, Katona I, Freund TF (2003) Interneurons are the local targets of hippocampal inhibitory cells which project to the medial septum. *Eur J Neurosci* **17:** 1861-1872

Gulyas AI, Miettinen R, Jacobowitz DM, Freund TF (1992) Calretinin is present in non-pyramidal cells of the rat hippocampus--I. A new type of neuron specifically associated with the mossy fibre system. *Neuroscience* **48:** 1-27

Gulyas AI, Miles R, Hajos N, Freund TF (1993) Precision and variability in postsynaptic target selection of inhibitory cells in the hippocampal CA3 region. *Eur J Neurosci* **5:** 1729-1751.

Gulyas AI, Toth K, Danos P, Freund TF (1991) Subpopulations of GABAergic neurons containing parvalbumin, calbindin D28k, and cholecystokinin in the rat hippocampus. *The Journal of comparative neurology* **312:** 371-378

Gutnick MJ, Connors BW, Prince DA (1982) Mechanisms of neocortical epileptogenesis in vitro. *Journal of neurophysiology* **48:** 1321-1335

Hajos N, Katona I, Naiem SS, MacKie K, Ledent C, Mody I, Freund TF (2000) Cannabinoids inhibit hippocampal GABAergic transmission and network oscillations. *Eur J Neurosci* **12:** 3239-3249

Hajos N, Ledent C, Freund TF (2001) Novel cannabinoid-sensitive receptor mediates inhibition of glutamatergic synaptic transmission in the hippocampus. *Neuroscience* **106:** 1-4

Halasy K, Buhl EH, Lorinczi Z, Tamas G, Somogyi P (1996) Synaptic target selectivity and input of GABAergic basket and bistratified interneurons in the CA1 area of the rat hippocampus. *Hippocampus* **6:** 306-329

Halász P, Rajna P (1990) *Epilepszia*, 0 edn. Budapest: Innomark.

Haller J, Matyas F, Soproni K, Varga B, Barsy B, Nemeth B, Mikics E, Freund TF, Hajos N (2007) Correlated species differences in the effects of cannabinoid ligands on anxiety and on GABAergic and glutamatergic synaptic transmission. *Eur J Neurosci* **25:** 2445-2456

Hampson RE, Deadwyler SA (1992) Information processing in the dentate gyrus. *Epilepsy Res***:** 291-299

Han ZS, Buhl EH, Lorinczi Z, Somogyi P (1993) A high degree of spatial selectivity in the axonal and dendritic domains of physiologically identified local-circuit neurons in the dentate gyrus of the rat hippocampus. *Eur J Neurosci* **5:** 395-410

Handelmann G, Meyer DK, Beinfeld MC, Oertel WH (1981) CCK-containing terminals in the hippocampus are derived from intrinsic neurons: an immunohistochemical and radioimmunological study. *Brain research* **224:** 180-184

Heinemann U, Konnerth A, Pumain R, Wadman WJ (1986) Extracellular calcium and potassium concentration changes in chronic epileptic brain tissue. *Adv Neurol* **44:** 641-661

Houser CR (1990) Granule cell dispersion in the dentate gyrus of humans with temporal lobe epilepsy. *Brain Res* **535:** 195-204.

Houser CR, Esclapez M (1996) Vulnerability and plasticity of the GABA system in the pilocarpine model of spontaneous recurrent seizures. *Epilepsy Res* **26:** 207-218.

Houser CR, Miyashiro JE, Swartz BE, Walsh GO, Rich JR, Delgado-Escueta AV (1990) Altered patterns of dynorphin immunoreactivity suggest mossy fiber reorganization in human hippocampal epilepsy. *J Neurosci* **10:** 267-282.

Howlett AC (2002) The cannabinoid receptors. *Prostaglandins Other Lipid Mediat* **68-69:** 619-631

Hsieh C, Brown S, Derleth C, Mackie K (1999) Internalization and recycling of the CB1 cannabinoid receptor. *Journal of neurochemistry* **73:** 493-501

Jinno S, Kosaka T (2002) Immunocytochemical characterization of hippocamposeptal projecting GABAergic nonprincipal neurons in the mouse brain: a retrograde labeling study. *Brain Res* **945:** 219-231

Jones NA, Hill AJ, Smith I, Bevan SA, Williams CM, Whalley BJ, Stephens GJ Cannabidiol displays antiepileptiform and antiseizure properties in vitro and in vivo. *J Pharmacol Exp Ther* **332:** 569-577

Kano M, Ohno-Shosaku T, Hashimotodani Y, Uchigashima M, Watanabe M (2009) Endocannabinoid-mediated control of synaptic transmission. *Physiol Rev* **89:** 309-380

Karlocai MR, Toth K, Watanabe M, Ledent C, Juhasz G, Freund TF, Magloczky Z (2011) Redistribution of CB1 cannabinoid receptors in the acute and chronic phases of pilocarpine-induced epilepsy. *PloS one* **6:** e27196

Karnup S, Stelzer A (2001) Seizure-like activity in the disinhibited CA1 minislice of adult guinea-pigs. *The Journal of physiology* **532:** 713-730

Kathmann M, Bauer U, Schlicker E, Gothert M (1999) Cannabinoid CB1 receptor-mediated inhibition of NMDA- and kainate-stimulated noradrenaline and dopamine release in the brain. *Naunyn Schmiedebergs Arch Pharmacol* **359:** 466-470

Katona I, Acsady L, Freund TF (1999a) Postsynaptic targets of somatostatin-immunoreactive interneurons in the rat hippocampus. *Neuroscience* **88:** 37-55

Katona I, Freund TF (2008) Endocannabinoid signaling as a synaptic circuit breaker in neurological disease. *Nat Med* **14:** 923-930

Katona I, Sperlagh B, Magloczky Z, Santha E, Kofalvi A, Czirjak S, Mackie K, Vizi ES, Freund TF (2000) GABAergic interneurons are the targets of cannabinoid actions in the human hippocampus. *Neuroscience* **100:** 797-804

Katona I, Sperlagh B, Sik A, Kafalvi A, Vizi ES, Mackie K, Freund TF (1999b) Presynaptically located CB1 cannabinoid receptors regulate GABA release from axon terminals of specific hippocampal interneurons. *J Neurosci* **19:** 4544-4558

Katona I, Urban GM, Wallace M, Ledent C, Jung KM, Piomelli D, Mackie K, Freund TF (2006) Molecular composition of the endocannabinoid system at glutamatergic synapses. *The Journal of neuroscience* **26:** 5628-5637

Katsumaru H, Kosaka T, Heizmann CW, Hama K (1988) Immunocytochemical study of GABAergic neurons containing the calcium-binding protein parvalbumin in the rat hippocampus. *Exp Brain Res* **72:** 347-362

Kawaguchi Y, Hama K (1988) Physiological heterogeneity of nonpyramidal cells in rat hippocampal CA1 region. *Exp Brain Res* **72:** 494-502

Keeler MH, Reifler CB (1967) Grand mal convulsions subsequent to marijuana use. Case report. *Dis Nerv Syst* **28:** 474-475

Klausberger T, Marton LF, Baude A, Roberts JD, Magill PJ, Somogyi P (2004) Spike timing of dendrite-targeting bistratified cells during hippocampal network oscillations in vivo. *Nat Neurosci* **7:** 41-47

Kosaka T, Katsumaru H, Hama K, Wu JY, Heizmann CW (1987) GABAergic neurons containing the Ca2+-binding protein parvalbumin in the rat hippocampus and dentate gyrus. *Brain Res* **419:** 119-130

Kosaka T, Kosaka K, Tateishi K, Hamaoka Y, Yanaihara N, Wu JY, Hama K (1985) GABAergic neurons containing CCK-8-like and/or VIP-like immunoreactivities in the rat hippocampus and dentate gyrus. *The Journal of comparative neurology* **239:** 420-430

Ledent C, Valverde O, Cossu G, Petitet F, Aubert JF, Beslot F, Bohme GA, Imperato A, Pedrazzini T, Roques BP, Vassart G, Fratta W, Parmentier M (1999) Unresponsiveness to cannabinoids and reduced addictive effects of opiates in CB1 receptor knockout mice. *Science* **283:** 401-404

Leite JP, Cavalheiro EA (1995) Effects of conventional antiepileptic drugs in a model of spontaneous recurrent seizures in rats. *Epilepsy Res* **20:** 93-104

Li XG, Somogyi P, Tepper JM, Buzsaki G (1992) Axonal and dendritic arborization of an intracellularly labeled chandelier cell in the CA1 region of rat hippocampus. *Exp Brain Res* **90:** 519-525

Litt B, Esteller R, Echauz J, D'Alessandro M, Shor R, Henry T, Pennell P, Epstein C, Bakay R, Dichter M, Vachtsevanos G (2001) Epileptic seizures may begin hours in advance of clinical onset: a report of five patients. *Neuron* **30:** 51-64

Lothman EW, Bertram EH, Bekenstein JW, Perlin JB (1989) Self-sustaining limbic status epilepticus induced by 'continuous' hippocampal stimulation: electrographic and behavioral characteristics. *Epilepsy Res* **3:** 107-119

Lourenco J, Matias I, Marsicano G, Mulle C (2011) Pharmacological activation of kainate receptors drives endocannabinoid mobilization. *J Neurosci* **31:** 3243-3248

Lowenstein DH, Simon RP, Sharp FR (1990) The pattern of 72-kDA heat shock protein-like immunoreactivity in the rat barin following flurothyl-induced status epilepticus. *Brain Res* **531:** 173-182

Ludanyi A, Eross L, Czirjak S, Vajda J, Halasz P, Watanabe M, Palkovits M, Magloczky Z, Freund TF, Katona I (2008) Downregulation of the CB1 cannabinoid receptor and related molecular elements of the endocannabinoid system in epileptic human hippocampus. *The Journal of neuroscience* **28:** 2976-2990

Lutz B (2002) Molecular biology of cannabinoid receptors. *Prostaglandins Leukot Essent Fatty Acids* **66:** 123-142

Lutz B (2004) On-demand activation of the endocannabinoid system in the control of neuronal excitability and epileptiform seizures. *Biochemical pharmacology* **68:** 1691-1698

Mackie K (2005) Distribution of cannabinoid receptors in the central and peripheral nervous system. *Handb Exp Pharmacol***:** 299-325

Mackie K (2008) Signaling via CNS cannabinoid receptors. *Mol Cell Endocrinol* **286:** S60-65

Mackie K, Stella N (2006) Cannabinoid receptors and endocannabinoids: evidence for new players. *Aaps J* **8:** E298-306

Magloczky Z, Acsady L, Freund TF (1994) Principal cells are the postsynaptic targets of supramammillary afferents in the hippocampus of the rat. *Hippocampus* **4:** 322-334.

Magloczky Z, Freund TF (1993) Selective neuronal death in the contralateral hippocampus following unilateral kainate injections into the CA3 subfield. *Neuroscience* **56:** 317-335.

Magloczky Z, Freund TF (1995) Delayed cell death in the contralateral hippocampus following kainate injection into the CA3 subfield. *Neuroscience* **66:** 847-860.

Magloczky Z, Freund TF (2005) Impaired and repaired inhibitory circuits in the epileptic human hippocampus. *Trends Neurosci* **28:** 334-340

Magloczky Z, Halasz P, Vajda J, Czirjak S, Freund TF (1997) Loss of Calbindin-D28K immunoreactivity from dentate granule cells in human temporal lobe epilepsy. *Neuroscience* **76:** 377-385

Magloczky Z, Toth K, Karlocai R, Nagy S, Eross L, Czirjak S, Vajda J, Rasonyi G, Kelemen A, Juhos V, Halasz P, Mackie K, Freund TF (2010) Dynamic changes of CB1-receptor expression in hippocampi of epileptic mice and humans. *Epilepsia* **51 Suppl 3:** 115-120

Magloczky Z, Wittner L, Borhegyi Z, Halasz P, Vajda J, Czirjak S, Freund TF (2000) Changes in the distribution and connectivity of interneurons in the epileptic human dentate gyrus. *Neuroscience* **96:** 7-25

Marsicano G, Goodenough S, Monory K, Hermann H, Eder M, Cannich A, Azad SC, Cascio MG, Gutierrez SO, van der Stelt M, Lopez-Rodriguez ML, Casanova E, Schutz G, Zieglgansberger W, Di Marzo V, Behl C, Lutz B (2003) CB1 cannabinoid receptors and on-demand defense against excitotoxicity. *Science* **302:** 84-88

Matsuda LA, Lolait SJ, Brownstein MJ, Young AC, Bonner TI (1990) Structure of a cannabinoid receptor and functional expression of the cloned cDNA. *Nature* **346:** 561-564

Matyas F, Freund TF, Gulyas AI (2004) Immunocytochemically defined interneuron populations in the hippocampus of mouse strains used in transgenic technology. *Hippocampus* **14:** 460-481

McBain CJ, DiChiara TJ, Kauer JA (1994) Activation of metabotropic glutamate receptors differentially affects two classes of hippocampal interneurons and potentiates excitatory synaptic transmission. *The Journal of neuroscience : the official journal of the Society for Neuroscience* **14:** 4433-4445

McNamara JO (1986) Kindling model of epilepsy. *Adv Neurol* **44:** 303-318

McNamara JO (1999) Emerging insights into the genesis of epilepsy. *Nature* **399:** A15-22

Mechoulam R, Ben-Shabat S, Hanus L, Ligumsky M, Kaminski NE, Schatz AR, Gopher A, Almog S, Martin BR, Compton DR, et al. (1995) Identification of an endogenous 2-monoglyceride, present in canine gut, that binds to cannabinoid receptors. *Biochemical pharmacology* **50:** 83-90

mice DogImgrsiitfoeaivumamm (2003) Determination of group I metabotropic glutamate receptor subtypes involved in the frequency of epileptiform activity in vitro using mGluR1 and mGluR5 mutant mice. *Neuropharmacology* **44:** 157-162.

Miles R, Toth K, Gulyas AI, Hajos N, Freund TF (1996) Differences between somatic and dendritic inhibition in the hippocampus. *Neuron* **16:** 815-823

Misner DL, Sullivan JM (1999) Mechanism of cannabinoid effects on long-term potentiation and depression in hippocampal CA1 neurons. *J Neurosci* **19:** 6795-6805

Monory K, Massa F, Egertova M, Eder M, Blaudzun H, Westenbroek R, Kelsch W, Jacob W, Marsch R, Ekker M, Long J, Rubenstein JL, Goebbels S, Nave KA, During M, Klugmann M, Wolfel B, Dodt HU, Zieglgansberger W, Wotjak CT, Mackie K, Elphick MR, Marsicano G, Lutz B (2006) The endocannabinoid system controls key epileptogenic circuits in the hippocampus. *Neuron* **51:** 455-466

Munro S, Thomas KL, Abu-Shaar M (1993) Molecular characterization of a peripheral receptor for cannabinoids. *Nature* **365:** 61-65

Naderi N, Haghparast A, Saber-Tehrani A, Rezaii N, Alizadeh AM, Khani A, Motamedi F (2008) Interaction between cannabinoid compounds and diazepam on anxiety-like behaviour of mice. *Pharmacol Biochem Behav* **89:** 64-75

Nadler JV, Perry BW, Cotman CW (1980) Selective reinnervation of hippocampal area CA1 and the fascia dentata after destruction of CA3-CA4 afferents with kainic acid. *Brain Res* **182:** 1-9.

Nó Ld (1934) Studies on the structure of the cerebral cortex. II. Continuation of the study of the Ammonic system. *J für Psychologie und Neurologie* **46**

Northcutt RG (1990) Ontogeny and Phylogeny - A Re-Evaluation of Conceptual Relationships and Some Applications. *Brain BehavEvol* **36:** 116-140

Nusser Z, Hajos N, Somogyi P, Mody I (1998) Increased number of synaptic GABA(A) receptors underlies potentiation at hippocampal inhibitory synapses. *Nature* **395:** 172-177

Nyiri G, Cserep C, Szabadits E, Mackie K, Freund TF (2005) CB1 cannabinoid receptors are enriched in the perisynaptic annulus and on preterminal segments of hippocampal GABAergic axons. *Neuroscience* **136:** 811-822

Ohno-Shosaku T, Tsubokawa H, Mizushima I, Yoneda N, Zimmer A, Kano M (2002) Presynaptic cannabinoid sensitivity is a major determinant of depolarization-induced retrograde suppression at hippocampal synapses. *J Neurosci* **22:** 3864-3872

Okamoto Y, Morishita J, Tsuboi K, Tonai T, Ueda N (2004) Molecular characterization of a phospholipase D generating anandamide and its congeners. *J Biol Chem* **279:** 5298-5305

Panuccio G, D'Antuono M, de Guzman P, De Lannoy L, Biagini G, Avoli M (2010) In vitro ictogenesis and parahippocampal networks in a rodent model of temporal lobe epilepsy. *Neurobiology of disease* **39:** 372-380

Peng Z, Houser CR (2005) Temporal patterns of fos expression in the dentate gyrus after spontaneous seizures in a mouse model of temporal lobe epilepsy. *J Neurosci* **25:** 7210-7220

Pertwee RG (1997) Pharmacology of cannabinoid CB1 and CB2 receptors. *Pharmacology & therapeutics* **74:** 129-180

Pertwee RG (2008) Ligands that target cannabinoid receptors in the brain: from THC to anandamide and beyond. *Addict Biol* **13:** 147-159

Piomelli D, Astarita G, Rapaka R (2007) A neuroscientist's guide to lipidomics. *Nature reviews* **8:** 743-754

Polack PO, Charpier S (2006) Intracellular activity of cortical and thalamic neurones during high-voltage rhythmic spike discharge in Long-Evans rats in vivo. *The Journal of physiology* **571:** 461-476

Racine RJ (1972) Modification of seizure activity by electrical stimulation: II. Motor seizure. *Electroencephalography and clinical neurophysiology* **32:** 281-294

Rios CD, Jordan BA, Gomes I, Devi LA (2001) G-protein-coupled receptor dimerization: modulation of receptor function. *Pharmacology & therapeutics* **92:** 71-87

Rocca WA, Sharbrough FW, Hauser WA, Annegers JF, Schoenberg BS (1987a) Risk factors for absence seizures: a population-based case-control study in Rochester, Minnesota. *Neurology* **37:** 1309-1314

Rocca WA, Sharbrough FW, Hauser WA, Annegers JF, Schoenberg BS (1987b) Risk factors for generalized tonic-clonic seizures: a population-based case-control study in Rochester, Minnesota. *Neurology* **37:** 1315-1322

Salzmann A, Perroud N, Crespel A, Lambercy C, Malafosse A (2008) Candidate genes for temporal lobe epilepsy: a replication study. *Neurol Sci* **29:** 397-403

Seress L (1988) Interspecies comparison of the hippocampal formation shows increased emphasis on the regio superior in the Ammon's horn of the human brain. *J Hirnforsch* **29:** 335-340

Sik A, Penttonen M, Buzsaki G (1997) Interneurons in the hippocampal dentate gyrus: an in vivo intracellular study. *Eur J Neurosci* **9:** 573-588

Sik A, Penttonen M, Ylinen A, Buzsaki G (1995) Hippocampal CA1 interneurons: an in vivo intracellular labeling study. *J Neurosci* **15:** 6651-6665.

Sik A, Ylinen A, Penttonen M, Buzsaki G (1994) Inhibitory CA1-CA3-hilar region feedback in the hippocampus. *Science* **265:** 1722-1724

Sloviter RS (1989) Calcium-binding protein (Calbindin-D28k) and parvalbumin immunocytochemistry: localization in the rat hippocampus with specific reference to the selective vulnerability of hippocampal neurons to seizure activity. *JCompNeurol* **280:** 183-196

Spencer DD, Spencer SS (1994) Hippocampal resections and the use of human tissue in defining temporal lobe epilepsy syndromes. *Hippocampus* **4:** 243-249.

Stein V, Nicoll RA (2003) GABA generates excitement. *Neuron* **37:** 375-378

Sugiura T, Kishimoto S, Oka S, Gokoh M (2006) Biochemistry, pharmacology and physiology of 2-arachidonoylglycerol, an endogenous cannabinoid receptor ligand. *Prog Lipid Res* **45:** 405-446

Sugiura T, Kondo S, Sukagawa A, Nakane S, Shinoda A, Itoh K, Yamashita A, Waku K (1995) 2-Arachidonoylglycerol: a possible endogenous cannabinoid receptor ligand in brain. *Biochemical and biophysical research communications* **215:** 89-97

Sullivan JM (1999) Mechanisms of cannabinoid-receptor-mediated inhibition of synaptic transmission in cultured hippocampal pyramidal neurons. *Journal of neurophysiology* **82:** 1286-1294

Sutula T, Cascino G, Cavazos J, Parada I, Ramirez L (1989a) Mossy fiber synaptic reorganization in the epileptic human temporal lobe. *Annals of neurology* **26:** 321-330

Sutula T, Steward O (1986) Quantitative analysis of synaptic potentiation during kindling of the perforant path. *JNeurophysiol* **56:** 732-746

Sutula TP, Cascino G, Cavazos JE, Ramirez L (1989b) Mossy fiber synaptic reorganization in the epileptic human temporal lobe. *AnnNeurol* **26:** 321-330

Szabadics J, Varga C, Molnar G, Olah S, Barzo P, Tamas G (2006) Excitatory effect of GABAergic axo-axonic cells in cortical microcircuits. *Science* **311:** 233-235

Tappe-Theodor A, Agarwal N, Katona I, Rubino T, Martini L, Swiercz J, Mackie K, Monyer H, Parolaro D, Whistler J, Kuner T, Kuner R (2007) A molecular basis of analgesic tolerance to cannabinoids. *The Journal of neuroscience : the official journal of the Society for Neuroscience* **27:** 4165-4177

Toth K, Eross L, Vajda J, Halasz P, Freund TF, Magloczky Z (2010) Loss and reorganization of calretinin-containing interneurons in the epileptic human hippocampus. *Brain* **133:** 2763-2777

Toth K, Freund TF (1992) Calbindin D28k-containing nonpyramidal cells in the rat hippocampus: their immunoreactivity for GABA and projection to the medial septum. *Neuroscience* **49:** 793-805

Toth K, Wittner L, Urban Z, Doyle WK, Buzsaki G, Shigemoto R, Freund TF, Magloczky Z (2007) Morphology and synaptic input of substance P receptor-immunoreactive interneurons in control and epileptic human hippocampus. *Neuroscience* **144:** 495-508

Turski L, Cavalhiero EA, Sieklucka-Dziuba M, Ikonomidou-Turski C, Czuczwar SJ, Turski WA (1986) Seizures produced by pilocarpine: Neuropathological sequelae and activity of glutamate decarboxylase in the rat forebrain. *Brain Res* **398:** 37-48

Turski WA, Cavalheiro EA, Bortolotto ZA, Mello LM, Schwarz M, Turski L (1984) Seizures produced by pilocarpine in mice: a behavioral, electroencephalographic and morphological analysis. *Brain research* **321:** 237-253

van den Pol AN, Obrietan K, Chen G (1996) Excitatory actions of GABA after neuronal trauma. *The Journal of neuroscience* **16:** 4283-4292

Varma N, Carlson GC, Ledent C, Alger BE (2001) Metabotropic glutamate receptors drive the endocannabinoid system in hippocampus. *The Journal of neuroscience* **21:** RC188

Wallace MJ, Blair RE, Falenski KW, Martin BR, DeLorenzo RJ (2003) The endogenous cannabinoid system regulates seizure frequency and duration in a model of temporal lobe epilepsy. *J Pharmacol Exp Ther* **307:** 129-137

Wittner L, Eross L, Czirjak S, Halasz P, Freund TF, Magloczky Z (2005) Surviving CA1 pyramidal cells receive intact perisomatic inhibitory input in the human epileptic hippocampus. *Brain* **128:** 138-152

Wittner L, Eross L, Szabo Z, Toth S, Czirjak S, Halasz P, Freund TF, Magloczky ZS (2002) Synaptic reorganization of calbindin-positive neurons in the human hippocampal CA1 region in temporal lobe epilepsy. *Neuroscience* **115:** 961-978

Wittner L, Magloczky Z, Borhegyi Z, Halasz P, Toth S, Eross L, Szabo Z, Freund TF (2001) Preservation of perisomatic inhibitory input of granule cells in the epileptic human dentate gyrus. *Neuroscience* **108:** 587-600

Woodin MA, Ganguly K, Poo MM (2003) Coincident pre- and postsynaptic activity modifies GABAergic synapses by postsynaptic changes in Cl- transporter activity. *Neuron* **39:** 807-820

Wyeth MS, Zhang N, Mody I, Houser CR (2010) Selective reduction of cholecystokinin-positive basket cell innervation in a model of temporal lobe epilepsy. *J Neurosci* **30:** 8993-9006

Zhang W, Yamawaki R, Wen X, Uhl J, Diaz J, Prince DA, Buckmaster PS (2009) Surviving hilar somatostatin interneurons enlarge, sprout axons, and form new synapses with granule cells in a mouse model of temporal lobe epilepsy. *J Neurosci* **29:** 14247-14256

11. List of publications underlying the thesis

Karlocai MR, Toth K, Watanabe M, Ledent C, Juhasz G, Freund TF, Magloczky Z (2011) Redistribution of CB1 cannabinoid receptors in the acute and chronic phases of pilocarpine-induced epilepsy. *PloS one* **6:** e27196

Magloczky Z, Toth K, Karlocai R, Nagy S, Eross L, Czirjak S, Vajda J, Rasonyi G, Kelemen A, Juhos V, Halasz P, Mackie K, Freund TF (2010) Dynamic changes of CB1-receptor expression in hippocampi of epileptic mice and humans. *Epilepsia* **51 Suppl 3:** 115-120

12. Acknowledgements

I wish to thank my supervisor Zsófia Maglóczky for the excellent support and education during the past years.

I am most grateful to prof. Tamás Freund for the opportunity of working in his laboratory in the Institute of Experimental Medicine.

My special thanks to Kinga Tóth for technical and intellectual support during my PhD

I would like to express my gratitude to Gábor Juhász and his Group of Proteomics, for technical support in carrying out *in vivo* recordings.

I wish to thank Viktor Varga for his support in analyzing *in vivo* results.

I would also like to thank the excellent technical assistance of Ms. E. Simon Szépné, K. Lengyel, K. Iványi and Mr. Gy. Goda.

I am grateful to Norbert Hájos, István Katona and Anikó Ludányi for inspiring discussions.

I also thank all immediate colleagues for their help and advices

I am very grateful to my family and friends for constant support.